

Host factors underlying susceptibility to enteric infection in humans

Sayo McCowin  
Charlottesville, Virginia

B.S., Biochemistry and Molecular Biology, University of Maryland-Baltimore  
County, 2016

A Dissertation presented to the Graduate Faculty of the University of  
Virginia in Candidacy for the Degree of  
Doctor of Philosophy

Department of Microbiology, Immunology, and Cancer Biology

University of Virginia  
April, 2022

## Table of Contents

<b>Table of Contents</b> .....	ii-iv
<b>Abstract</b> .....	v-viii
<b>Acknowledgements</b> .....	ix-xi
<b>1. Chapter 1: Introduction</b> .....	<b>1</b>
1.1. <i>Cryptosporidium</i> spp. importance and prevalence .....	2
1.2. The <i>Cryptosporidium</i> life cycle .....	2-6
1.3. Morphology of <i>Cryptosporidium</i> spp .....	7-8
1.4. <i>Cryptosporidium</i> parasite effectors for adherence and invasion .....	9-15
1.5. Models for <i>Cryptosporidium</i> infection .....	16-17
1.6. Host actin cytoskeleton remodeling is a requisite for invasion .....	17-21
1.7. Protein Kinase C- $\alpha$ (PKC $\alpha$ ) the disease regulator .....	22-25
1.8. PKC $\alpha$ linked to susceptibility of <i>Cryptosporidium</i> infection .....	26-29
1.9. Regulation of <i>PRKCA</i> during <i>Cryptosporidium</i> infection .....	30-32
1.10.    Limitations of Pharmacologic Inhibitor Studies .....	32
1.11.    Human Leukocyte Antigen (HLA) and Infection .....	32-35
1.12.    Conclusions .....	36-37
<b>2. Chapter 2: Human Leukocyte Antigen (HLA) class I and II alleles and     their role in susceptibility to enteric infection</b> .....	<b>38</b>
2.1. Introduction .....	39-41
2.2. Materials and Methods .....	41-45
2.3. Results	

2.3.1. HLA classes I and II alleles associated with resistance or susceptibility to specific enteric pathogens.....	46-55
2.3.2. HLA haplotype associations with enteric pathogen infection....	55-58
2.3.3. HLA classes I and II alleles associated with resistance or susceptibility to overall diarrhea.....	59-60
2.3.4. Enteric pathogen susceptibility not driven by differences in exclusive breastfeeding.....	61
2.4. Discussion.....	61-68
<b>3. Chapter 3: PKC<math>\alpha</math> and its Role in Early <i>Cryptosporidium</i> Infection of Intestinal Epithelial Cells.....</b>	<b>69</b>
3.1. Introduction.....	70-72
3.2. Materials and Methods.....	73-79
3.3. Results	
3.3.1. <i>C. parvum</i> activates host PKC $\alpha$ during invasion.....	79-84
3.3.2. A stoplight assay for differentiation of sporozoite adherence from invasion.....	85-90
3.3.3. Pharmacologic inhibition of PKC $\alpha$ decreases <i>Cryptosporidium parvum</i> infection.....	91-99
3.3.4. Pharmacologic activation of PKC $\alpha$ increases <i>Cryptosporidium parvum</i> infection.....	100-103
3.4. Discussion.....	104-112
<b>4. Conclusions and Future Directions.....</b>	<b>113-115</b>
4.1. PKC $\alpha$ a mediator of <i>Cryptosporidium</i> infection.....	115-119

4.2. HLA, <i>Cryptosporidium</i> , and other common enteric infections.....	119-122
4.3. Future Directions.....	122
4.3.1. Ca <sup>2+</sup> influx as an activator of PKC $\alpha$ during invasion.....	123-133
4.3.2. PKC $\alpha$ regulation of F-actin as a mechanism of action.....	133-138
4.3.3. A genetic role for PKC $\alpha$ in the host immune response.....	139-143
4.3.4. Functional differences in HLA class I and II alleles.....	143-146
4.4. Final Conclusions.....	146-151
<b>5. References.....</b>	<b>152-201</b>

## Abstract

Host factors are indispensable for infectious disease processes and influence disease susceptibility and severity. Many pathogens usurp host factors by direct binding to or use of specialized secretion systems to exploit the downstream signaling processes facilitating infection. Thus, the host-pathogen interactions implicated in development of disease are key components of infection and transmission. In disease control, the host elicits a myriad of defense mechanisms entailing interplay between the innate and adaptive immune response to clear the infectious agent. Hence, communication between non-immune and immune cells is integral in the host response. Understanding how host factors are involved with and effect disease outcome offers an opportunity for new insight into pathogenesis and therapy.

The apicomplexan parasite *Cryptosporidium* is the causative agent of cryptosporidiosis, a disease that primarily consists of but is not limited to watery diarrhea. Cryptosporidiosis is a leading cause of diarrhea-associated morbidity and mortality in young children, globally. Notably, clinical presentation of *Cryptosporidium* infection is variable in severity; some patients experience severe diarrheal illness while others remain asymptomatic. Though the cause for this wide spectrum of disease is poorly understood, several studies have demonstrated long-term clinical implications of both asymptomatic and symptomatic infection. Importantly, nitazoxanide, currently the only FDA-approved drug for *Cryptosporidium* infection has poor efficacy in patients most

at-risk, immunocompromised persons. Thereby, the identification of novel host factors as potential therapeutic targets to combat cryptosporidiosis is warranted.

The highly diverse, classical human leukocyte antigen (HLA) genes are traditional genetic determinants of immunity. We systematically evaluated the impact of HLA alleles and haplotypes on susceptibility to 12 common enteric infections during the first year of life. A birth cohort of 601 Bangladeshi infants was prospectively monitored for diarrheal disease. We compared the frequency of HLA class I (A and B) alleles, class II (DRB1, DQA1, and DQB1) alleles, and haplotypes between infected and uninfected infants. We identified six individual allele associations and one five-locus haplotype association. Two alleles *B\*38:02* and *DQA1\*01:01* were associated with increased risk of *Cryptosporidium* infection, however no protective HLA-*Cryptosporidium* associations were identified. We discovered an additional three alleles associated with increased risk to other enteric infections: *A\*24:17*—typical EPEC, *B\*15:01*—astrovirus, *B\*38:02*—astrovirus. One allele, *A\*24:02*, was associated with protection from EAEC infection. A single five-locus haplotype was associated with protection: *A\*11:01~B\*15:02~DRB1\*12:02~DQA1\*06:01~DQB1\*03:01*—adenovirus 40/41. Our findings validate the role for HLA in susceptibility to five pathogens. Understanding the genetic contribution of HLA in susceptibility has important implications for vaccine design and understanding regional differences in incidence of enteric infection.

To discover novel genetic links to cryptosporidiosis alternate to those with traditional roles in immunity (e.g., HLA), our lab performed a genome-wide

association study (GWAS) of a birth cohort in an endemic area of Dhaka, Bangladesh during the first year of life. Our lab discovered single nucleotide polymorphisms (SNP) in an intron region of the human protein kinase C alpha (*PRKCA*) gene associated with increased susceptibility to *Cryptosporidium*. Protein Kinase C- $\alpha$  (PKC $\alpha$ ) is a host serine/threonine kinase that has been shown to modulate susceptibility to several enteric infections through regulation of the actin cytoskeleton. *Cryptosporidium* infection has been linked to changes in *PRKCA* expression and PKC $\alpha$  activity *in vitro*, independently. Previous work has found *Cryptosporidium* requires host cell actin polymerization at the site of invasion while in-parallel identifying critical actin-associated mediators. However, a role for host PKC $\alpha$  during *Cryptosporidium* invasion remains unexplored. Since PKC $\alpha$  is a primary regulator of the actin cytoskeleton, and during intracellular invasion *Cryptosporidium* sporozoites induce host cell actin remodeling we examined the role of PKC $\alpha$  during this process.

Here, we used an established *Cryptosporidium in vitro* model of infection: HCT-8 intestinal epithelial cells and infection with *Cryptosporidium parvum* sporozoites from excysted oocysts. To delineate the role of PKC $\alpha$  in infection, we developed a fluorescence-based imaging assay to differentiate adherent from invaded parasite. We tested pharmacologic agonists and antagonists of PKC $\alpha$  activity and measured the effect on *C. parvum* sporozoite adherence and invasion. We demonstrated both PKC $\alpha$  agonists and antagonists significantly alter parasite adherence and invasion of HCT-8 cells. We additionally found HCT-8 cell PKC $\alpha$  is activated by *C. parvum* infection. Altogether, our findings

suggest intestinal epithelial cell PKC $\alpha$  as a host therapeutic target for cryptosporidiosis and implicate PKC $\alpha$  activity as a mediator of parasite adherence and invasion.

The results from these studies present a primary role for the host in response to enteric infection and demonstrate that differences in activity of host factors directly influence susceptibility. The work presented in this thesis will focus on host-pathogen interactions in generating a protective or deleterious response to various infectious agents. Overall, this thesis furthers our understanding of the host immune response in enteric infection and explicitly implicates a host-derived kinase, PKC $\alpha$ , in *Cryptosporidium* pathogenesis.

## Acknowledgements

First and foremost, I would like to thank my co-mentors Chelsea Marie and Bill Petri for their unwavering support and guidance during this journey. I am honored to be Chelsea's first "official" graduate student. Her work ethic is unbelievable and enthusiasm for all areas of science is inspiring. I am thankful to her for her continuous motivation and investment in my growth as I searched to find my scientific independence. I will always appreciate her for bestowing me with autonomy in pursuance of my own hypotheses and supporting me when scientific discoveries were far and in between. She presented me with countless opportunities for growth and challenged me. Independent of her scientific prowess, it is her daily kindness and compassion that made my graduate student experience enjoyable. I will never forget the countless zoom meetings, phone calls, texts, and impromptu office chats both scientific and non-scientific alike. I am grateful to her for always putting my professional needs before her own and finding time for me at a moment's notice. Everything I have experienced during my graduate career is due to the admirable mentorship I have received. Thank you, Chelsea.

I would also like to thank my mentor Bill for his continuous support and exceptional leadership during my time as his graduate student. His knowledge on all things medicine and science has been instrumental to my development as a physician-scientist. Under his tutelage I learned to be excited yet critical of my science and that sometimes simplicity results in the biggest discoveries. I am also grateful to Bill for surrounding me with so many special members from his

lab to whom I was able to present, discuss, reflect, and develop my science. I will always remember the weekly lab meetings with Bodo's bagels, journal clubs, mentor-mentee conferences, round table talks, early morning rounds on the general medicine service, and facilitating collaborations with leaders in my field. He is an outstanding role model who I aim to emulate in all aspects of my personal and professional career. I am appreciative of his constant kindness and dedication to my success which made my graduate school journey even more pleasant. From my mentors I will take with me scientific rigor, competence, patience, and passion as I embark on this next step of my scientific career. I truly have seen further by standing on the shoulders of Giants.

A resounding thank you to my committee members Alison Criss, Hervé Agaisse, Isabelle Dérre, and Jim Casanova. All members of my committee have been an integral part of my scientific growth from helping to design my experiments to interpretation of my results. I am full of gratitude for their guidance as I navigated through graduate school and investment both in time and effort as members of my thesis committee. Your dedication to the department and to the students is well noted, and I thank you for being a part of my experience.

I would like the members of my lab, who are all models for how science should be conducted. Thank you to the members of "Team C. diff", "Team Amoeba", "Team Neuro", "Team COVID" and "Team Crypto" for your scientific input, support, and most of all fun these past four years. Whether it be brief conversations in the hallway or in depth discussions at your workspace, I am

forever grateful to you all for sharing your thoughts. Having each and every one of you as colleagues has been as meaningful as I could have ever hoped.

Finally I would like to thank my friends and family. To the friends I have made before, and during, this journey I am filled with joy when I am reminded that I am surrounded by such smart, passionate, driven, and supportive people. To my family, you have been and continue to be my biggest support system. All I have accomplished would not be possible without your consistent love and support. A special thank you to my partner Samantha, who finds any reason to celebrate my accomplishments and makes me believe all things are possible. Collectively, you all have instilled in me confidence, modesty, and compassion. I am so grateful for each and every day I get to share with all of you.

## Chapter 1: Introduction

This chapter has been adapted from: McCowin, S., Marie, C., 2020. The Role of Host PKC $\alpha$  During Intracellular *Cryptosporidium* Infection, in: Guillen, N. (Ed.), Eukaryome Impact on Human Intestine Homeostasis and Mucosal Immunology. Springer International Publishing, Cham, pp. 213–223.

This chapter has been adapted from: McCowin, S., Marie, C., Petri, W.A., 2021. Parasite protein pirates host cytoskeletal modulator during invasion. Trends Parasitol 37, 937–939.

## 1.1 *Cryptosporidium* spp. importance and prevalence

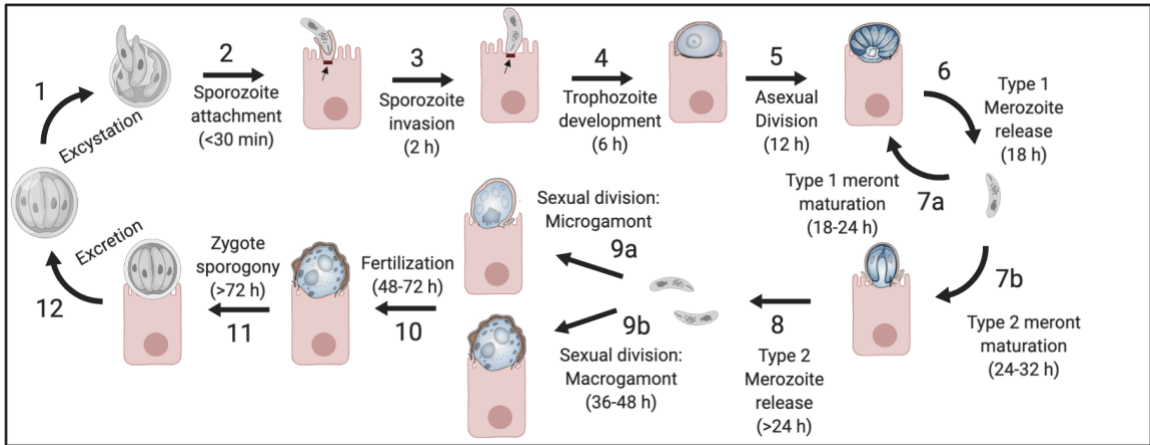
With over 40 *Cryptosporidium* spp. and their inherent ability to infect a broad range of vertebrates including humans, mammals, and wildlife, the footprint of infection is vast (Leitch et al., 2011). The clinical manifestations of cryptosporidiosis are variable but most commonly include watery diarrhea accompanied by abdominal pain (Checkley et al., 2015). These symptoms are further complicated by the immunocompetency of the host, with immunocompromised persons such as HIV/AIDS patients exhibiting more severe and chronic diarrhea that can be fatal. Additionally, due to their immature immune system and therefore high susceptibility to infection, cryptosporidiosis largely adversely affects infants accounting for 30-50% of deaths in infants and young children worldwide (Khan et al., 2019). In the absence of mortality, pediatric cryptosporidiosis has been linked to poor nutritional status, long-term cognitive developmental delays, and growth deficits (Mondal et al., 2009; Checkley et al., 1998; Guerrant et al., 1999). The burden of *Cryptosporidium* infection is the highest in developing countries, leading to over 200,000 deaths annually in children under the of age 2 in Africa and South Asia (Sow et al., 2016; Kotloff et al., 2013). This factor is further complicated as no vaccine is available for *Cryptosporidium* infection and nitazoxanide, the only approved drug, has low efficacy in immunocompromised patients and is not approved for use in children under 1 year of age (Khalil et al., 2018). Therefore, work to identify novel therapeutic targets to develop more effective drugs against *Cryptosporidium* infection is of high importance.

## 1.2 The *Cryptosporidium* life cycle

The entirety of the *Cryptosporidium* life cycle is completed in the intestinal epithelium of humans (**Fig. 1.1**). The preferred site of infection is the ileum of the small intestine however extraintestinal infection has also been described particularly in immunocompromised persons (Leitch et al., 2011). Enteric infection is initiated through ingestion of chlorine-resistant oocysts in the environment and subsequent excystation of sporozoites in the gastrointestinal tract. Each oocyst contains four motile sporozoites which exit the oocyst (i.e., excyst) through a fissure in the oocyst shell. Several host-dependent factors such as temperature, bile salts, ion content, and pH play a pivotal role in the success of this excystation process (Reduker et al., 1985). Once excysted, *Cryptosporidium* sporozoites use gliding motility to reach and adhere to epithelial cells of the intestinal brush border (Forney et al., 1998; Wetzel et al., 2005). The sporozoites adhere to the host epithelium via interactions with galactose and galactose-N-acetylgalactosamine (Gal-GalNAc) host cell surface ligands and sporozoite surface lectins (Joe et al., 1994; Nesterenko et al., 1999). A *Cryptosporidium*-derived lectin, p30, has been reported to recognize Gal-GalNAc surface sugars and mediate sporozoite adherence (Bhat et al., 2007). Once adherent, sporozoites induce encapsulation with the host cell apical membrane forming the parasitophorous vacuole at the infection site. Here, the sporozoite differentiates into a trophozoite then undergoes asexual division to form the type 1 meront consisting of eight motile merozoites. Then, the type 1 meront is breached permitting escape of the type 1 merozoites and attachment to adjacent

intestinal epithelial cells. At this stage, type 1 merozoites can either repeat type 1 meront formation or continue the life cycle producing type II meronts containing four type II merozoites. Type II merozoites release from type II meronts and undergo sexual division to produce microgamont (male) or macrogamont (female) progeny. The microgamont contains 16 nucleated microgametes which exit and fertilize nearby macrogamonts resulting in the sole diploid stage, the zygote. The *Cryptosporidium* zygote develops into an oocyst which then further differentiates to be thin- or thick-walled. Thick-walled oocysts are excreted from the infected host into the environment while thin-walled oocysts remain in the lumen of the small intestine to cause autoinfection of the host. Markedly, *Cryptosporidium* thick-walled oocysts are infectious upon excretion into the environment thus permitting immediate fecal-oral transmission between hosts.

Figure 1.1



Created with BioRender.com

**Figure 1.1: The *Cryptosporidium* life cycle.** Following ingestion, oocysts excyst in the upper small intestine, presenting four sporozoites with gliding motility that interact with the mucosal epithelium. The sporozoites attach to host epithelium via interactions with galactose-N-acetylgalactosamine (Gal-GalNAc) host cell surface ligands and *C. parvum* sporozoite surface lectins. Following attachment, the host initiates a signaling cascade to aggregate F-actin at the infection site (black arrow) and form a membrane protrusion resulting in the encapsulation of the sporozoite in an extra-cytoplasmic parasitophorous vacuole. Once inside the host cell, the parasite transforms into a trophozoite. The parasite then undergoes asexual reproduction (merogony) followed by sexual reproduction (gametogony) generating microgamonts (male) and macrogamonts (female) progeny. Upon fertilization of the macrogamont by the microgamont, an undifferentiated zygote is formed. From this zygote, thin-walled oocysts are produced causing autoinfection while thick-walled oocysts are excreted to infect a new host. Figure adapted from Bouzid et al., 2013.

### 1.3 Morphology of *Cryptosporidium* spp.

The characteristics of *Cryptosporidium* morphology largely depend on the stage of the parasite under investigation. Oocysts are spherical in shape with a smooth surface and possess a unilateral cleft permitting excystation of sporozoites under suitable conditions (Borowski et al., 2010). Sporozoites are characterized as rough on the surface and spindle-shaped, displaying a pointed apical end with a rounded posterior. The sporozoite contains micronemes and a rhoptry bulb at this apical end, dense granules in the center portion, and a single nucleus at the posterior end (Tetley et al., 1998). These apical organelles of sporozoites are secreted and facilitate the invasion of the sporozoite into the host epithelial cell (Guérin et al., 2021). The next stage, trophozoite, is depicted as having a smooth surface and develops a hood-like structure at the basal membrane (Borowski et al., 2010). Before merozoite development, cytoplasmic granulation of trophozoites has been reported (Borowski et al., 2010). Type I and II meronts exhibit similar morphology persisting as epicellular with a smooth surface. The only notable difference between these *Cryptosporidium* stages is size. Type I merozoites resemble sporozoites in structure with an elongated apical region and rough surface while type II merozoites are more ovular in shape. The microgamont and macrogamont progeny from type II merozoites are spherical with a rough surface. These sexual reproductive stages reside in a more extracellular location than their predecessors but remain in contact with the host cell apical membrane (Borowski et al., 2010). The stage-specific morphology of the *Cryptosporidium* life cycle is summarized in **Table 1.1**.

**Table 1.1: *Cryptosporidium in vitro* developmental characteristic**

<b>Life cycle stage</b>	<b>Morphology</b>
Oocyst (0 h)	Spherical, 4 nuclei, inner/outer cell wall, ~5 µm
Sporozoite (2 h)	Banana-shaped (pointed apical region, rounded posterior region), secretory vesicles (micronemes), ~5x0.6 µm
Trophozoite (6 h)	Spherical, epicellular, electron dense band (actin), PV, feeder-organelle, 1.5-2.5 µm
Type 1 Meront (12-24 h)	Epicellular, smooth surface, 6-8 nuclei, 1.5 µm
Type 1 Merozoite (18-24 h)	Rod-like shape, secretory vesicles (micronemes), 0.4 x 1 µm
Type 2 Meront (24-32 h)	Epicellular, smooth surface, thick membrane, 3-4 nuclei, 3.5 µm
Microgamont (36-48 h)	Extracellular, 16 nuclei densely packed (microgametes), 2 x 2 µm
Macrogamont (36-48 h)	Extracellular, spherical, rough surface, 4 x 5 µm

#### 1.4 *Cryptosporidium* parasite effectors for adherence and invasion

*Cryptosporidium* spp. express virulence factors that are used for the infection processes of adherence, invasion, and host immune cell evasion. Apicomplexan parasites in particular possess unique secretory organelles termed the rhoptry bulb, micronemes, and dense granules known to play essential roles in invasion of the host cells (Borowski et al., 2010). Identification of virulence factors for *Cryptosporidium* has been lacking relative to other apicomplexan parasites due to its inherent difficulty persisting in *in vitro* culture. Unlike most intracellular pathogens, *Cryptosporidium* exists in a unique membrane-bound compartment at the periphery of the intestinal epithelium. Despite this, *Cryptosporidium* is capable of damaging the host intestinal epithelium directly or indirectly through recruitment of immune cells or secretion of inflammatory cytokines at the infectious site.

The initial step of *Cryptosporidium* infection is the adherence of the sporozoite to the host epithelium. Several parasite adherence factors have been described via immunological or molecular techniques (**Table 1.2**). Circumsporozoite-like (CSL) glycoprotein was shown to be released as a soluble glycoprotein and bind directly via ligand to a receptor on the surface of intestinal epithelial cells (Riggs et al., 1997; Langer and Riggs 1999). Glycoprotein 900 (gp900) is located in the sporozoite microneme and is known to mediate invasion as antibodies against gp900 block infection *in vitro* (Barnes et al., 1998; Petersen et al., 1997). Glycoprotein 60 (gp60) is primarily used as a genetic marker for species of *Cryptosporidium* (Jex and Gasser 2010). However, during infection,

gp60 is tethered to the parasite membrane via a glycosylphosphatidylinositol (GPI) anchor and has been found to mediate parasite adherence and invasion of host cells (Strong and Nelson 2000). Furthermore, a parasite surface protein complex involving gp15, gp40, and gp60 has also been reported (Strong and Nelson., 2000). Gp15 is anchored to the sporozoite membrane via a GPI-anchor while gp40 remains soluble (O'Connor et al., 2007). Still, gp40 and gp15 colocalize to the membrane of sporozoites, co-immunoprecipitate, and function to link the parasite to the host cell surface (O'Connor et al., 2007). A surface protein, p23, is deposited in trails during the gliding motility of the sporozoite, linking this protein to motility. Monoclonal antibodies against p23 were found to reduce infection in mice and protect against cryptosporidiosis (Boulter-Bitzer et al., 2007). P30 is a *Cryptosporidium*-derived lectin that recognizes Gal-GalNAc host cell surface sugars and mediates sporozoite adherence (Bhat et al., 2007). *Cryptosporidium* p30 does not contain predicted adhesive domains nor does the lectin share homology with other mammalian lectins (Bhat et al., 2007). Similarly, the protozoan parasite *E. histolytica* expresses a Gal-GalNAc-specific lectin shown to mediate adherence though it also lacks adhesive domains and homology to other lectins (Petri et al., 2002). Microneme proteins (MICs) localize in micronemes at the apical end of the sporozoite. These proteins share sequence and structural homology with members of adherence proteins in other apicomplexan parasites such as *Toxoplasma* and *Plasmodium* spp (Soldati et al., 2001). Upon signaling, MICs translocate from the apical complex to the surface of the sporozoite to mediate the processes of host cell adherence and

subsequent invasion (Spano et al., 1998; Putignani et al., 2008). Notably, gp900, gp40, gp15, p23, and MICs all possess a mucin-type O-glycosylation suggesting this post-translational modification as critical in parasite adherence and invasion of the host cell.

Calcium has been linked to many stages of the *Cryptosporidium* life cycle such as effector secretion, adherence, invasion, and gliding motility (Billker et al., 2009; Chen et al., 2004c). In the parasite, calcium ions are regulated in response to activity of calcium-dependent protein kinases (CDPKs). To date, there have been 11 CDPKs reported through whole-genome sequencing analysis of *C. parvum* life cycle stages (Lippuner et al., 2018). *Cryptosporidium* CDPK1 (CpCDPK1) has been studied almost exclusively as it is expressed in all stages and thus serves as an attractive therapeutic target (Castellanos-Gonzalez et al., 2016; Kuhlenschmidt et al., 2015). A recent study found that CpCDPK1 knockdown decreased parasite invasion and growth by approximately 50% *in vitro* (Castellanos-Gonzalez et al., 2016). CpCDPK1 is expressed later in infection, peaking at 24 h post-infection and continuing to 48 h *in vitro* (Etzold et al., 2014). A novel class of pharmacologic agents termed bumped kinase inhibitors (BKIs) have been developed, selectively targeting CDPKs of apicomplexan pathogens (Doggett et al., 2014). Combining CDPK1 knockdown with BKI treatment synergistically decreased parasite growth by approximately 95% (Castellanos-Gonzalez et al., 2016; Hulverson et al., 2017). This finding partially confirms the specificity of BKI for CpCDPK1, however, it does not exclude the possibility that this BKI acts additively with CDPK1 inhibition via an

off-target effect on host cell kinases. Some BKIs have been shown to have efficacy against mammalian c-Src, which has known activity in parasite invasion, suggesting a potential for an off-target effect (Hulverson et al., 2017). An independent analysis found that many BKI analogs with potent activity toward purified CDPK1 had little or no effect on parasite growth in HCT-8 cells despite favorable absorption in mammalian cells highlighting a potential difference in infection of these two cell types (Kuhlenschmidt et al., 2015). Compound optimization has led to the development of BKIs that are reportedly >200-fold more active against parasite CDPK1 than 20 representative human kinases *in vitro* (Van Voorhis et al., 2017). However, this study reported that even these optimized BKIs had the highest off-target effects on protein kinase D3 (PKD3), a relative of protein kinase C. This finding suggests that the efficacy of BKIs may be at least partially mediated via inhibition of host cell kinases. Notably, no results for conventional PKC isoforms were reported. CpCDPK3 has been reported to play a role in the intracellular development of *Cryptosporidium* (Zhang et al., 2020). More recently, CpCDPK4, CpCDPK5, and CpCDPK6 were examined for expression and function (Zhang et al., 2021). These CpCDPKs are expressed at differing time points of *Cryptosporidium* infection and localized to distinct areas of the sporozoite. Furthermore, CpCDPK4 and CpCDPK6 were found to mediate parasite invasion while CpCDPK5 had no effect on invasion suggesting different roles for CpCDPKs during the parasite life cycle (Zhang et al., 2021). The functions of the remaining CpCDPKs have not been reported.

The invasive form of *Cryptosporidium*, the sporozoite, contains a single rhoptry bulb at the apical end of the parasite. In other apicomplexan parasites, such as *Toxoplasma* or *Plasmodium* spp., this secretory organelle is involved in parasite adherence and invasion (Okhuysen and Chappell 2002). A recent analysis exploring *Cryptosporidium* rhoptry proteins identified 54 co-transcribed rhoptry protein candidates expressed during invasion (Guérin et al., 2021). Of these, six candidates displayed localization to the sporozoite rhoptry bulb only, suggesting these as potential rhoptry effectors. These six rhoptry candidates are secreted during invasion and localize to diverse compartments in the host cell, implying rhoptry effectors target various host cell processes and structures (Guérin et al., 2021). Rhoptry protein 1 (ROP1) accumulated in the cytoplasm of the host cell at the cell periphery where *C. parvum* invasion occurs. Using a high-throughput yeast 2-hybrid screen of the N-terminus of ROP1, 149 positive clones associated with a host protein LMO7 were identified. In LMO7 KO mice infected with *Cryptosporidium*, ROP1 localization at the infection site was absent, suggesting LMO7 recruits ROP1. Furthermore, when quantifying infection, the presence of ROP1 was found to be critical for parasite infection *in vitro* and *in vivo* (Guérin et al., 2021). Further investigation into these remaining rhoptry effectors and direct or indirect associations with host PKC $\alpha$  may yield vital information on the mechanisms of invasion.

In summary, the identification of molecules involved in the earliest stages of *Cryptosporidium* infection advances our understanding of pathogenesis. A shared commonality is the expression of these proteins on the surface of the

infectious sporozoite and for some proteins, the merozoite stage as well. Given the broad range of hosts susceptible to infection by *Cryptosporidium* spp. we postulate the expression of a seemingly redundant parasite adherence and invasion effectors as critical to supporting this virulence.

**Table 1.2: Parasite effectors involved in adherence and invasion**

Virulence factor	Localization	Function	Reference(s)
CSL glycoprotein	Apical end of sporozoite and merozoite	Adherence	Riggs et al., 1997; Langer and Riggs., 1999
Gp900	Microneme (apical end of sporozoite)	Adherence	Petersen et al., 1997; Barnes et al., 1998
Gp15/40/60	Surface of sporozoite, extracellular	Adherence	Strong and Nelson., 2000; O'Connor et al., 2007
P23	Surface of sporozoite	Adherence, locomotion	Boulter-Bitzer et al, 2007
P30	Surface of sporozoite	Adherence	Bhat et al., 2007
MICs	Microneme (apical end of sporozoite)	Adherence, invasion, locomotion	Soldati et al., 2001; Spano et al., 1998; Putignani et al., 2008
CpCDPK1	Sporozoite, Merozoite, Type 1 Meront	Invasion	Kuhlenschmidt et al., 2015; Castellanos-Gonzalez et al., 2016; Hulverson et al., 2017; Van Voorhis et al., 2017
CpCDPK2	Not reported	Not reported	
CpCDPK3	Sporozoite, Merozoite	Intracellular development	Zhang et al., 2020
CpCDPK4	Anterior and mid-anterior sporozoite	Invasion, intracellular development	Zhang et al., 2021
CpCDPK5	Entire sporozoite	Egress	Zhang et al., 2021
CpCDPK6	Punctate distribution on sporozoites	Invasion, intracellular development	Zhang et al., 2021
CpCDPK7	Not reported	Not reported	
CpCDPK8	Not reported	Not reported	
CpCDPK9	Not reported	Not reported	
CpCDPK10	Not reported	Not reported	
CpCDPK11	Not reported	Not reported	
ROP1	Parasitophorous vacuole, host cell periphery	Invasion	Guérin et al., 2021
ROP2	Parasitophorous vacuole	Invasion	Guérin et al., 2021
ROP3	Parasitophorous vacuole, host cell cytoplasm	Invasion	Guérin et al., 2021
ROP4	Parasitophorous vacuole	Invasion	Guérin et al., 2021
ROP5	Ring structure, host-parasite interface	Invasion	Guérin et al., 2021
ROP6	Ring structure, host-parasite interface	Invasion	Guérin et al., 2021

### 1.5 Models for *Cryptosporidium* infection

Human transformed cell lines have been used traditionally to model *Cryptosporidium* infection *in vitro*. Human ileocecal colorectal adenocarcinoma (HCT-8) cells are the most commonly used transformed cell line. HCT-8 intestinal epithelial cells were found to support the greatest degree of infection for *C. parvum* producing nearly twice the number of intracellular parasite developmental stages than any other transformed cell line (Upton et al., 1994; Meloni et al., 1996). Furthermore, upon increasing the multiplicity of infection (MOI), HCT-8 cells consistently exhibited higher numbers of infected parasites than other host cell lines (Upton et al., 1994).

There exist established murine models for studying *Cryptosporidium* infection *in vivo* such as the IFN $\gamma$  deletion, IL-12 deletion, and severe combined immunodeficiency (SCID) mice (Mead et al., 1991; You et al., 1998; Jakobi et al., 2008; von Oettingen et al., 2008; Tessema et al., 2009; McDonald et al., 2021). Most murine models of cryptosporidiosis are performed in an immunosuppressed background (Costa et al., 2012). Still, these *in vivo* models help to delineate critical host-derived factors involved in *Cryptosporidium* infection within an entire living organism. Importantly, there does not yet exist an *in vivo* model to explicitly isolate distinct *Cryptosporidium* life cycle events such as sporozoite adherence or invasion. Furthermore, a timeline for stage-specific progression of *Cryptosporidium* infection has not been described *in vivo*.

A resounding strength of using the HCT-8 cell system to study *Cryptosporidium* infection is the ease of acquisition and maintenance in culture,

degree of infection, and well-characterized timeline of life cycle stage progression. Thus, permitting explicit investigation of parasite and host factors potentially involved in a specific stage of development. The primary limitation of the HCT-8 cell system as an infectious model is the inability to generate significant oocyst production to maintain infected cultures due to inefficient fertilization (Upton et al., 1994; Müller et al., 2013). Hence, the entirety of the *Cryptosporidium* life cycle cannot be completed *in vitro*. As such, stem cell-derived systems have been developed to recapitulate *in vivo* conditions permitting increased parasite yields along with longer parasite propagation (Heo et al., 2018; Wilke et al., 2019). However, though capable of supporting long-term *Cryptosporidium* infection, these stem cell-derived models exhibit a delayed timeline of infection relative to the traditionally used HCT-8 cell model. Furthermore, a limitation of using these stem-cell-derived systems is their finite lifespan thus inducing the need for a continued supply of these cells from human or animal tissues.

### **1.6 Host actin cytoskeleton remodeling is a requisite for invasion**

As an obligate intracellular parasite, *Cryptosporidium* depends on the host cell machinery to complete its life cycle. During invasion, an electron-dense band with an underlying network of filamentous actin (F-actin) forms at the host-parasite interface, separating the parasite from the host cell cytoplasm (Elliott et al., 2000). This invasion event happens rapidly ( $\leq 2$  minutes) with the apical end of the sporozoite fixed to the host cell while the basal end contorts (Guérin et al., 2021). This event is subsequently followed by the sporozoite straightening and

resulting in engulfment by the host plasma membrane. F-actin polymerizes and continues to develop in structure but is limited to the location of the sporozoite apex (Forney et al., 1999; Guérin et al., 2021). However, the complete parasitic effector proteins involved in this host F-actin rearrangement and their molecular targets have not been revealed.

Many studies have documented the requirement for host cell actin during cellular invasion by *Cryptosporidium* (Elliott et al., 2000; Elliott et al., 2001; Guérin et al., 2021), which is regulated by PKC $\alpha$  (Song et al., 2002; Nakashima 2002). Both *C. parvum* and *C. hominis* induced host cell actin rearrangements in immortalized cell lines (Hashim et al., 2004) and colocalized with actin in primary human intestinal cells during infection (Hashim et al., 2006). Further underscoring the necessity of host actin rearrangements, pre-treatment of intestinal cells with cytoskeletal inhibitors cytochalasin B and cytochalasin D blocked parasite infection (Hashim et al., 2006). Mechanistic studies of *C. parvum*-induced cytoskeleton remodeling have shown that parasites rapidly trigger tyrosine phosphorylation at the site of attachment (Forney et al., 1999). Further work identified activation of c-Src, a membrane-associated protein tyrosine kinase, and phosphatidylinositol 3-kinase (PI3K) leading to subsequent recruitment of host Rho-GTPase Cdc42 and the Cdc42-associated GEF, frabin (Chen et al., 2004b). This phosphorylation cascade results in N-WASP activation and subsequent recruitment and activation of the actin nucleation and branching complex of proteins, Arp2/3 (Chen et al., 2004a; Chen et al., 2004b). Inhibition of Arp2/3 (Elliott et al., 2001), PI3K (Forney et al., 1999; Chen et al.,

2003), Cdc42, and N-WASP (Chen et al., 2004a) blocked parasite infection implicating these actin-associated proteins as essential. *Cryptosporidium* parasites have also been observed to induce volume increases via activation of host aquaporin 1 (AQP1) and the sodium/glucose transporter (SGLT1) at the site of host cell attachment which is thought to further contribute to actin-dependent host cell invasion (Chen et al., 2005; Borowski et al., 2008). Silencing of AQP1 gene expression results in an impairment in the organization of host cell actin in human endothelial and melanoma cell lines (Monzani et al., 2009). Based on this prior evidence we have developed a hypothetical pathway of PKC $\alpha$ -actin-mediated *Cryptosporidium* invasion of host cells (**Fig. 1.2**).

Recent research focused on the action of parasite effectors during *Cryptosporidium* invasion has begun to characterize these host-pathogen interactions. A *Cryptosporidium* rhoptry protein, ROP1, binds to a component of the F-actin network, LIM domain only 7 (LMO7). LMO7 is a host protein that regulates emerin activity (Holaska et al., 2006) and functions to stabilize the growing ends of F-actin (Holaska et al., 2004). Mutations in LMO7 or emerin are associated with impairment of actin dynamics (Du et al., 2019; Ranade et al., 2019). Hence, the *Cryptosporidium* sporozoite has evolved to hijack actin-associated protein LMO7 via secretion of ROP1 to enhance parasite invasion.

Figure 1.2

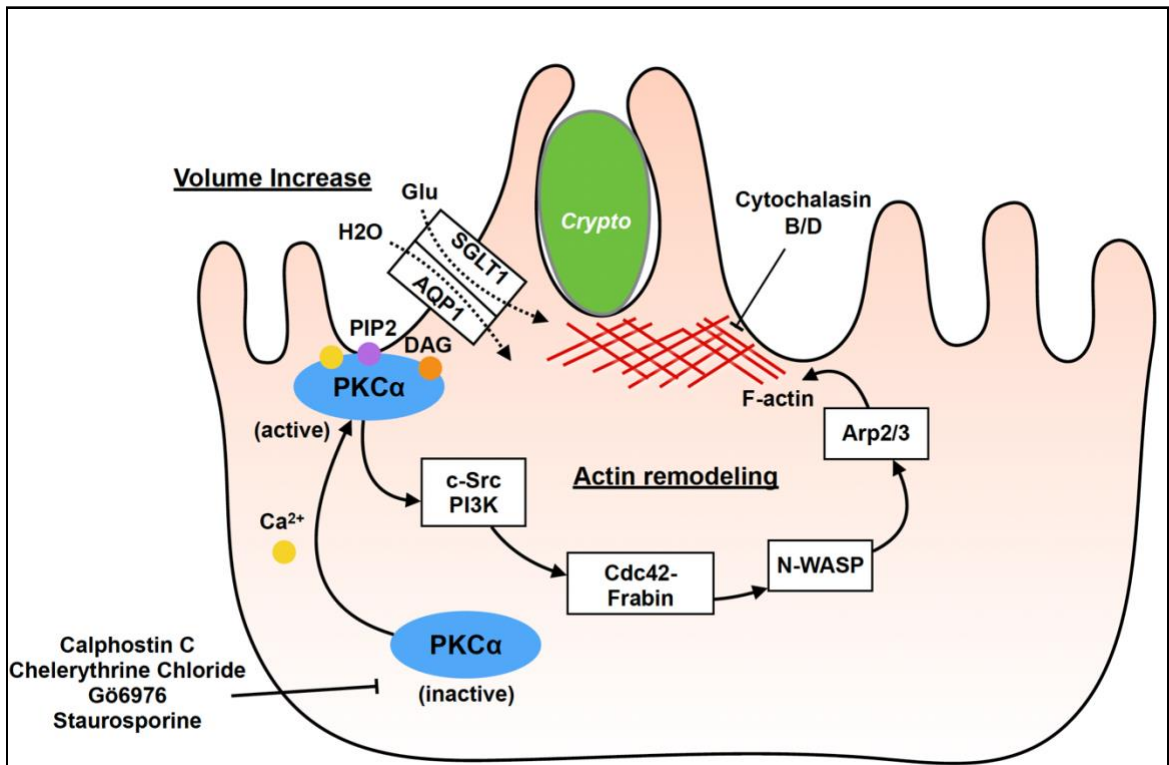


**Figure 1.2: PKC $\alpha$  mediated *Cryptosporidium* invasion of host cells.**

Adherence of *Cryptosporidium* results in recruitment of host factors necessary for invasion. During parasite invasion, activation and translocation of host PKC $\alpha$  occurs to the site of infection at the plasma membrane. Activated PKC $\alpha$  initiates a phosphorylation cascade in the host cytoplasm causing activation of the Arp2/3 complex and subsequent remodeling of the actin cytoskeleton.

Concurrently, host cell contact with *Cryptosporidium* leads to activation of SGLT1/AQP1 and a volume increase, from co-transport of glucose and water, further contributing to the actin remodeling required for infection. Pharmacologic inhibition of *Cryptosporidium* invasion by several small compounds targeting actin or actin-associated proteins has been reported.

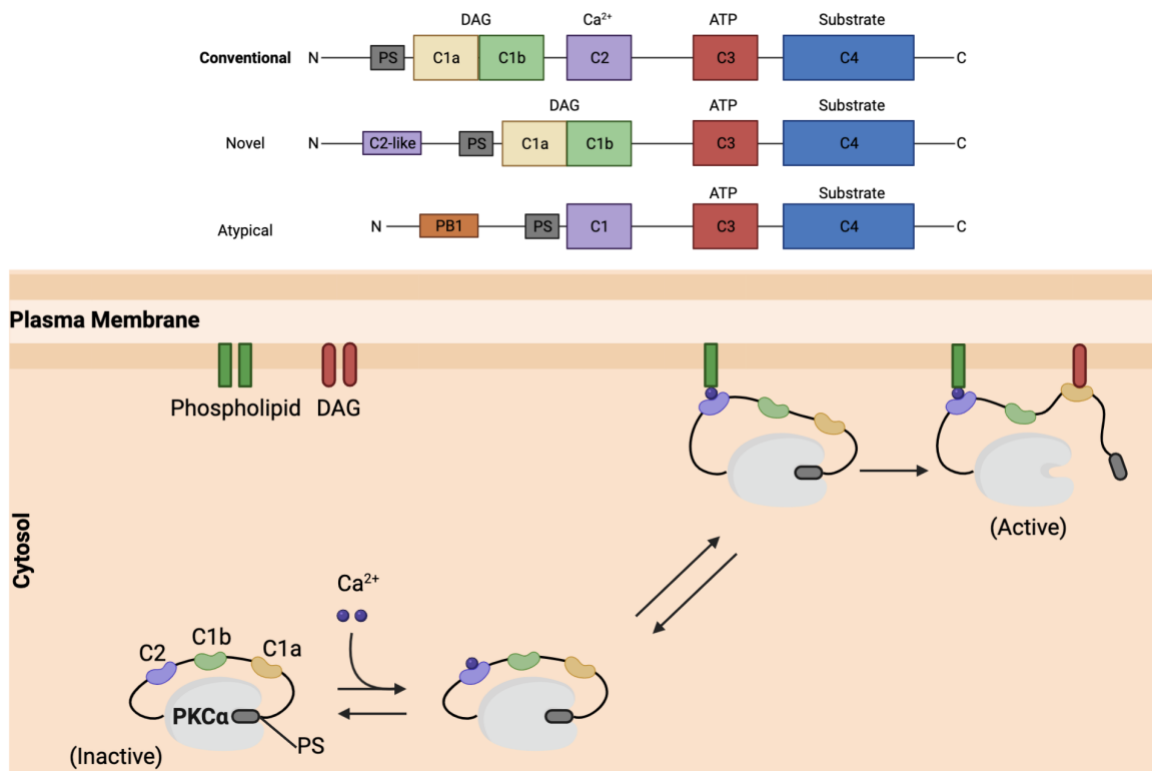
### 1.7 Protein Kinase C- $\alpha$ (PKC $\alpha$ ) the disease regulator

The protein kinase C (PKC) family is classified into three distinct groups based on their regulation (Newton 1995). The conventional isoforms ( $\alpha$ ,  $\beta$ ,  $\gamma$ ) contain a diacylglycerol (DAG)-binding C1 domain and a  $\text{Ca}^{2+}$ -binding C2 domain (**Fig. 1.3**). Novel PKC isoforms ( $\delta$ ,  $\epsilon$ ,  $\theta$ ,  $\eta$ ) require only DAG for activation while atypical PKCs ( $\zeta$  and  $\iota/\lambda$ ) activity is independent of secondary messengers and calcium. Instead, atypical PKC isoforms contain a protein domain and are regulated through protein-protein interactions. The PKC family of serine/threonine kinases has been a focus of drug discovery due to their role in a variety of pathogenic conditions including diabetes, cancer, heart disease, Parkinson's disease, Alzheimer's disease, bipolar disease, psoriasis, and inflammatory bowel disease (Hempel et al., 1997; Koivunen et al., 2004; Palaniyandi et al., 2009; Bar-Am et al., 2004; Talman et al., 2016; Hahn et al., 1999; Skvara et al., 2008; Yang and Yan 2014). This has led to FDA-approved clinical trials using PKC pharmacologic modulators (Ishii et al., 1996; Packer et al., 1993; Fischer et al., 2010) though to our knowledge none have been tested for clinical efficacy against cryptosporidiosis.

PKC $\alpha$  activity specifically has been implicated in numerous enteric infections (Sukumaran et al., 2002; Mittal et al., 2016; Bhalla et al., 2017). PKC $\alpha$  plays an important role in the invasion of human endothelial cells by *Escherichia coli*. Like *Cryptosporidium*, *E. coli* induces host actin condensation at the site of invasion and immunocytochemical studies indicated that activated PKC $\alpha$  co-localized with actin at the bacterial entry site (Sukumaran et al.,

2002). An analogous role for PKC $\alpha$  was described for *Pseudomonas aeruginosa* invasion of middle ear epithelial cells (Mittal et al., 2016). A bacterial effector was found to be a corequisite for phosphorylation of host PKC $\alpha$  which then translocated to the site of bacterial invasion and actin condensation. In *Listeria monocytogenes* infection, PKC $\alpha$  was directly associated with bacterial internalization and accumulation of host actin filaments (Bhalla et al., 2017). Altogether, these findings support the exploitation of PKC $\alpha$  activity by diverse enteric pathogens to alter host processes to promote pathogenesis.

Figure 1.3



Created with BioRender.com

**Figure 1.3: PKC regulatory domains and co-factors for activation.** Protein kinase C (PKC) is a family of serine/threonine kinases classified based on their post-translational regulation. PKC $\alpha$  is a serine/threonine kinase member of the conventional PKC isoforms. As a conventional PKC, PKC $\alpha$  requires binding of calcium, DAG, and phospholipids for catalytic competency. Novel PKCs require DAG only while atypical PKCs rely on protein-protein interactions for activation. After maturation and priming, activation of PKC $\alpha$  involves binding of free Ca<sup>2+</sup> to the C2 domain resulting in translocation from the host cytoplasm to the plasma membrane. Once bound to the membrane, the C1a domain of PKC $\alpha$  binds to DAG releasing the pseudosubstrate from the catalytic active site. At this stage, PKC $\alpha$  is tightly-associated with the plasma membrane and highly active to facilitate downstream molecular interactions.

## 1.8 PKC $\alpha$ linked to susceptibility of *Cryptosporidium* infection

*Cryptosporidium* infection is a major cause of pediatric diarrhea in low- and middle-income countries (Kotloff et al., 2013). These countries typically include rural, impoverished areas, primarily in sub-Saharan Africa and South Asia (Khalil et al., 2018). In Dhaka, Bangladesh the leading causes of diarrhea during infancy were *Campylobacter jejuni/coli* (*C. jejuni/coli*), rotavirus, astrovirus, *Shigella*/enteroinvasive *Escherichia coli* (EIEC), ST-EPEC, norovirus GII, sapovirus, astrovirus, and *Cryptosporidium* (Schnee et al., 2018). Risk factors for increased risk of *Cryptosporidium* infection during infancy include poverty, overcrowding, and poor water filtration (Bouزيد et al., 2018). Despite efforts to improve the burden of *Cryptosporidium*, in Dhaka, Bangladesh nearly two-thirds of children residing in this region were found to be infected with *Cryptosporidium* by 2 years of age, while one-fourth reported more than one episode (Korpe et al., 2018). Moreover, children with cryptosporidiosis were at an increased risk of becoming malnourished by 2 years of age (Steiner et al., 2018). Yet, in these areas endemic to cryptosporidiosis, there remains variability in clinical outcomes between infants. Putative explanations for this discrepancy in *Cryptosporidium* infection symptomology include pathogen virulence and host genetics. Still, the host cell signaling cascades and proteins seized by *Cryptosporidium* during infection are not well understood.

To identify novel host factors involved in *Cryptosporidium* infection our lab compared the genotypes of infants living in an endemically exposed area of Dhaka, Bangladesh who contracted cryptosporidiosis to those that did not (177

cases, 866 controls). This study evaluated pediatric cryptosporidiosis in three independent cohorts within Dhaka, Bangladesh, and conducted a meta-analysis to determine highly significant associations. This genome-wide association study identified an intronic region in the gene encoding host protein kinase C alpha (*PRKCA*) significantly associated with susceptibility to cryptosporidiosis within the first year of life (Wojcik et al., 2020).

While the role of host cell PKC $\alpha$  has not been explicitly investigated previously, several lines of evidence suggested that PKC $\alpha$  may also be a critical host factor for the establishment of intracellular *Cryptosporidium* infection (Hashim et al., 2006; Love et al., 2017; Liu et al., 2018). Two studies have independently characterized the anticryptosporidial activity of the inhibitor Gö6976. Gö6976 is a potent selective inhibitor of PKC (isotypes  $\alpha$  and  $\beta$ 1) as well as the tyrosine kinases JAK2 and the checkpoint kinases Chk1/2 (Martiny-Baron et al., 1993; Grandage et al., 2006). The first study characterized the effects of a variety of protein kinase inhibitors on *Cryptosporidium* infection of HCT-8 and primary epithelial cells (Hashim et al., 2006). Gö6976, reduced invasion of *C. hominis* and *C. parvum* invasion by approximately 50% for both HCT-8 and primary epithelial cells. The protein kinase C inhibitors calphostin C and chelerythrine chloride also displayed inhibitory effects on infection of HCT-8 cells by *C. hominis* and *C. parvum*, respectively, but neither had activity in primary epithelial cells. Staurosporine, a general protein kinase inhibitor, completely abolished *C. parvum* and *C. hominis* infection of both HCT-8 cells

and primary epithelial cells. Importantly, dual inhibitor experiments showed that staurosporine acted primarily via inhibition of PKC signaling.

The second study to suggest inhibition of host PKC $\alpha$  may exert anticryptosporidial activity was independently observed in a high throughput phenotypic screen of 78,942 compounds (Love et al., 2017). This study identified twelve small compound inhibitors with potent sub-micromolar anticryptosporidial activity, including the PKC $\alpha/\beta$ 1 inhibitor Gö6976. Gö6976 strongly inhibited both *C. parvum* and *C. hominis* infection of HCT-8 cells with similar half-maximal effective concentrations (*C. parvum* EC<sub>50</sub> = 2.5 nM  $\pm$  1.8 nM and *C. hominis* (EC<sub>50</sub> = 5 nM  $\pm$  2.6 nM). In contrast to earlier work, this study experimentally determined the EC<sub>50</sub> and demonstrated this value to be 10-fold lower than the half-maximal cytotoxic concentration. The precise determination of EC<sub>50</sub> in this report further suggests that Gö6976 may act via inhibition of PKC $\alpha$  which is inhibited at lower concentrations than PKC $\beta$ 1 (PKC $\alpha$  IC<sub>50</sub> = 2.3 nM, PKC $\beta$ 1 IC<sub>50</sub> = 6.2 nM) (Martiny-Baron et al., 1993).

**Table 1.2: Anticryptosporidial activity of PKC inhibitors**

PKC Inhibitor	Mode of action	Inhibitory conc.	Parasite and cell type
Staurosporine	Non-specific	2.5 $\mu$ M	100% inhibition of <i>C. hominis</i> and <i>C. parvum</i> infection of HCT-8*  Reduced <i>C. hominis</i> invasion of primary IECs from 95.2% $\pm$ 0.2% to 60.0% $\pm$ 0.2%*  Reduced <i>C. parvum</i> primary IECs 97.3% $\pm$ 0.2% to 60.4% $\pm$ 0.4%*
Gö6976	Ca <sup>2+</sup> -dependent PKC $\alpha$	2.5 nM $\pm$ 1.8 nM 5.0 nM $\pm$ 2.6 nM  80 nM	EC <sub>50</sub> <i>C. parvum</i> HCT-8** EC <sub>50</sub> <i>C. hominis</i> HCT-8**  Reduced <i>C. hominis</i> infection of HCT-8 from ~55% to ~35%*  Reduced <i>C. parvum</i> infection of HCT-8 from 91.4% $\pm$ 0.5% to 59.9% $\pm$ 2.6%*  Reduced <i>C. hominis</i> infection of primary IECs from 95.2% $\pm$ 0.2% to 60.0% $\pm$ 0.2%*  Reduced <i>C. parvum</i> infection of primary IECs from 97.4% $\pm$ 0.2% to 49.6% $\pm$ 1.6%*
Chelerythrine chloride	Inhibits the catalytic domain of PKC	660 nM	Reduced <i>C. parvum</i> infection of HCT-8 cells from 91.4% to ~46%*  No effect on <i>C. hominis</i> infection of HCT-8
Calphostin C	Competes at the binding site of diacylglycerol and phorbol esters of PKC	5 $\mu$ M  0.5 $\mu$ M	Reduced <i>C. hominis</i> infection of HCT-8 from ~57% to ~38%* No effect on <i>C. parvum</i> infection of HCT-8 cells (tested at 10-fold lower conc.)*

\*Hashim et al., 2006

\*\*Love et al., 2017

### 1.9 Regulation of *PRKCA* during *Cryptosporidium* infection

*PRKCA* was identified as the most significantly down-regulated gene in a transcriptomic analysis of HCT-8 cells infected with *C. parvum* (Liu et al., 2018), providing a genetic line of evidence for the involvement of PKC $\alpha$  in *Cryptosporidium* pathogenesis. In this study, HCT-8 cells were infected with *C. parvum* and differentially expressed genes were identified by RNA-sequencing 24 hours post-infection. In addition to *PRKCA*, other differentially regulated genes in this analysis corresponded to inflammation, anti-apoptosis, and initiation and regulation of mucosal response pathways. As inhibitor studies have established a compelling link between blockade of host PKC $\alpha$  and decreased parasite invasion, this may reflect a protective response to prevent further infection. We hypothesize that down-regulation of *PRKCA* decreases parasite-induced actin rearrangements that are necessary for parasite invasion and intracellular proliferation. Notably, the study found opposing trends in overall mRNA expression during infection of two different *C. parvum* subtypes highlighting different pathogenic mechanisms between species and subspecies, however down-regulation of *PRKCA* remained consistent.

An independent study assessed the transcriptome of intestinal epithelial human organoids following infection with *C. parvum* over time (Heo et al., 2018). Several changes in the host cell transcriptome in response to infection were noted at 24 and 72 hours post-infection, supporting distinct host transcriptional responses at various stages of infection. While *PRKCA* was not among the significantly differentially expressed genes in this analysis, a

significant enrichment of upregulated genes related to 'cytoskeleton' and 'cell mobility' was identified at 24 hours post-infection, of which PKC $\alpha$  is a key regulator. A paired analysis of *C. parvum* gene expression over the course of intracellular infection found an enrichment of transcripts for parasite kinases later in infection (24 hours = 0%, 72 hours = 5%) suggesting that parasite kinases may be necessary for invasion or proliferation in the organoid model. Similarly, no significant changes in expression of *PRKCA* interacting proteins were observed. This may be a consequence of the low efficiency of *Cryptosporidium* infection in the stem cell-derived organoids compared to HCT-8 intestinal epithelial cells. In the setting of a low burden of infection, the uninfected-dominant population of cells may dilute or confound the identification of differential gene expression due to infection. To address this challenge, a study analyzed the transcriptome of uninfected and *Cryptosporidium*-infected cells individually (Yang et al., 2010). The authors sorted uninfected and *Cryptosporidium*-infected HCT-8 intestinal epithelial cells from the same monolayer to identify differentially transcribed genes as a direct consequence of infection. The authors observed 31 down-regulated genes associated with the functional category termed 'cytoskeleton'. Interestingly, protein kinase C epsilon (PKC $\epsilon$ ) was significantly downregulated in infected cells compared to uninfected controls, which has opposing effects to PKC $\alpha$  on F-actin stability in the intestinal epithelium (Song et al., 2002). Importantly, regulation of PKC $\alpha$  occurs beyond transcription but also post-translationally. Therefore, while the

expression of *PRKCA* may be constant, differences in downstream PKC $\alpha$  signaling as a result of signal transduction factors can still be observed.

### 1.10 Limitations of Pharmacologic Inhibitor Studies

Host-targeted therapies (HTTs) offer a promising new class of compounds for the treatment of infectious diseases, particularly for intracellular pathogens with limited drug targets such as *Cryptosporidium*, or high levels of antimicrobial resistance. A fundamental limitation of pharmacologic inhibitor studies is the difficulty to differentiate between the inhibition of host and *Cryptosporidium* targets. The use of irreversible inhibitors or removal of inhibitors from host cells before infection can alleviate some of this overlap. Furthermore, all of the PKC $\alpha$  pharmacologic inhibitors, including Gö6976, act on multiple targets complicating our results as to if the observed anticryptosporidial activity is due to specific inhibition of PKC $\alpha$  or an alternative host kinase. Notably, no known homologs of PKC isoforms have been reported in any *Cryptosporidium* spp. to date. Furthermore, the anticryptosporidial activity of Gö6976 supports a host-directed target as indicated by wash-out assays of the selective PKC $\alpha$  inhibitor prior to challenge with *Cryptosporidium in vitro* (Love et al., 2017).

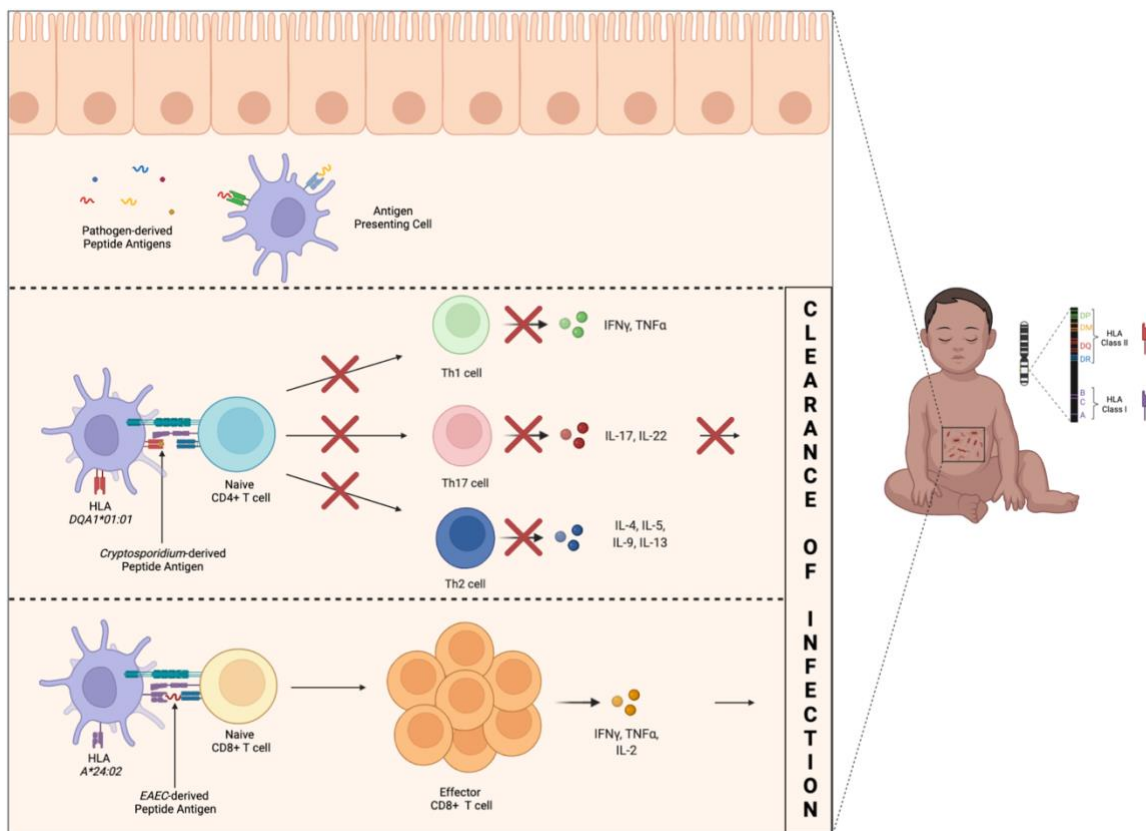
### 1.11 Human Leukocyte Antigen (HLA) and Infection

The human leukocyte antigen (HLA) complex is a vital part of the host immune system encoded by a set of genes located on chromosome 6. HLA molecules that present peptide antigens to CD8+ and CD4+ T cells are divided

into 2 primary classes: HLA class I and HLA class II, respectively. The classical HLA class I molecules are encoded by genes at the HLA-A, HLA-B, and HLA-C loci. The classical HLA Class II molecules are encoded by genes at the HLA-DR, HLA-DQ, HLA-DM, or HLA-DP loci. The ability of HLA molecules to present peptide antigens to T cells cements their significance in the adaptive immune response by initiating and maintaining T cell immunity (**Fig. 1.4**). HLA genes are some of the most polymorphic genes in humans with thousands of alleles encoding functional molecules (Little et al., 1999; Robinson et al., 2014). This high degree of polymorphism equips the host immune system to respond to a diversity of pathogen-derived peptide antigens.

Genetic association studies to identify candidate regions of the human genome contributing to specified disease outcomes are critical. Due to their role in immunity, genetic associations between HLA loci and infection have been extensively explored (Kirkpatrick et al., 2008; Elahi et al., 2011; Ribas-Silva et al., 2013). HLA alleles that are associated with natural protection from infection offer crucial information for vaccine development, particularly in cases where the pathogenic peptide antigen is unidentified. Identifying HLA molecules capable of recognizing and presenting protective pathogen-derived peptide antigens provides insight into pathogenesis. Furthermore, examining HLA-pathogen associations can aid in our understanding of the protective T cell response to combat infection. Hence, determining functional links between specific HLA alleles and susceptibility to infectious diseases merits further inquiry.

Figure 1.4



Created with BioRender.com

**Figure 1.4: HLA presentation and activation of T cells during infection.** The host adaptive immune response plays a vital role during enteric infection. This role can be protective by promoting adequate host defenses or harmful by contributing to tissue pathology. HLA loci encode cell-surface proteins important in the processing and presentation of pathogen-derived peptide antigens to naïve T cell populations. HLA class I molecules are ubiquitously expressed while HLA class II molecules are exclusively expressed on antigen-presenting cells (APCs) such as dendritic cells. During enteric infection, HLA class I and II molecules deliver pathogen-derived peptide antigens to the cell surface where they are exposed to CD8+ or CD4+ T cells, respectively. HLA class II presentation to a naïve CD4+ T cell results in expansion of T helper (Th) type 1 - Th1, Th17, and Th2 cytokine-producing cells. HLA class I presentation to a naïve CD8+ T cell results in activation and expansion of effector CD8+ T cells and related cytokines. For each instance, HLA molecule presentation leads to a specific T cell activation response to promote protection and clearance of infection. In the case of poor peptide antigen recognition or presentation by an HLA class I or II molecule (e.g., *DQA1\*01:01*), naïve T cell activation and thus cytokine release is absent resulting in the persistence of infection.

## 1.12 Conclusions

Host factors can play a critical role in pathogenesis and studying them can aid our understanding of microorganism virulence. For many pathogens, the natural host immune response contributes to the clearance of the disease. Therefore, distinguishing and manipulating host factors may serve to combat disease progression. The proposed goal of this dissertation will be to discuss the identification of host factors that influence susceptibility to enteric infection with a focus on *Cryptosporidium* infection, specifically.

The HLA complex has been implicated as a primary driver of susceptibility and severity for enteric infections. The burden of enteric infection disproportionately targets pediatric populations, particularly during the first two years of life. However, the impact of genetic variation in HLA on susceptibility to enteric infections during early childhood remains undefined. Therefore, we analyzed the relationship between HLA allele variation and 12 enteric infections in infants during the first year of life. We identified seven novel associations between HLA class I and II alleles and susceptibility to five enteric pathogens. The structure and function of these encoded HLA molecules can be further examined to identify functional epitopes that lead to a protective or detrimental immune response. These findings have implications for vaccine design and much-needed therapeutics for pediatric diarrheal disease.

Like HLA, there is strong evidence linking PKC isoforms to disease susceptibility (Hempel et al., 1997; Koivunen et al., 2004; Palaniyandi et al., 2009; Bar-Am et al., 2004; Talman et al., 2016; Hahn et al., 1999; Skvara et al.,

2008; Yang and Yan 2014). Our finding that a region of *PRKCA* genome is important in susceptibility and severity to cryptosporidiosis provided compelling evidence for further exploration of host PKC $\alpha$  as a target for the treatment of cryptosporidiosis. We found modulating PKC $\alpha$  activity *in vitro* has a significant effect on *Cryptosporidium parvum* adherence and invasion of human intestinal epithelial cells. Furthermore, *C. parvum* independently activates host PKC $\alpha$  via an undescribed mechanism. Altogether, this work denotes that host factor PKC $\alpha$  plays a critical role in early *Cryptosporidium* infection.

## **Chapter 2: HLA class I and II alleles and their role in susceptibility to enteric infection**

This chapter was adapted from: McCowin, S.E., Moreau, G.B., Haque, R., Noble, J.A., McDevitt, S.L., Donowitz, J.R., Alam, M.M., Kirkpatrick, B.D., Petri, W.A., Marie, C., 2021. HLA class I and II associations with common enteric pathogens in the first year of life. *eBioMedicine* 67.

SEM and GBM performed the statistical data analyses. SEM, WAP, CM, JD, GBM, and JAN contributed to interpretation of data. SEM, JAN, WAP, and CM wrote the manuscript. RH, MA, BDK, and WAP contributed to study design and preparation of ethical protocols. RH and MA enrolled mothers and children in the study. RH, MA, and BDK collected clinical data. JAN and SLM performed HLA genotyping and analysis at Children's Hospital Oakland Research Institute. WAP and CM directed the research.

## 2.1 Introduction

Enteric infection and diarrheal disease have an adverse impact on early childhood development in low-and middle-income countries (Petri et al., 2008). Diarrheal disease is estimated to be responsible for 10% of child mortality in children under five years old (Troeger et al., 2018). Even in the absence of mortality, negative growth impacts and poor cognitive development have also been attributed to recurrent enteric infection in infants and young children (Checkley et al., 2008; Nataro et al., 2017).

Diarrheal disease caused by enteric infection can arise from a broad range of pathogens including viruses, bacteria, and parasites. Recently, the Global Enteric Multicenter Study (GEMS) reported *Shigella* spp., rotavirus, adenovirus, heat-stable toxin enterotoxigenic *Escherichia coli* (ST-ETEC), *Cryptosporidium* spp., and *Campylobacter* spp. as the most common pathogens associated with moderate-to-severe diarrhea in infants and young children in low-resource settings (Kotloff et al., 2013; Liu et al., 2016). Several other enteric pathogens including norovirus GII, sapovirus, enteroaggregative *Escherichia coli* (EAEC), and typical enteropathogenic *Escherichia coli* (EPEC) were also significantly associated with moderate-to-severe diarrhea (Kotloff et al., 2013). In Bangladesh, the major causes of diarrhea during the first year of life were *Campylobacter jejuni/coli* (*C. jejuni/coli*), rotavirus, astrovirus, *Shigella*/enteroinvasive *Escherichia coli* (EIEC), ST-ETEC, norovirus GII, sapovirus, astrovirus, and *Cryptosporidium* (Schnee et al., 2018).

Genetic association studies are powerful tools for discovery of genetic variants associated with disease and provide insight into the prediction, prevention, and treatment of disease (Duggal et al., 2011; Wojcik et al., 2018; Wojcik et al., 2020). The human leukocyte antigen (HLA) complex is the human version of the major histocompatibility complex (MHC), a gene group that is highly associated with infection, immunity, and autoimmunity (Trowsdale et al., 2013). HLA classes I and II molecules expressed on the cell surface present pathogen-derived peptides to CD8+ and CD4+ T cells, respectively. The highly polymorphic nature of HLA genes and the corresponding specificity of their molecules for peptide ligands are fundamental for immune responses to a broad range of infections. Host HLA genotype has been associated with the balance between asymptomatic and symptomatic disease progression for a multitude of pathogens (Lekstrom-Himes et al., 1999; Blackwell et al., 2009; Lanteri et al., 2011; Matzaraki et al., 2017; Kirkpatrick et al., 2008). Altogether, variation in HLA genes has been extensively associated with differential susceptibility to both infectious and non-infectious diseases.

In this study, we investigated associations between HLA class I and II genes and 12 common enteric infections in a cohort of 601 infants from a longitudinal birth cohort study in Dhaka, Bangladesh (Schnee et al., 2018; Kirkpatrick et al., 2015). Stool specimens were collected from diarrheal episodes during the first year of life and the presence of enteric pathogens was detected using the TaqMan Array Card (TAC) system, a highly sensitive molecular

diagnostic (Jones et al., 2008). The results of the TAC pathogen detection in this cohort have been published previously (Schnee et al., 2018).

## 2.2 Materials and Methods

**Study design and population:** The PROVIDE study was a prospective clinical trial of polio and rotavirus vaccine interventions, which enrolled a birth cohort of 700 children and their mothers, from Mirpur Dhaka, Bangladesh. Study design including randomization and sample size calculations have been published previously (Kirkpatrick et al., 2015) of the 700 children enrolled in the study, 640 children were HLA genotyped. HLA genotyping was performed at the Children's Hospital Oakland Research Institute. The 640 HLA-genotyped infants were all born to Bangladeshi mothers from the northern ward of Mirpur, Dhaka living in an endemic area (Kirkpatrick et al., 2015). The racial composition of the population of Mirpur, Bangladesh is highly homogenous with 98% of the population identifying as Bengali while the remainder is comprised of an indigenous population (Jones et al., 2008). A total of 601 HLA-genotyped children who completed the first year of the study were included in these analyses. All 601 children included in this study were vaccinated against tuberculosis, diphtheria, tetanus, whooping cough, hepatitis B, haemophilus influenzae type *b*, poliovirus, measles, and rubella. Of the 601 children included in these analyses, 301 children were vaccinated against rotavirus.

**Enteric pathogen detection:** Twice weekly diarrhea surveillance occurred in the homes by trained field research assistants. Diarrhea was defined as three or more abnormally loose stools in 24 h according to the mother. To be

considered separate diarrheal episodes, a 72 h diarrhea-free period was required. Children with diarrhea were referred to the study clinic for evaluation and treatment, and a diarrheal stool specimen was collected. Stool samples were evaluated for the presence of enteric pathogens by multiplex TAC (Liu et al., 2013).

**Identification of cases and controls:** The 12 enteric pathogens with the highest incidence, based on the proportion of positive diarrheal stool samples in the PROVIDE cohort, were selected for analysis. The presence of infection for each pathogen was identified by PCR detection of nucleic acid in collected diarrheal stool samples. Primers used for the detection of pathogens have been reported previously (Liu et al., 2013). For each pathogen, cases were defined by detection of pathogen nucleic acid by TAC in diarrheal stool ( $0 < \text{CT-value} < 35$ ). Controls were defined as no detection of the pathogen nucleic acid by TAC in diarrheal stool ( $\text{CT-value} \geq 35$ ) (Liu et al., 2013). Identification of cases and controls for each pathogen was performed in R (version 4.0.2) using the tidyverse package (version 1.3.0) (R Core Team 2020; Wickham et al., 2019).

**HLA genotyping:** HLA sequence data were generated on the Roche 454 GS Junior System. Amplicons were generated from genomic DNA using fusion primers consisting of a locus-specific primer on the 3' end, a 10 bp multiplex ID (MID) tag, and either an "A" or "B" 454 specific primer sequence on the 5' end. The MID tag served as a sample barcode recognized by Conexio ASSIGN™ ATF genotyping software (version 1.1.0.35, Conexio Genomics, Freemantle, Western Australia). Amplicons were purified with AMPure beads (Becton Dickinson,

Franklin Lakes, NJ), quantified using PicoGreen (Life Technologies, Foster City, CA), diluted, and pooled into libraries. Emulsion PCR, bead enrichment, and sequencing on the GS Junior System were performed using Titanium Series kits (454 Life Sciences) (Bentley et al., 2009; Holcomb et al., 2011). Allele calls were generated from sequence data using customized versions of Conexio Genomics HLA ASSIGN™ ATF genotyping software and Sequence COmpilation and REarrangement (SCORE™) software (Graz, Austria) (Helmberg et al., 1998). All HLA genotyping results are reported at the two-field level. The HLA genotyping system used for this work is exon-based. Only the exons that encode the peptide-binding groove on the HLA molecule were sequenced. These include exons 2 and 3 for HLA class I loci and exon 2 for HLA class II loci. Therefore, alleles that are identical in the sequenced exons but differ elsewhere in the gene cannot be distinguished. For example, *DQB1\*02:01* and *DQB1\*02:02* are identical for exon 2 but differ in exon 3. In this report, all instances of these alleles are called *DQB1\*02:01*. Given that the number of HLA alleles named to date is greater than 27,000, a complete list of all potential ambiguities is not feasible. Ambiguities in common alleles that may be of note in this report include *DQB1\*03:01* vs. *DQB1\*03:19* and *DRB1\*14:01* vs. *DRB1\*14:54*.

**HLA-pathogen association tests:** Alleles at the HLA class I loci *HLA-A*, *HLA-B* and class II loci *HLA-DRB1*, *HLA-DQA1*, and *HLA-DQB1* of children were analyzed for associations with 12 common enteric pathogens during the first year of life. Association analyses of HLA genotype data and enteric infection were performed using the Bridging ImmunoGenomic Data-Analysis Workflow Gaps

(BIGDAWG) software (version 2.3; IDAWG, Oakland, CA, USA) (Pappas et al., 2016) in R (version 1.2.5033). BIGDAWG is an integrated data-analysis pipeline designed for automated association analyses of highly polymorphic genetic data (e.g., HLA genes). BIGDAWG combines rare variants (expected frequency  $<5$  in cases and controls) to a common class to account for sparse cells in tables as described (Pappas et al., 2016; Hollenbach et al., 2012). Nine novel HLA alleles were observed; however, they were binned in the analysis due to rare frequency. Extended haplotype frequencies were mathematically calculated by an EM algorithm using the BIGDAWG package in R. Association tests were performed at the allele and haplotype levels. A false-discovery rate (FDR) cut-off of 0.15 was selected to balance the number of HLA alleles deemed significant for further validation while minimizing potential type 1 error from multiple comparisons. Furthermore, when selecting the FDR cut-off, we also considered the biological plausibility of discovering a true genetic role for HLA in host susceptibility to enteric infection. Jvenn, an integrated data-analysis tool for comparing variables with Venn diagrams, was used to compare children with FDR-significant HLA alleles (Bardou et al., 2014).

**Socioeconomic status (SES) and exclusive breastfeeding:** Surveys were conducted to collect data regarding the child's environment and socioeconomic status (SES). Infants were analyzed for significant differences in several key metrics for SES deemed relevant to enteric pathogen susceptibility. These variables included source of drinking water, water treatment methods, toilet facility, number of household members, household food availability,

parental education, number of living children, number of siblings under five years of age, housing quality (floor, wall, roof), and total monthly income/expenditure. Maximum number of days of exclusive breastfeeding was determined for each child enrolled prior to analysis.

**Hardy-Weinberg equilibrium (HWE) analysis:** In these analyses, we compared 156 alleles across five HLA loci in a cohort of 601 infants during the first year of life. Testing for Hardy-Weinberg equilibrium (HWE) was performed using BIGDAWG (version 2.3) software in R (version 1.2.5033) on cases and controls. There were no deviations from HWE in this cohort study.

**Statistical analysis:** Statistical analyses were done using the GraphPad Prism software package (version 8.4.2; GraphPad Software, La Jolla, CA, USA). The chi-squared test was used for comparison of categorical variables between groups such as exclusive breastfeeding days. The Benjamini-Hochberg procedure was performed to correct for multiple comparisons across alleles with an FDR of 0.15 (15%) (Benjamini et al., 2001). For this procedure, p-values calculated in the BIGDAWG analyses were adjusted by the ratio of total alleles analyzed per locus and p-value rank order (determined by magnitude) of the designated HLA allele at that locus.

## **2.3 Results**

### **2.3.1 HLA classes I and II alleles associated with resistance or susceptibility to specific enteric pathogens**

To investigate genetic susceptibility to enteric infection, we compared the incidence of infection for the 12 enteric pathogens with highest incidence (**Table**

**2.1**) in a cohort of 601 infants during the first year of life. For analysis of HLA and susceptibility to rotavirus infection only, we performed the analysis on 300 rotavirus unvaccinated infants. A total of 156 alleles across five loci were compared (33 for *HLA-A*, 58 for *HLA-B*, 39 for *HLA-DRB1*, eight for *HLA-DQA1*, 18 for *HLA-DQB1*) at the two-field level (e.g., *A\*01:01*). We found associations ( $P$ -value  $<0.05$ ) for 27 HLA alleles (11 *HLA-A*, ten *HLA-B*, two *HLA-DRB1*, two *HLA-DQA1*, two *HLA-DQB1*) shown in **Fig. 2.1**. After correction for multiple comparisons, we identified six allele-pathogen associations that withstood an FDR cut-off of 0.15 (**Table 2.2**). The distribution of infants with FDR-significant alleles is shown in **Fig. 2.2**. The six allele-pathogen associations correspond to one viral pathogen, two bacterial pathogens, and one parasite described below.

**Table 2.1: Incidence of the 12 most common enteric pathogens in the first year of life.**

Pathogen	Controls	Cases	Incidence (%)
EAEC	145	456	76
Adenovirus 40/41	251	350	58
LT-ETEC	261	340	57
ST-ETEC	283	318	53
Typical EPEC	289	312	52
Rotavirus	329	272	45
<i>C. jejuni/coli</i>	335	266	44
Norovirus GII	337	264	44
Sapovirus	344	257	43
Astrovirus	394	207	34
EIEC & Shigella	458	143	24
<i>Cryptosporidium</i>	499	102	17

Case = infant with detection of pathogen nucleic acid by TAC in a diarrheal stool sample ( $0 < \text{CT-value} < 35$ ).

Control = infants with no detection of the pathogen nucleic acid by TAC in diarrheal stool ( $\text{CT-value} \geq 35$ ).

Incidence (%) = proportion of positive diarrheal stool samples relative to the total displayed as a percentage.

Figure 2.1

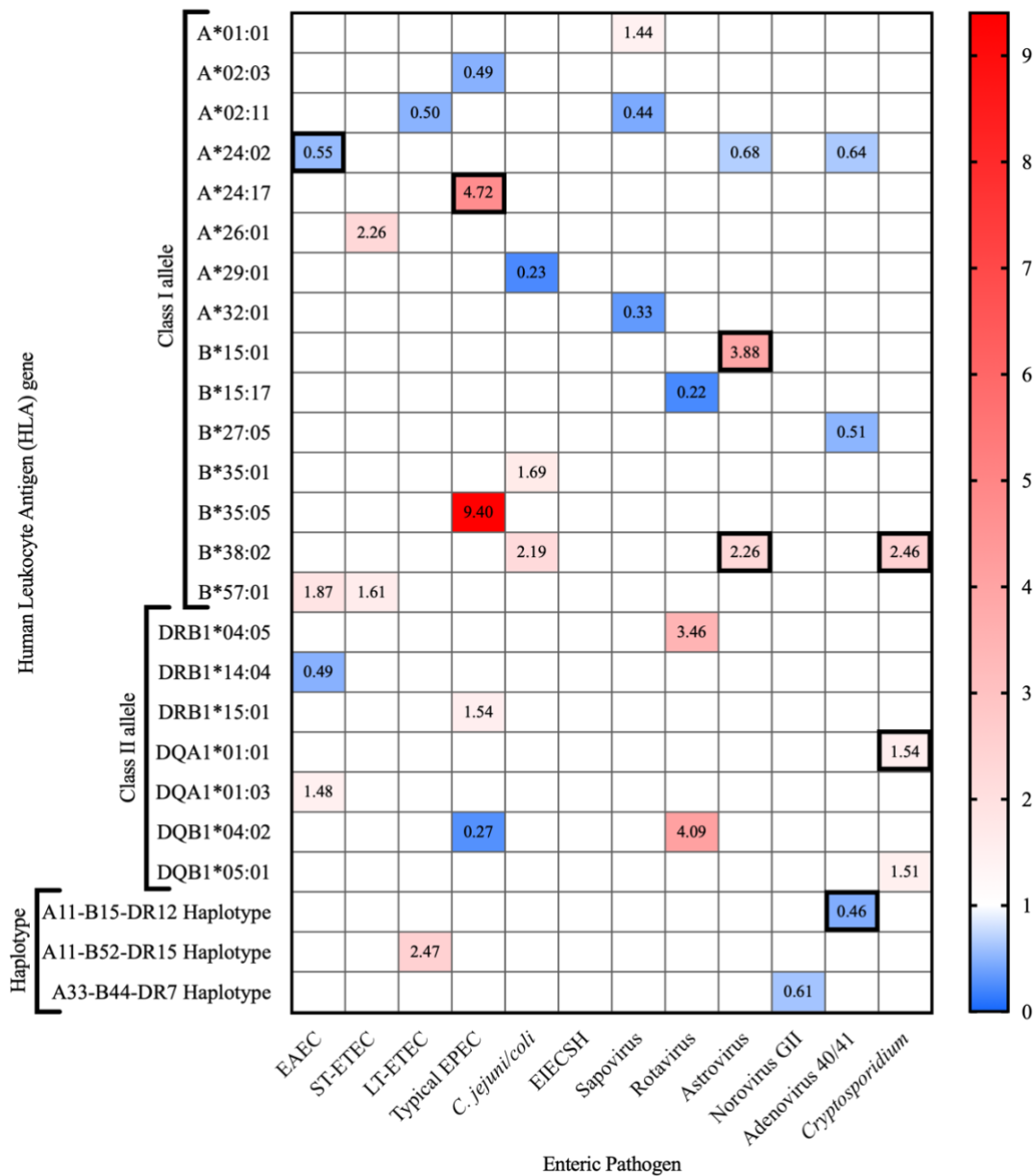


**Figure 2.1: HLA class I and II allele enteric pathogen associations.**

Associations between five HLA loci (A~B~DRB1~DQA1~DQB1) analyzed and the 12 most common enteric infections in a cohort of 601 infants during the first year of life. Pathogens are arranged by class (bacteria, virus, protozoa). Odds-ratios (OR) for HLA-pathogen associations with P-value<0.05 are shown. Red = increased susceptibility to infection, blue = decreased susceptibility to infection. Bolded boxes indicate significant HLA-pathogen associations after correction for multiple comparisons (FDR<0.15).

**Table 2.2: HLA class I/II allele-pathogen associations after correction for multiple comparisons.**

Pathogen	Allele	Controls	Cases	Frequency (controls)	Frequency (cases)	Frequency	P_Chi sq	Chis q	d f	O R	CI L9 5%	CI U9 5%	P-value	P_adj*
EAEC	A*24:02	50	94	0.17	0.10	0.14	0.11	18	12	0.55	0.38	0.82	0.0015	0.018
Typical EPEC	A*24:17	3	15	0.0052	0.024	0.15	0.19	21	16	4.7	1.3	26	0.0072	0.11
Astrovirus	B*15:01	5	10	0.0064	0.024	0.015	0.49	18	19	3.9	1.2	15	0.0082	0.078
	B*38:02	20	23	0.025	0.056	0.040	0.49	18	19	2.3	1.2	4.4	0.0074	0.14
<i>Cryptosporidium</i>	B*38:02	29	14	0.029	0.069	0.049	0.069	21	13	2.5	1.2	4.9	0.0056	0.072
	DQA1*01:01	178	51	0.18	0.25	0.21	0.23	9.3	70	1.5	1.1	2.2	0.018	0.14

\*P\_adj = Adjusted p-value for multiplicity of testing by number of comparisons for each pathogen.

Figure 2.2

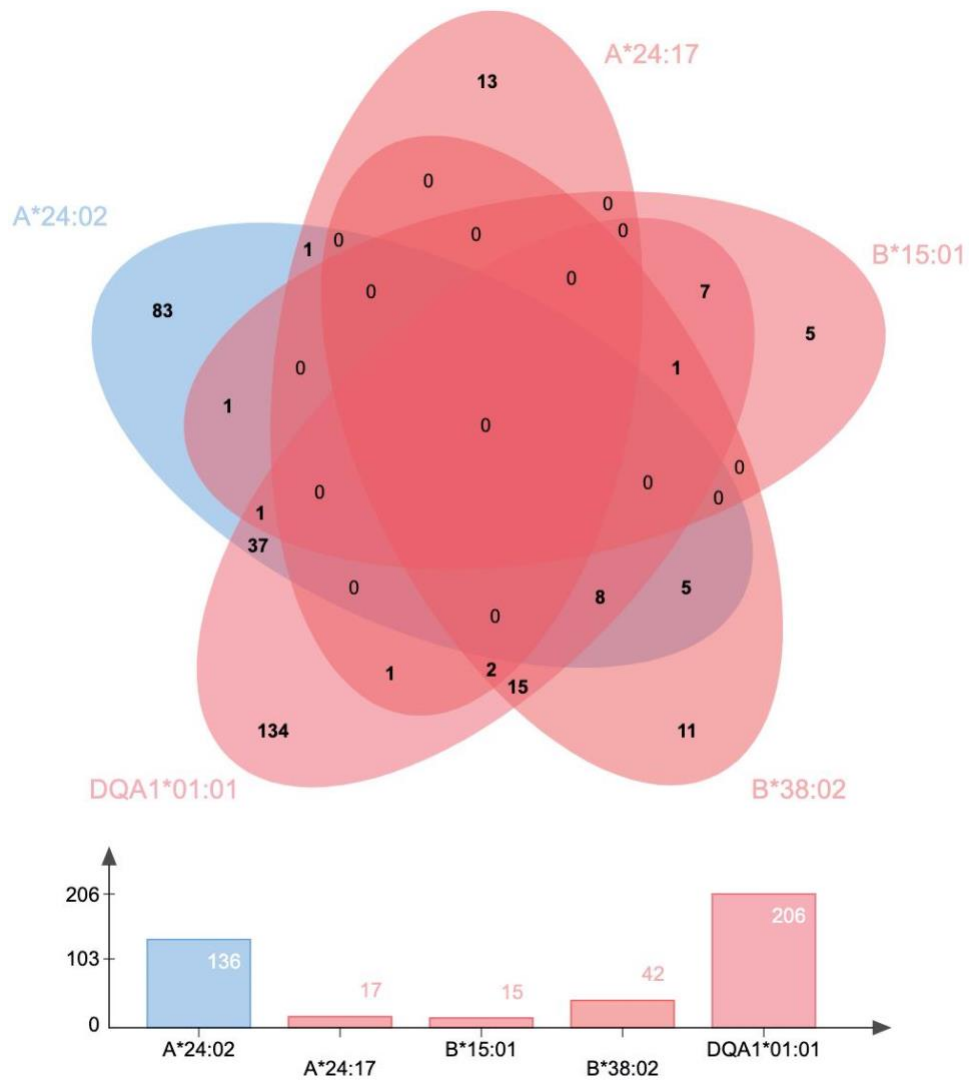


**Figure 2.2: Venn diagram overlap of infants with FDR-significant HLA class I and II alleles.** Five HLA loci (*A~B~DRB1~DQA1~DQB1*) were analyzed for associations with 12 common enteric pathogens in 601 infants during the first year of life. Allele-enteric pathogen associations were corrected for multiple comparisons at an FDR cut-off of 0.15. Numeric values for infants with at least one copy of an allele are shown. The bar graph displays the total number of infants with a corresponding FDR-significant allele. Red = increased susceptibility to infection, blue = decreased susceptibility to infection. Bolded values indicate infants sharing two or more designated significant HLA alleles.

**Cryptosporidium:** *Cryptosporidium* infection has been identified as a leading cause of moderate-to-severe diarrhea in infants, second only to rotavirus (Sow et al., 2016). Cryptosporidiosis was reported to account for 30–50% of deaths in infants and children (Khan et al., 2019). In this study, 102 of the 601 infants (17%) had at least one *Cryptosporidium*-positive diarrheal episode during the first year of life. We found two associations for *Cryptosporidium* infection. The HLA class I allele *B\*38:02* was associated with increased risk of *Cryptosporidium* infection ( $P$ -value = 0.0056 [Chi-square test], OR = 2.5, 95% CI = 1.2–4.9). The *B\*38:02* allele was also found to be associated with increased risk of astrovirus infection in this cohort. Additionally, the HLA class II allele *DQA1\*01:01* was associated with increased risk of *Cryptosporidium* infection during the first year of life ( $P$ -value= 0.018 [Chi-square test], OR = 1.5, 95% CI = 1.1–2.2).

**Astrovirus:** Astrovirus is a common cause of pediatric diarrhea and is of particular significance as chronic infections (>14 days) have been linked to infant mortality (Unicomb et al., 1998). In this study, 207 of the 601 infants (34%) had at least one astrovirus-positive diarrheal episode (Table 1). We identified two associations for astrovirus infection. The HLA class I allele *B\*15:01* was associated with increased risk of astrovirus infection ( $P$ -value= 0.0082 [Chi-square test], OR = 3.9, 95% CI = 1.2–15). This association is the second largest of the six allele-pathogen associations. The HLA class I allele *B\*38:02* was also associated with increased risk of astrovirus infection ( $P$ -value= 0.0074 [Chi-square test], OR = 2.3, 95% CI = 1.2–4.4).

**Enteroaggregative *E. coli* (EAEC):** Enteroaggregative *E. coli* (EAEC) was the most common enteric pathogen in this study with 456 of the 601 infants (76%) having at least one EAEC-positive diarrheal episode during the first year of life. Infants were also prone to repeat EAEC infection as the average infant had at least two EAEC-positive diarrheal episodes. We found that the HLA class I allele *A\*24:02* was associated with protection from EAEC infection ( $P$ -value = 0.0015 [Chi-square test], OR = 0.55, 95% CI = 0.38–0.82). The association between *HLA-A\*24:02* and EAEC is the most statistically significant  $P$ -value after correction for multiple comparisons ( $P_{\text{adj}} = 0.018$ ) for any enteric pathogen analyzed where EAEC also had the highest incidence of infection in this study.

**Typical enteropathogenic *E. coli* (EPEC):** Enteropathogenic *E. coli* (EPEC) is a common cause of bacterial gastroenteritis affecting the developing world and the leading cause of diarrhea-associated mortality in developing countries for infants under 12 months of age as reported in GEMS (Kotloff et al., 2013). Typical EPEC is differentiated as expressing the EPEC adherence factor plasmid (pEAF), a key virulence factor that mediates adherence of EPEC to host cells of the intestine (Teixeira et al., 2015). In this study, 312 of the 601 infants (52%) had at least one typical EPEC-positive diarrheal episode during the first year of life. We found a single association for typical EPEC infection: the HLA class I allele *A\*24:17* was associated with an increased risk of typical EPEC infection ( $P$ -value = 0.0072 [Chi-square test], OR = 4.7, 95%

CI =1.3–26). The *A\*24:17* allele showed the largest association for risk of infection of any of the six allele-pathogen associations identified in this study.

### 2.3.2 HLA haplotype associations with enteric pathogen infection

To explore HLA haplotype associations with the common enteric pathogens analyzed here, we compared the incidence of infection in 601 infants during the first year of life. In the cohort of 601 infants, a total of 630 unique haplotypes for five loci (*A~B~DRB1~DQA1~DQB1*) were compared in these analyses at the two-field level. We analyzed associations between eight unique haplotypes carried by >1% of the infants in cases and controls. We found associations ( $P$ -value <0.05) for three HLA five-locus haplotypes (**Fig. 2.1**). We identified one haplotype demonstrating significance after correction for multiple comparisons ( $P_{adj}$  <0.15) for adenovirus 40/41 infection.

**Adenovirus 40/41:** Adenovirus types 40/41 are well established as causes of pediatric acute gastroenteritis during the first year of life. Adenovirus 40/41 infection and pediatric gastroenteritis have been linked to socio-economic status disproportionally impacting low-income and middle-income countries (Lee et al., 2020). In this study, 350 of the 601 infants (58%) had at least one adenovirus 40/41 positive diarrheal episode during the first year of life. We identified one haplotype association for adenovirus 40/41 infection in our cohort (**Table 2.3**). The *A11-B15-DR12* haplotype (*HLA-A\*11:01~B\*15:02~DRB1\*12:02~DQA1\*06:01~DQB1\*03:01*) was associated with protection from adenovirus 40/41 infection ( $P$ -value = 0.017 [Chi-square test], OR = 0.46, 95% CI = 0.22–0.92).

***Cryptosporidium***: We found three haplotype associations for *Cryptosporidium* infection during the first year of life that were deemed insignificant (**Table 2.4**). The A01-B57-DR07 haplotype (*HLA-A\*01:01~B\*57:01~DRB1\*07:01~DQA1\*02:01~DQB1\*03:03*) was associated with protection from *Cryptosporidium* infection (*P*-value = 0.26 [Chi-square test], OR = 0.55, 95% CI = 0.14–1.6). The A11-B15-DR12 haplotype (*HLA-A\*11:01~B\*15:02~DRB1\*12:02~DQA1\*06:01~DQB1\*03:01*) was associated with protection from *Cryptosporidium* infection (*P*-value = 0.48 [Chi-square test], OR = 0.71, 95% CI = 0.21–1.9). The A33-B44-DR07 haplotype (*HLA-A\*33:013~B\*44:03~DRB1\*07:01~DQA1\*02:01~DQB1\*02:01*) was associated with an increased risk of *Cryptosporidium* infection (*P*-value = 0.64 [Chi-square test], OR = 1.2, 95% CI = 0.61–2.1). We postulate the lack of significance for these haplotype associations to be the consequence of a combination of factors. First, a total of 630 unique haplotypes were generated thereby fractioning the frequency of cases and controls (i.e., sample size) and limiting the power of the haplotype analyses. Second, the incidence of *Cryptosporidium* infection in this study was the lowest of all pathogens investigated. Lastly, due to the design of this study, only diarrhea stool samples were collected (i.e., symptomatic *Cryptosporidium* infection), yet asymptomatic *Cryptosporidium* infection is also associated with malnutrition and growth stunting (Mondal et al., 2009; Checkley et al., 1998; Moore et al., 2010). Hence, expanding our analysis to include asymptomatic *Cryptosporidium* infection may increase the significance of these associations.

**Table 2.3: HLA class I/II haplotype-pathogen associations after correction for multiple comparisons.**

Pathogen	Haplotype (A~B~DRB1~DQA1~DQB1)	Controls	Cases	Frequency (controls)	Frequency (cases)	Frequency	P_Chisq	Chi sq	d f	O R	CI L95%	CI U95%	P-value	P_adj*
Adenovirus 40/41	11:01~15:02~12:02~06:01~03:01	23	15	0.046	0.021	0.034	0.32	7.0	6	0.46	0.22	0.92	0.017	0.10

\*P\_adj = Adjusted p-value for multiplicity of testing by number of comparisons for each pathogen.

**Table 2.4: HLA class I/II haplotype associations with *Cryptosporidium* infection.**

Pathogen	Haplotype (A~B~DRB1~DQA1~DQB1)	Controls	Cases	Frequency (controls)	Frequency (cases)	Frequency	P_Chisq	Chi sq	d f	O R	CI L95%	CI U95%	P-value	P_adj*
<i>Cryptosporidium</i>	01:01~57:01~07:01~02:01~03:03	35	4	0.035	0.02	0.03	0.58	2.0	3	0.5	0.14	1.6	0.26	0.77
	11:01~15:02~12:02~06:01~03:01	34	5	0.034	0.025	0.03	0.58	2.0	3	0.7	0.21	1.9	0.48	0.72
	33:03~44:03~07:01~02:01~02:01	69	16	0.069	0.078	0.074	0.58	2.0	3	1.2	0.61	2.1	0.64	0.64

\*P\_adj = Adjusted p-value for multiplicity of testing by number of comparisons for each pathogen.

### 2.3.3 HLA classes I and II alleles associated with resistance or susceptibility to overall diarrhea

In this study, 529 of the 601 infants (88%) had at least one diarrheal stool sample positive for an enteric pathogen during the first year of life. We identified four HLA alleles associated with overall diarrhea development deemed significant ( $P$ -value  $<0.05$ ). Of the four HLA alleles, we identified one allele, *HLA-DQA1\*01:03*, demonstrating significance after correction for multiple comparisons (**Table 2.5**). Interestingly, we also identified an association between *HLA-DQA1\*01:03* and increased susceptibility to EAEC infection during the first year of life ( $P$ -value=0.044 [Chi-square test], OR = 1.5, 95% CI = 1.0–2.2). We acknowledge a limitation of this HLA-overall diarrhea analysis is the low sample size of the control group due to the high incidence of infection in this cohort, specifically with EAEC (76%). This high incidence of EAEC infection during the first year of life may be confounding our HLA associations with overall diarrheal development.

**Table 2.5: HLA class I/II associations with overall diarrhea after correction for multiple comparisons.**

Pathogen	Allele	Controls	Cases	Frequency (controls)	Frequency (cases)	Frequency	P_Chisq	Chi sq	df	OR	CI 95%	CI U95%	P-value	P_adj*
Overall Diarrhea	DQA1*01:03	14	190	0.097	0.18	0.14	0.079	13	7.0	2.0	1.1	3.9	0.014	0.11

\*P\_adj = Adjusted p-value for multiplicity of testing by number of comparisons for overall diarrhea.

### **2.3.4 Enteric pathogen susceptibility not driven by differences in exclusive breastfeeding**

Beyond socioeconomic status (SES), early childhood susceptibility to enteric infection has also been linked to the duration of exclusive breastfeeding (Lamberti et al., 2011; Morrow et al., 2004). Human breast milk protection likely arises due to diminished pathogen exposure and breast milk's anti-microbial, anti-inflammatory, and immunoregulatory components (Morrow et al., 2004). Furthermore, an early transition away from exclusive breastfeeding in the first month of life in infants was observed in the MAL-ED study (Patil et al., 2015). We analyzed infants for an association between exclusive breastfeeding and enteric infection. No significant associations between length of exclusive breastfeeding and susceptibility to enteric infection during the first year of life were observed by chi-squared analysis (data not shown). We, therefore, concluded that this metric is not responsible for observed differences in susceptibility to enteric infection.

## **2.4 Discussion**

We discovered seven novel HLA associations with five common enteric pathogens in infants. Analysis of enteric infections from birth offers insights into the development of host immunity during infancy, particularly in a region endemic to enteric infection. Prospective monitoring from birth allows for examination of SES and genetic factors on the risk of early enteric infection between infected and uninfected infants. Of note, we identified several associations with previously reported associations to other infectious diseases, as well as alleles that increased susceptibility across classes of enteric pathogens. Furthermore, to

gain insight into the relationship between HLA and pathogen burden we compared CT-values from primary infection for each HLA-pathogen association. Our analysis revealed no significant differences in mean CT-value when comparing children with a protective/susceptible HLA allele to children without [Student's *T*-test]. This does not decrease our confidence in these associations as there are numerous mechanisms by which HLA may impact susceptibility independently of pathogen burden such as varying antigen recognition or altering adaptive immune responses.

Our findings should be considered in relation to those previously published investigating HLA pathogen associations. In a study investigating COVID-19 positive patients genotyped for HLA loci, *HLA-B\*15:27* was found to be associated with the occurrence of COVID-19 infection (*P*-value = 0.001 [Fisher's exact test], OR = 3.59, 95% CI = 1.7–7.5) (Wang et al., 2020). The strength of this increased susceptibility association between *HLA-B\*15:27* and COVID-19 infection is similar to the associations we have identified in our study. This observed increase in susceptibility to COVID-19 suggests the *HLA-B\*15:27* molecule has reduced recognition of an immunodominant COVID-19 viral antigen when compared to controls. A separate study discovered an association between *HLA-DRB1\*11:01* (*P*-value <0.00001 [Chi-square test], OR = 2.0, 95% CI = 1.6–2.6) and *HLA-DQB1\*03:01* (*P*-value <0.00001 [Chi-square test], OR = 2.4, 95% CI = 1.6–3.4) and viral clearance (Hong et al., 2005). Again, this HLA-pathogen analysis yielded associations that parallel the strength of those we identified. For this study, however, we do acknowledge that these

HLA associations have higher significance than those we discovered which we postulate stems from their combining of multiple studies. An HLA association analysis with human immunodeficiency virus type 1 (HIV-1) susceptibility identified *HLA-DRB1\*01:01* to be protective ( $P$ -value = 0.0003 [log rank test], incidence response ratio (IRR)= 0.22, 95% CI = 0.06-0.60) supporting the well-established role of class II CD4 effector cells in response to HIV-1 infection (MacDonald et al., 2000). The strength of this association matches several of our identified protective associations. In a congenital study examining 122 fetuses for toxoplasmosis where HLA class II molecules play a crucial role in immunity, *HLA-DQA1\*01:03* ( $P$ -value = 0.0002 [Chi-square test], OR = 3.1) and *HLA-DQA1\*03:02* ( $P$ -value = 0.0001 [Chi-square test], OR = 9.6) were found to be associated with increased susceptibility to congenital toxoplasmosis (Shimokawa et al., 2016). The magnitude of the *HLA-DQA1\*03:02* association is similar to our *HLA-B\*35:05* association with typical EPEC but is far stronger than any other HLA association identified. These HLA-pathogen analyses parallel the findings from our study in both the strength of association and methodology.

While all allele-pathogen associations identified in this study are novel, some of the HLA alleles we identified have been implicated in susceptibility to other infections. *HLA-B\*15:01* has previously been linked to an increased incidence of hepatitis C virus (HCV) infection (Xiong et al., 2015), where we identified an increased risk association between this allele and astrovirus infection. *HLA-B\*38:02* has been associated with a reduced risk of disease severity for both dengue hemorrhagic fever and dengue shock syndrome

(Mercado et al., 2015; Appanna et al., 2010), however, in this study, we identified an association for increased risk of both astrovirus and *Cryptosporidium* infection. The association between *HLA-B\*27* and arthritis is one of the strongest known relationships between HLA loci and a disease. Here, we identified a relationship between *HLA-B\*27:05* and protection from adenovirus 40/41 infection during the first year of life. In a study from the UK, where the frequency of *HLA-B\*27* is roughly 8%, it was found to be associated with 60–90% of patients with reactive arthritis (Sheehan et al., 2004). In our study, 43 of 601 (7.2%) infants harbored an *HLA-B\*27* allele. Given the high incidence of infection, particularly with causative agents of reactive arthritis such as *Shigella* and *C. jejuni/coli* (Ajene et al., 2013), paired with the frequency of *HLA-B\*27* it is plausible these infants may experience an increased risk for reactive arthritis later in life.

The majority of the associations identified were with HLA class I alleles. We found HLA allele *A\*24:02* was protective for risk of EAEC infection. This is not surprising as some EAEC strains have been shown to invade and replicate within intestinal epithelial cells *in vitro*. Therefore, it is plausible intracellular antigens from EAEC can be processed and presented via class I. A class I allele associated with protection from infection is likely acting via presentation of a peptide to the receptor of a CD8+ T cell generating a protective cell-mediated immune response. This difference in peptide presentation which confers increased protection from infection may be a consequence of enhanced binding

affinity for the peptide resulting in CD8+ T cell activation (Tian et al., 2007; Chervin et al., 2009).

We also identified class I associations that increased risk of infection: *A\*24:17* for typical EPEC, *B\*15:01* and *B\*38:02* for astrovirus, and *B\*38:02* for *Cryptosporidium*. Viral replication requires host cell machinery supporting a role for class I allele presentation. While typical EPEC has been characterized as an extracellular pathogen, intracellular EPEC has been described previously in human infection highlighting a potential class I association (Bulgin et al., 2009). Additionally, as *Cryptosporidium* is known to invade intestinal epithelial cells and exist in an intracellular extra-cytoplasmic niche, observation of both classes I and II associations is not surprising (Tzipori et al., 1998). This increased risk of infection association we observe in this study for these class I alleles may be due to a poorer presentation of peptides derived from these pathogens.

HLA class II allele *DQA1\*01:01* increased risk of *Cryptosporidium* infection. Presentation of bacterial antigens by HLA class II molecules following macroautophagy and lysosomal degradation is critical for the CD4+ T cell enhanced antibody response to that pathogen (Schmid et al., 2007; Lünemann et al., 2009). We hypothesize that the association between the *DQA1\*01:01* molecule and *Cryptosporidium* infection could be due to an inability to present *Cryptosporidium*-derived antigens.

These results should also be considered in light of some potential limitations. First, to detect enteric infection, we collected diarrheal stool samples from infants, which may underestimate cases as sub-clinical infection is common

(Platts-Mills et al., 2015). In our analysis, any infection in an infant that did not result in a corresponding diarrheal episode would have gone undetected. Second, detection of multiple enteric pathogens during an episode of diarrhea is common in this population (Taniuchi et al., 2013). In these instances, the presence of an enteric pathogen was considered an infection. Third, though we attempt to correct for multiple comparisons by using the Benjamini-Hochberg procedure, the magnitude of comparisons performed in this analysis may limit findings. Validation of the allele-pathogen associations identified in this study in additional studies could provide valuable insight. Lastly, pathogens with multiple strains were defined based on known shared biological processes and pathogenesis (EAEC, ST-EPEC, typical EPEC, rotavirus, *Cryptosporidium*).

In this analysis, *HLA-A\*24:02* was associated with protection from EAEC infection during the first year of life. It is notable that we previously identified a protective association between *HLA-A\*24:02* and *Cryptosporidium* infection in Bangladeshi children ages 2–5 (Kirkpatrick et al., 2008). The identification of multiple enteric pathogen associations for *HLA-A\*24:02* suggests the peptide binding region for the *A\*24:02* molecule has a wide repertoire capable of recognizing and presenting peptide ligands derived from EAEC and *Cryptosporidium*. Moreover, we previously identified associations between alleles *HLA-B\*15*, *HLA-DQB1\*03:01*, and haplotype *HLA-DRB1\*11:01/HLA-DQB1\*03:01* with increased incidence of asymptomatic and symptomatic *Cryptosporidium* infection (Kirkpatrick et al., 2008). In this current study *HLA-B\*38:02* and *HLA-DQA1\*01:01* were associated with increased risk of

*Cryptosporidium* infection. These discrepancies in HLA associations identified and *Cryptosporidium* may be explained by the differences in age of the children as specific alleles could influence the duration of immune response into early childhood. Furthermore, the present study used the TAC assay for molecular diagnostics which is reported to have an average sensitivity and specificity of 85 and 77% when compared to conventional tests such as the ELISA used by the previous study (Liu et al., 2013). In the current study, 102 children (17%) had a *Cryptosporidium*-positive diarrheal episode compared to the previous cohort of 58 children (26%). Finally, the previous study examined the association between HLA and *Cryptosporidium* infection, including both symptomatic and asymptomatic infection, while this study focuses on the relationship between HLA and symptomatic *Cryptosporidium* infection (i.e., diarrhea).

A major strength of this study was the ability to compare HLA genotypes and susceptibility to multiple enteric pathogens during the first year of life, thus permitting the investigation of early immune responses in an immunologically naïve population from an area that has a high incidence of pediatric enteric infection. Second, the children in this study were closely monitored for episodes of diarrhea to collect all relevant samples for pathogen detection. Third, pathogen detection was determined using molecular diagnostics (TAC), allowing for higher sensitivity and quantitative detection of each enteric pathogen when compared to conventional methods (Liu et al., 2013). Lastly, this study was performed in a single ethnic population which may have made HLA signals more apparent due to the homogeneity of this group.

In summary, our study has successfully identified novel HLA associations with susceptibility to common enteric pathogens in Bangladeshi infants and highlights the impact of host genetics on pathogen susceptibility. Future studies investigating the functional role of HLA-mediated antigen presentation in this setting may be crucial for defining the process by which we develop mucosal immunity to enteric infection and has implications for oral vaccine development.

### **Chapter 3: PKC $\alpha$ and its Role in Early *Cryptosporidium* Infection of Intestinal Epithelial Cells**

This chapter was adapted from: McCowin S, Petri WA Jr, Marie C. Protein Kinase C- $\alpha$  Is a Gatekeeper of *Cryptosporidium* Sporozoite Adherence and Invasion. *Infect Immun*. 2022 Mar 17;90(3):e0067921. doi: 10.1128/iai.00679-21.

Epub 2022 Jan 18. PMID: 35099276; PMCID: PMC8929341.

S.M., C.M., and W.A.P. conceived and designed the experiments. S.M. performed the experiments and analyzed the data. S.M. drafted the manuscript with input from all authors. S.M., C.M., and W.A.P. purchased the reagents and materials.

### 3.1 Introduction

*Cryptosporidium spp.* are a family of obligate intracellular parasites with increasing importance in global health. Though there are over 20 species relevant to humans, *C. parvum*, *C. hominis*, and *C. meleagridis* are responsible for the vast majority of infections (Leitch and He 2011; Ryan et al., 2014; Steiner et al., 2018). *Cryptosporidium* infection causes diarrhea that can be life-threatening and in immunocompromised individuals (e.g., HIV/AIDS) this diarrhea can be prolonged. The burden of infection is most severe in low- and middle-income countries, with cryptosporidiosis classified as the second leading cause of diarrhea-associated mortality in young children (Kotloff et al., 2013; Sow et al., 2016). In addition to morbidity and mortality, pediatric cryptosporidiosis is associated with malnutrition and long-term developmental deficits (Mondal et al., 2009; Checkley et al., 1998; Guerrant et al., 1999). At present, no vaccine is available for cryptosporidiosis and the only approved drug, nitazoxanide, has poor efficacy in immunocompromised patients and malnourished children (Sears et al., 2007; Khalil et al., 2018).

During human infection, *Cryptosporidium* oocysts excyst in the upper small intestine, presenting four sporozoites with gliding motility that interact with the mucosal epithelium (Forney et al., 1998; Wetzel et al., 2005). These motile sporozoites attach to the host epithelium through interactions with host cell surface ligands (Joe et al., 1994) and sporozoite surface lectin (Nesterenko et al., 1999; Bhat et al., 2007). Upon interaction, glycoproteins on the surface of the host cell membrane initiate a signaling cascade aggregating F-actin to the site of

sporozoite contact and form a host membrane protrusion resulting in the encapsulation of the sporozoite (Forney et al., 1999; Elliott et al., 2000; Guérin et al., 2021). Henceforth, *Cryptosporidium* exists in an intracellular yet extra-cytoplasmic vacuole formed by and partitioned off from the host cell by F-actin (O'Hara et al., 2011). The formation of this F-actin pedestal at the site of infection has been directly linked to the actin-associated signaling pathways of the neural Wiskott-Aldrich syndrome protein (N-WASP) and the Arp 2/3 complex (Elliott et al., 2001). The membrane protrusions encapsulating *Cryptosporidium* during invasion are additionally dependent on localized volume increases mediated by glucose and water influxes (Chen et al., 2005; Delling et al., 2019). Recruitment of Na<sup>+</sup>/glucose cotransporter (SGLT1) and aquaporin 1 (AQP1) to the site of infection contributes to this actin-dependent cellular invasion. Analysis of the *C. parvum* transcriptome during development has identified the expression of stage-specific genes over the course of infection (Yang et al., 2010; Mauzy et al., 2012; Tandel et al., 2019). Paired with microscopy imaging, a timeline for *Cryptosporidium* development and propagation *in vitro* has been well-characterized. This entire life cycle has been modeled *in vitro* primarily using immortalized cell lines (Upton et al., 1994). However, the complete host cell repertoire that is usurped by *Cryptosporidium spp.* to achieve this has not yet been described.

Many studies have identified factors involved in *Cryptosporidium* infection on both sides of the parasite-host interface (Guérin et al., 2021; Hashim et al., 2006; Castellanos-Gonzalez et al., 2016). Recently, we found variation within the

*PRKCA* gene was associated with increased susceptibility to cryptosporidiosis in children (Wojcik et al., 2020). Here, we asked the question, is human PKC $\alpha$  mechanistically involved in *Cryptosporidium* infection *in vitro*. In a recent study, a high-throughput phenotypic screen identified a selective protein kinase C- $\alpha/\beta$ 1 (PKC $\alpha/\beta$ 1) inhibitor, Gö6976, to have potent anticryptosporidial activity *in vitro* (Love et al., 2017). Gö6976 reduced infection of HCT-8 cells with both *C. parvum* and *C. hominis* at nanomolar doses with an EC<sub>50</sub> (half-maximal effective concentration) for inhibition of *C. parvum* infection coinciding with the reported Gö6976 IC<sub>50</sub> for PKC $\alpha$  (Martiny-Baron et al., 1993). Furthermore, HCT-8 cell *PRKCA* mRNA expression is significantly decreased after *C. parvum* infection when compared to controls (Liu et al., 2018). From this evidence, we focused on exploring human intestinal epithelial cell PKC $\alpha$  further during *Cryptosporidium* infection.

In this study, we investigated the role of human intestinal epithelial cell PKC $\alpha$  during *C. parvum* infection *in vitro*. PKC $\alpha$  has been implicated in regulation of host actin cytoskeletal remodeling, a requirement of parasite invasion, therefore we targeted PKC $\alpha$  activity during this event. We found that PKC $\alpha$  mediated the earliest stages of *C. parvum* infection, sporozoite adherence and invasion, into human intestinal epithelial cells. Additionally, host PKC $\alpha$  was activated during sporozoite invasion. Our work exposes PKC $\alpha$  as a potential anticryptosporidial host target through inhibition of *C. parvum* adherence and invasion. Collectively, this work advances the understanding of *Cryptosporidium* pathogenesis and links a host protein to early infection.

## 3.2 Materials and Methods

**HCT-8 intestinal epithelial cell culture:** Human ileocecal adenocarcinoma (HCT-8; ATCC CCL 244) cells were purchased from the American Type Culture Collection. Cells were maintained in T-75 (75-cm<sup>2</sup>) tissue culture flasks as adherent monolayers in growth medium: RPMI 1640 medium (Catalog #:11875093) supplemented with L-glutamine, 10% heat-inactivated fetal bovine serum (FBS). Cells were stored in a 37°C humidified incubator in 5% CO<sub>2</sub> until confluency. One day prior to infection, cells were washed once with 1x PBS, collected at 37°C with 0.25% Trypsin-EDTA and resuspended in growth medium. Cells were then plated (500 µL/well) into 24-well assay plates at a density of 1.14x10<sup>5</sup> cells/well. Cells were allowed to grow for 24 h at 37°C with 5% CO<sub>2</sub> in a humidified incubator.

***Cryptosporidium parvum* oocysts:** Oocysts of *Cryptosporidium parvum* (Iowa strain) were purchased from Waterborne Inc. and stored at 4°C for ≤ 3 months in PBS with antibiotics (penicillin, streptomycin, Amphotericin B, gentamicin, and 0.01% Tween20).

**Pharmacologic compounds:** Four compounds were used to modulate PKCα activity prior to *Cryptosporidium parvum* infection *in vitro*. All compounds were commercially sourced from reputable vendors and supplied as high-purity (≥95%) solids. Gö6976 and PMA were purchased from Abcam. Calphostin C was purchased from Calbiochem. Bryostatin 1 was purchased from Sigma Aldrich. Compounds were pre-diluted in dimethyl sulfoxide (DMSO) at 1 mg/mL. All

experiments using pharmacologic compounds were performed in biological triplicate.

***C. parvum* infection of HCT-8 cells:** Oocysts were excysted 24 h after seeding of HCT-8 cells, as described previously (Pawlowic et al., 2017). Briefly, the oocysts were centrifuged at 16,000×g for 3 min in a microcentrifuge at 4°C. Oocysts were then incubated in a 1:4 bleach solution on ice for 5 min and then centrifuged at 16,000×g for 3 min at 4°C. The supernatant was gently aspirated, and the oocysts were resuspended in 1 mL of 1xPBS then centrifuged for a total of three washes at 4°C. After the final wash, the supernatant was gently removed and the oocysts resuspended in 0.5 mL of 0.75% sodium taurocholate and incubated at 15°C for 10 min. After incubation in bile salts, the oocysts were stored in a 37°C heat block and incubated for 1 h. For heat-killed *C. parvum*, sporozoites from excysted oocysts were then incubated at 75°C for 60 seconds (Moriarty et al., 2005). After incubation, the oocysts were centrifuged at 3,000×g for 1 min and resuspended in 0.5 mL of assay medium: RPMI 1640 medium (-) phenol red (Catalog #:11835030), supplemented with 2% heat-inactivated FBS. Oocysts were then enumerated using a disposable hemocytometer to determine the percentage of sporozoite excystation. The growth medium was gently removed from the 24-well assay plate of seeded HCT-8 cells and replaced with 0.5 mL of assay medium. Sporozoites from excysted oocysts were added to each well ( $5.7 \times 10^5$  sporozoites/well) of the 24-well assay plate. Plates were then spun at 150×g for 3 min in a benchtop

centrifuge at room temperature. Infected cells were incubated at 37°C with 5% CO<sub>2</sub> in a humidified incubator for 2 h.

**Stoplight immunofluorescence assay for *C. parvum* adherence and invasion:** Post-infection, assay medium containing infectious parasites was aspirated and cells were washed with pre-warmed assay medium to remove unbound parasites. Cells were then fixed with 4% paraformaldehyde for 15 min at room temperature followed by 3 washes with 1xPBS for 3 min at room temperature. To prevent non-specific binding, the cells were blocked with Dilution/Blocking (DB) buffer (Waterborne, Inc.) for 30 min at room temperature. Cells were stained with TRITC-conjugated Sporo-Glo (Waterborne, Inc.) diluted 1:20 in DB buffer for 1 h at room temperature protected from light. Cells were washed three times with 1xPBS supplemented with 0.01% Tween 20 (1xPBST) for 3 min. After washing, each well was permeabilized with 0.1% Triton X-100 diluted in 1xPBS for 15 min at room temperature, and then washed 3 times with 1xPBST. Cells were then stained with FITC-conjugated Sporo-Glo (Waterborne, Inc.) diluted 1:20 in DB buffer for 1 h at room temperature protected from light. Cells were washed three times with 1xPBST for 3 min. To visualize HCT-8 cell nuclei, cells were stained with 4',6-diamidino-2-phenylindole (DAPI) diluted 1:1000 in 1xPBS for 10 min at room temperature protected from light. Lastly, cells were washed 3 times with 1xPBST. The cells were imaged with a ZEISS LSM 700 confocal microscope (Carl Zeiss, Inc.) using a 20x objective. Three channels were used: 405 nm for DAPI-stained nuclei, 488 nm for FITC-

labeled *Cryptosporidium* parasites, and 543 nm for TRITC-labeled *Cryptosporidium* parasites.

For each assay (pharmacologic inhibition/activation, dose-response, and time-course) 2 fields were captured for each well in biological triplicate. The ZEN 2.1 Black Edition software was used to obtain z-stacks through the entire height of the cells with confocal z-slices of 1.0  $\mu\text{m}$  (z-stack=26  $\mu\text{m}$ ). HCT-8 cytotoxicity (number of nuclei relative to DMSO-treated controls) and contrasts in *Cryptosporidium* sporozoite adherence and invasion (cell counts relative to DMSO-treated controls) were determined. Images were processed using Fiji is Just ImageJ (FIJI) software (Version 2.0.0-rc-41/1.50d). HCT-8 cells nuclei were counted using the analyze particles command selecting for units 50-1000  $\mu\text{m}^2$  in size. TRITC-labeled *Cryptosporidium* parasites and FITC-labeled *Cryptosporidium* parasites were counted using the analyze particles command selecting for units 2-20  $\mu\text{m}^2$  in size.

**Immunofluorescent assay for PKC $\alpha$  localization:** Assay medium containing infectious parasites was aspirated and cells were washed with pre-warmed assay medium to remove unbound parasites. Cells were then fixed with 4% paraformaldehyde for 15 min at room temperature. Each well was then washed three times with 1xPBS for 3 min at room temperature. After washing, each well was permeabilized with 0.1% Triton X-100 diluted in 1xPBS for 15 min at room temperature, and then washed three times with 1xPBS. To prevent non-specific binding, the cells were blocked with DB buffer for 30 min at room temperature. *C. parvum* parasites were then stained with FITC-conjugated

Sporo-Glo diluted 1:20 in DB buffer for 1 h at room temperature protected from light. Cells were washed three times with 1xPBST for 3 min. HCT-8 cell PKC $\alpha$  were stained with an anti-PKC $\alpha$  antibody (Abcam, ab32376) used at a dilution of 1:200 in 1xPBS supplemented with 1% bovine serum albumin (BSA) for 1 h at room temperature. A secondary goat anti-rabbit Cy3 antibody (Abcam, ab6939) was used at a dilution of 1:1000 in 1xPBS supplemented with 1% BSA for 1 h at room temperature protected from light. Cells were washed three times with 1xPBST for 3 min. HCT-8 cell nuclei were stained with DAPI diluted 1:1000 in 1xPBS for 10 min at room temperature protected from light. Lastly, cells were washed three times with 1xPBST and covered. The 24-well plates were imaged on a ZEISS LSM 700 confocal microscope (Carl Zeiss, Inc.) at 63x objective with immersion oil. Three channels were used: 405 nm for DAPI-stained nuclei, 488 nm for FITC-labeled *Cryptosporidium* parasites, and 543 nm for Cy3-labeled PKC $\alpha$ . For each well 2 fields were captured. The ZEN 2.1 Black Edition software was used to obtain z-stacks through the entire height of the cells with confocal z-slices of 1.0  $\mu\text{m}$  (z-stack=16  $\mu\text{m}$ ). HCT-8 cytotoxicity (number of nuclei relative to DMSO-treated controls) was determined. Images were processed using FIJI software.

**Cell fractionation and immunoblot analysis:** After completion of infection, cells were washed with pre-warmed assay medium to remove unbound parasites. Each well containing *Cryptosporidium*-infected cells was treated with 0.25% Trypsin-EDTA for 10 min at 37°C and collected in Eppendorf tubes. A small aliquot of cells was removed for enumeration and the remaining cells were

pelleted at 300×g for 10 min. After centrifugation, cell fractionation was performed by using a commercially available cell fractionation kit (Abcam, ab109719) according to the manufacturer's instructions. Briefly, cells were resuspended in 0.1 mL of 1x Buffer A (Abcam) supplemented with a 1x Halt protease and phosphatase inhibitor cocktail (ThermoFisher). Cells were permeabilized with Detergent I (Abcam) then pelleted at 5,000×g for 2 min and repeated at 10,000×g for 2 min at 4°C. The resultant supernatant was collected as the cytoplasmic fraction. The cytoplasm-depleted pellet was resuspended in 0.1 mL of 1X Buffer A. Protein concentration in each fraction was quantified using a Qubit fluorometer (ThermoFisher). Samples were prepared 1:1 with 2x Laemmli sample buffer (Bio-Rad) and boiled for 5 min at 100°C. Samples were run on an Any kD Mini-PROTEAN TGX polyacrylamide gel (Bio-Rad), transferred to a nitrocellulose membrane, and blocked with Intercept (PBS) blocking buffer (LI-COR biosciences). Anti-PKC $\alpha$  antibody was used at a dilution of 1:1000. A secondary donkey anti-rabbit IR dye 680 (LI-COR biosciences) was used at a dilution of 1:10,000. Anti-GAPDH antibody (Cell Signaling Technology #97166) was used at a dilution of 1:1000. A secondary goat anti-mouse IR dye 800 (LI-COR) was used at a dilution of 1:10,000. Blots were imaged with a LI-COR biosciences Odyssey imaging system. Images were analyzed using the analysis feature in ImageStudioLite software (Version 5.2.5, LI-COR biosciences). Band intensity for PKC $\alpha$  for each experimental condition was measured using the analysis feature in ImageStudioLite software (Version 5.2.5, LI-COR biosciences). PKC $\alpha$  activation (percent of PKC $\alpha$  in membrane fraction relative to

cytoplasmic fraction) was calculated for each condition relative to DMSO-treated vehicle controls.

**HCT-8 cell cytotoxicity:** HCT-8 cells were assessed for cytotoxicity of pharmacologic compounds using two methods, propidium iodide (PI) staining and HCT-8 cell nuclei count relative to DMSO-treated controls. In each case, cells were seeded (500  $\mu$ L/well) into 24-well assay plates at a density of  $1.14 \times 10^5$  cells/well. Cells were exposed to each experimentally-matched concentration of pharmacologic compounds resuspended in assay medium. Cells were incubated at 37°C with 5% CO<sub>2</sub> in a humidified incubator for 2 h. After incubation, cells were exposed to a PI/RNase A solution (Phoenix Flow Systems, Inc.). After a 30 min incubation at room temperature, the live cells were imaged on a ZEISS LSM 700 confocal microscope at 20x objective. The number of PI-labeled cells for exposure to each compound was calculated relative to a maximum cytotoxicity control. For further confirmation, the total number of nuclei per field for compound-exposed cells relative to DMSO-treated controls was measured.

**Data and Statistical Analysis:** Prism 9 (GraphPad Software, La Jolla CA) was used for generation of graphs and statistical analysis. Image quantification was evaluated for significance using the unpaired Student's t or one-way ANOVA and Tukey's post hoc test to determine statistical differences between means of groups of data from all tissue culture experiments. All data show the results from 1 of 2 independent experiments (n) in biological triplicate.

### 3.3 Results

#### 3.3.1. *C. parvum* activates host PKC $\alpha$ during invasion

We investigated PKC $\alpha$  localization as a measure of activation during *C. parvum* invasion of HCT-8 cells. After binding the requisite cofactors for activation (phosphatidylserine, calcium, and diacylglycerol), activated PKC $\alpha$  translocates from the host cytoplasm to the membrane (Black and Black 2013). We used a traditional *in vitro* fluorescence-based microscopy assay to simultaneously visualize *C. parvum* and intestinal epithelial cell PKC $\alpha$ . As a positive control for activation of PKC $\alpha$ , we treated HCT-8 cells with phorbol-12-myristate 13-acetate (PMA). PMA is a well-established activator and induces the translocation of PKC to the cell membrane where it is tightly bound and highly active (Pontremoli et al., 1986; Strulovici et al., 1989; Abdullah et al., 1997). As predicted, exposure to 200 nM PMA for 1 h caused ubiquitous PKC $\alpha$  colocalization with the host membrane (**Fig. 3.1A**). Contrarily, we observed a decrease in membrane-associated PKC $\alpha$  when HCT-8 cells were treated with the PKC $\alpha$  inhibitor Gö6976 (2.5 nM) for 1 h (**Fig. 3.1A**). When HCT-8 cells were infected with *C. parvum* sporozoites at a multiplicity of infection (MOI) of 4:1 (sporozoite: cell) for 2 h, we observed an increase in membrane-associated PKC $\alpha$  (**Fig. 3.1A**). Notably, the increase in *C. parvum*-induced membrane-associated PKC $\alpha$  is not limited to the *Cryptosporidium*-infected HCT-8 cell but can result in adjacent uninfected HCT-8 cell PKC $\alpha$  activation suggesting a cell-to-cell signaling event during invasion.

To confirm *C. parvum* activation of intestinal epithelial cell PKC $\alpha$ , we examined this interaction using quantitative immunoblot. We performed cellular fractionation of HCT-8 cells after treatment with 2.5 nM Gö6976, 200 nM PMA, or

*C. parvum* at an MOI of 4:1. We generated cytoplasmic and membranous fractions and probed all fractions for glyceraldehyde 3-phosphate dehydrogenase (GAPDH) and PKC $\alpha$ . GAPDH localizes to the host cell cytoplasm, is constitutively expressed, is stable in HCT-8 cells, and was used to denote the cytoplasmic fraction. We confirmed that pharmacologic inhibition with Gö6976 decreased membrane-associated PKC $\alpha$  while treatment with PMA resulted in increased membrane-associated PKC $\alpha$  (**Fig. 3.1B**). After infection with *C. parvum*, we observed increased membrane-associated PKC $\alpha$  (**Fig. 3.1B**). The percentage of PKC $\alpha$  in the membranous fraction after infection with *C. parvum* is significantly elevated ( $39.29\% \pm 1.235$ ,  $P < 0.0001$ ) relative to vehicle controls (**Fig. 3.1C**). Next, we asked if the activation of PKC $\alpha$  during *C. parvum* invasion correlated with the rate of HCT-8 cell infection. To address this, we tested if heat-killed *C. parvum* sporozoites were capable of activating PKC $\alpha$  (**Fig. 3.1D**). Heat-killed *C. parvum* sporozoites did not induce a significant difference in membrane-associated PKC $\alpha$  relative to vehicle controls (**Fig. 3.1E**). This phenotype remained true when increasing the MOI for heat-killed *C. parvum* to 20:1 (**Fig. 3.1E**). Furthermore, we increased the MOI of live *C. parvum* to 20:1 then compared PKC $\alpha$  in the membranous fraction (**Fig. 3.1D**) and found elevating the MOI resulted in a significant increase in membrane-associated PKC $\alpha$  ( $19.20\% \pm 1.902$ ,  $P = 0.0005$ ) supporting activation of PKC $\alpha$  by *C. parvum* sporozoite invasion (**Fig. 3.1E**). Moreover, when comparing membrane-associated PKC $\alpha$  for live *C. parvum* at an MOI of 4:1 to an MOI of 20:1 we observed an additional significant increase ( $4.522\% \pm 0.7185$ ,  $P = 0.0033$ ) (**Fig. 3.1E**). Altogether, these

findings show host intestinal epithelial cell PKC $\alpha$  is activated during *C. parvum* invasion *in vitro* in two distinct assays.

Figure 3.1

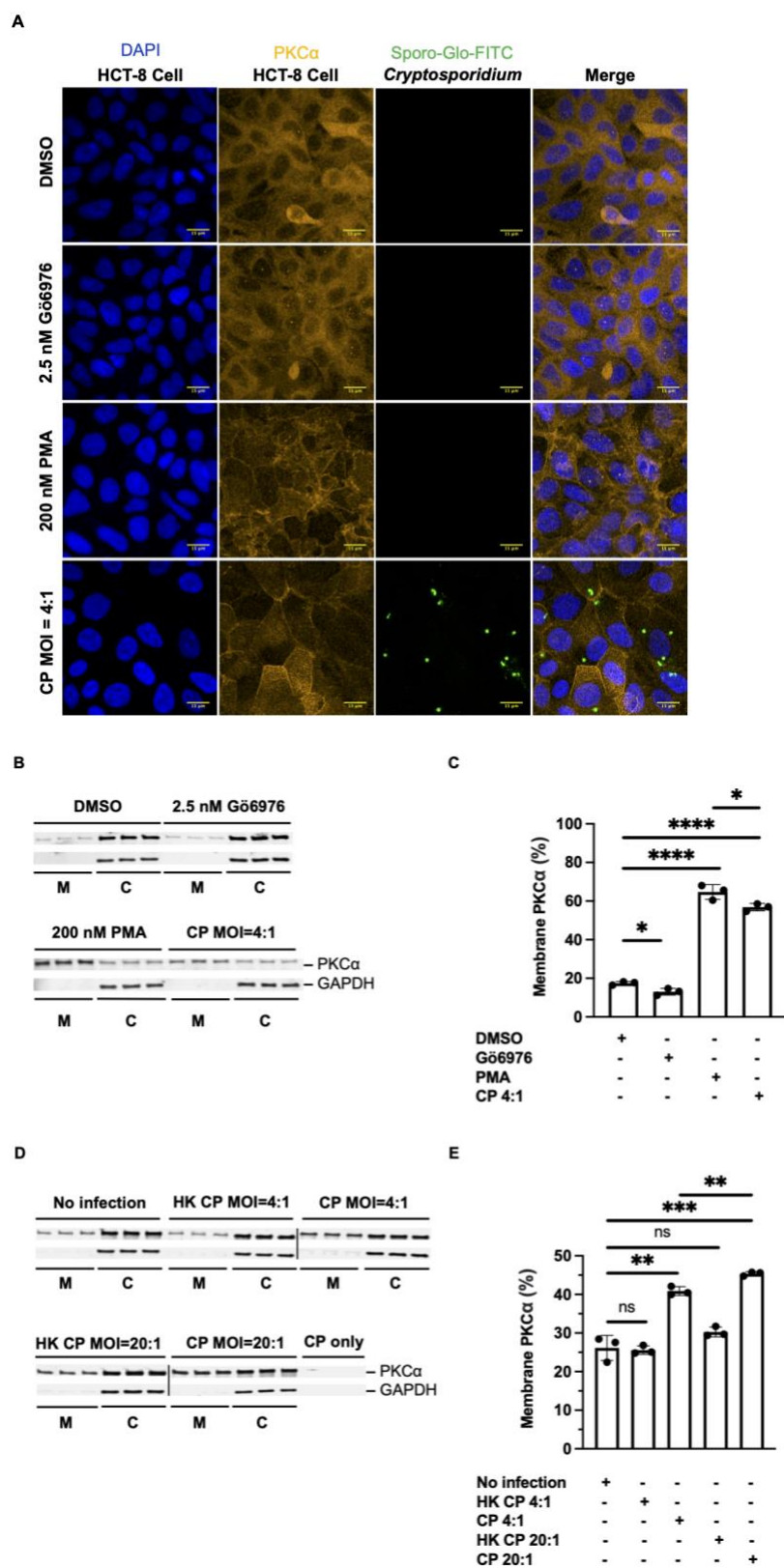


**Figure 3.1: *C. parvum* activates host PKC $\alpha$  during invasion.** (A) Intestinal epithelial cells were treated with DMSO, 2.5 nM Gö6976, 200 nM PMA, or *C. parvum* at an MOI of 4:1 as described in the Materials and Methods section. High magnification (63x objective) confocal fluorescence microscopy images of DAPI (HCT-8 cell nucleus), anti-PKC $\alpha$ -Cy3 (PKC $\alpha$ ), FITC-conjugated Sporo-Glo (total *C. parvum*), and merged channels. One of two independent experiments is shown. (B) Intestinal epithelial cells were treated with DMSO, 2.5 nM Gö6976, 200 nM PMA, or *C. parvum* at an MOI of 4:1. Immunoblot of cell membrane and cytoplasmic fractions are displayed in biological triplicate (n=2). (C) Bar graph depicts quantification of membrane-associated PKC $\alpha$  (activation) after exposure to treatment. (D) Intestinal epithelial cells were treated with infection media, heat-killed *C. parvum* at an MOI of 4:1, live *C. parvum* at an MOI of 4:1, and heat-killed *C. parvum* at an MOI of 20:1, or live *C. parvum* at an MOI of 20:1 for 2 h. Immunoblot of cell membrane and cytoplasmic fractions (-) *C. parvum*, heat-killed *C. parvum* at an MOI of 4:1, live *C. parvum* at an MOI of 4:1, heat-killed *C. parvum* at an MOI of 20:1, and live *C. parvum* at an MOI of 20:1 in biological triplicate (n=2). (E) Bar graph depicts quantification of membrane-associated PKC $\alpha$  (activation) after exposure to treatment. Asterisks denote results of one-tailed unpaired Student's t-test used to analyze PKC $\alpha$  membrane association. (\*P<0.05;\*\*P<0.01;\*\*\*P<0.001;\*\*\*\*P<0.00001).

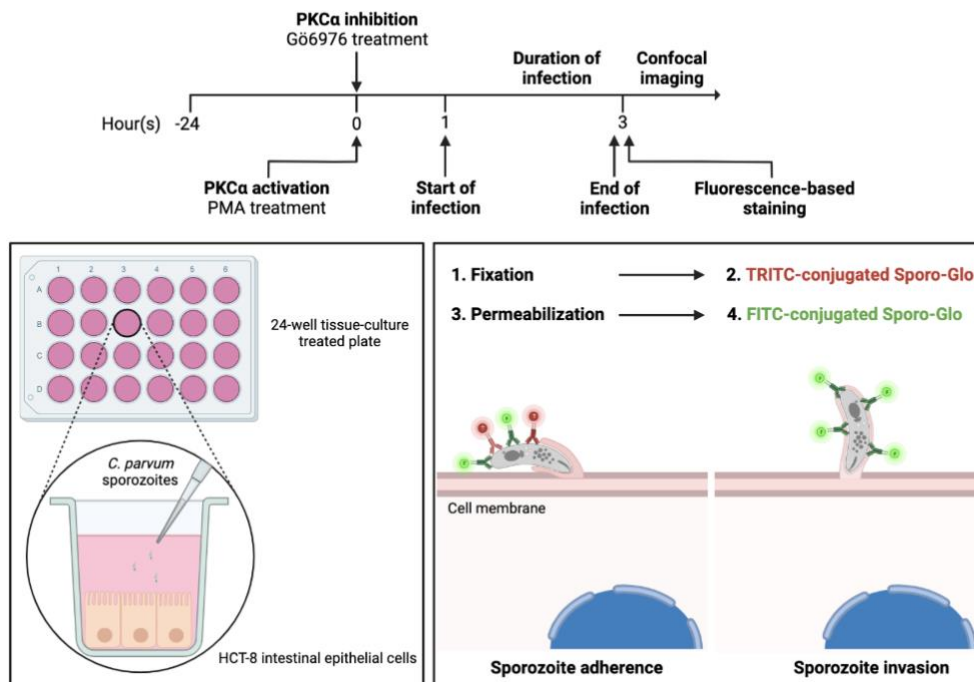
### 3.3.2. A stoplight assay for differentiation of sporozoite adherence from invasion

To distinguish the earliest steps of the *C. parvum* infection, adherence and invasion, we developed a dual-color “stoplight” immunofluorescence assay (IFA). Antibody labeling of *C. parvum*-infected HCT-8 cells has been established previously to measure *C. parvum* development and propagation (Karanis et al., 2011). However, we aimed to characterize sporozoite invasion which is complete in 2 h *in vitro* after exposure to *C. parvum* sporozoites (Guérin et al., 2021; Mele et al., 2004; Borowski et al., 2010). To differentiate sporozoite adherence and invasion we used two identical *C. parvum*-specific antibodies, conjugated to different fluorophores, coupled with staining before and after cell permeabilization (**Fig. 3.2A**). This assay was tested in *C. parvum*-infected HCT-8 cells to determine the assay selectivity for *C. parvum* sporozoite adherence and invasion. We report two distinct populations of labeled *C. parvum*-infected HCT-8 cells representative of sporozoite adherence and invasion (**Fig. 3.2B**). Adherent *C. parvum* sporozoites are dual-labeled with fluorescein isothiocyanate (FITC)-conjugated Sporo-Glo (a monoclonal antibody that binds to *Cryptosporidium*) and tetramethylrhodamine (TRITC)-conjugated Sporo-Glo while invaded sporozoites are single-labeled with FITC-conjugated Sporo-Glo only. We performed single antibody stains of *C. parvum*-infected HCT-8 cells separately and observed no spectral overlap between FITC and TRITC fluorophores (**Fig. 3.3A**). Additionally, we stained *C. parvum*-infected HCT-8 cells with both antibodies simultaneously and observed 100% dual-labeled sporozoites as expected (**Fig. 3.3A**). To further

evaluate the specificity of our assay to discriminate sporozoite adherence from invasion, we challenged fixed HCT-8 cells with *C. parvum* sporozoites which should only support parasite adherence. When fixed HCT-8 cells were exposed to *C. parvum*, we observe 100% dual-labeled *C. parvum* sporozoites, characteristic of exclusively adherent sporozoites (**Fig. 3.3B**). Together, these results validate that our stoplight assay can distinguish *C. parvum* adherence from invasion.

Figure 3.2

A



Created with BioRender.com

B

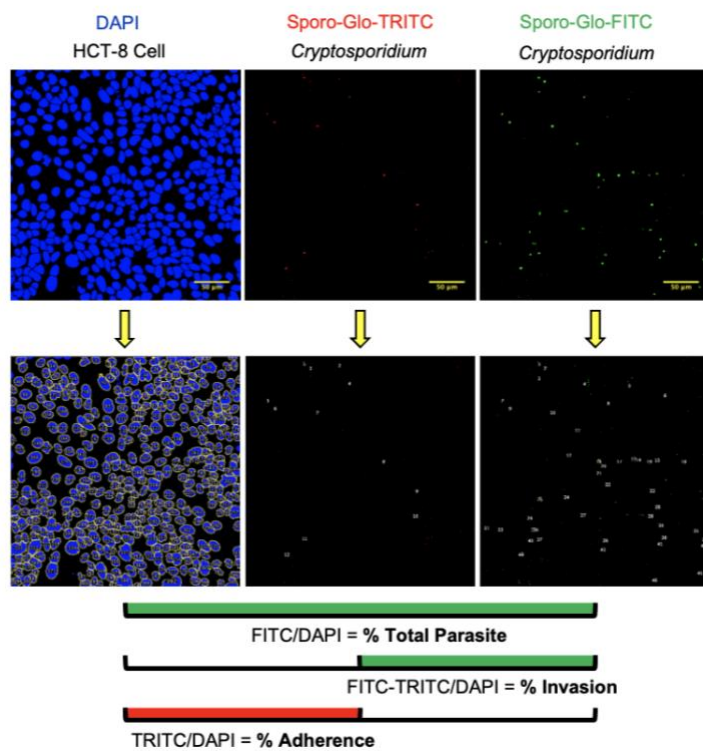
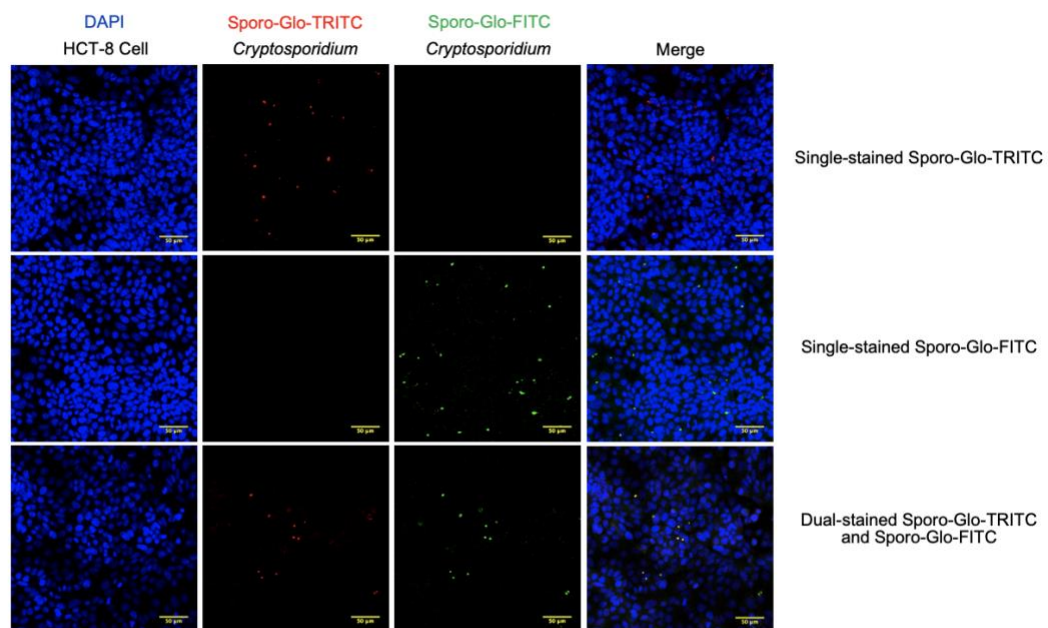


**Figure 3.2: Imaging “stoplight” assay to differentiate *C. parvum* adherence**

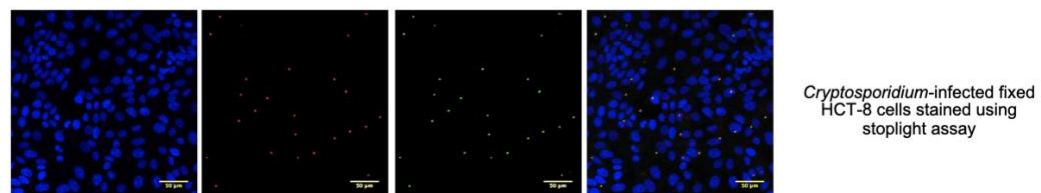
**from invasion *in vitro*.** (A) HCT-8 intestinal epithelial cells were seeded into a 24-well tissue culture treated plate. 24 h later, each well containing HCT-8 cells was treated with a PKC $\alpha$  pharmacologic inhibitor or activator to alter PKC $\alpha$  activity. Next, cells were challenged with *C. parvum* at an MOI of 4:1 for 2 h. After infection, *Cryptosporidium*-infected HCT-8 cells were fixed with 4% paraformaldehyde and then stained with a TRITC-conjugated Sporo-Glo antibody specific to *Cryptosporidium*. Next, the *Cryptosporidium*-infected HCT-8 cells were permeabilized with 0.1% Triton X-100 and subsequently stained with a FITC-conjugated Sporo-Glo antibody. This method of staining produces two populations of labeled *Cryptosporidium*, dual-labeled (TRITC+/FITC+) extracellular sporozoites and single-labeled (FITC+) intracellular sporozoites. (B) Confocal microscopy (20x objective) images of DAPI (HCT-8 cell nucleus), TRITC-conjugated Sporo-Glo (adherent *C. parvum*), FITC-conjugated Sporo-Glo (total *C. parvum*). Quantification of each image using spot counts is shown below with numerical values indicating a positive event. Calculations for *C. parvum* total parasite number, adherence, and invasion were performed using recorded spot counts for FITC/DAPI, TRITC/DAPI, and FITC-TRITC/DAPI, respectively.

Figure 3.3

A



B



**Figure 3.3: Evaluating stoplight assay for fluorescent overlap and**

**specificity.** (A) HCT-8 intestinal epithelial cells were seeded into a 24-well tissue culture treated plate. 24 h later, each well containing HCT-8 cells was challenged with *C. parvum* at an MOI of 4:1 for 2 h. After infection, *Cryptosporidium*-infected HCT-8 cells were fixed with 4% paraformaldehyde and then permeabilized with 0.1% Triton X-100. Next, the *Cryptosporidium*-infected HCT-8 cells were stained with either the TRITC-conjugated Sporo-Glo antibody, the FITC-conjugated Sporo-Glo antibody, or both. (B) HCT-8 intestinal epithelial cells were seeded into a 24-well tissue culture treated plate. 24 h later, each well containing HCT-8 cells was fixed with 4% paraformaldehyde and then challenged with *C. parvum* at an MOI of 4:1 for 2 h. Each well was then fixed again with 4% paraformaldehyde and then stained with the TRITC-conjugated Sporo-Glo antibody. Lastly, the *Cryptosporidium*-infected fixed-HCT-8 cells were permeabilized with 0.1% Triton X-100 and then stained with the FITC-conjugated Sporo-Glo antibody.

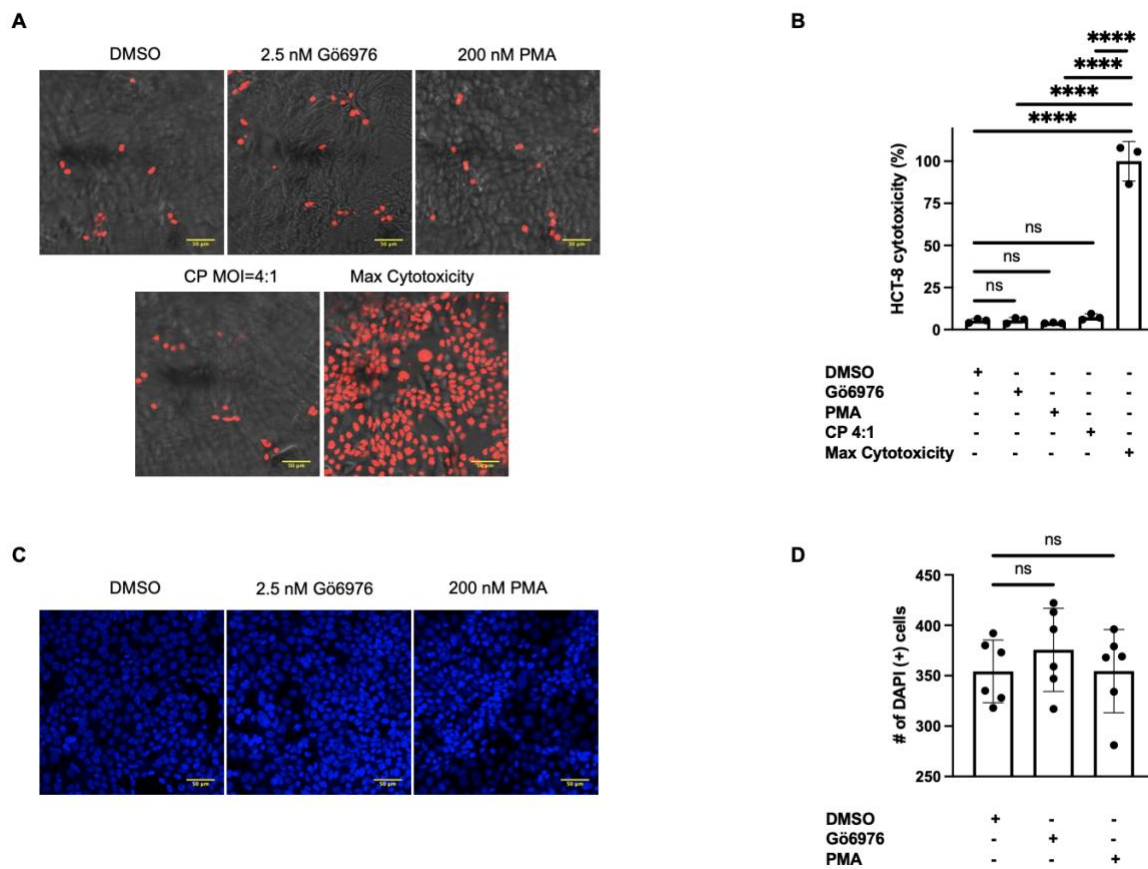
### 3.3.3. Pharmacologic inhibition of PKC $\alpha$ decreases *Cryptosporidium parvum* infection

We chose Gö6976 as the primary antagonist for our *in vitro* inhibitor studies due to its previously defined anticryptosporidial activity at PKC $\alpha$ -selective concentrations (Love et al., 2017) and because it prevented PKC $\alpha$  activation in uninfected HCT-8 cells (**Fig. 3.1A and 3.1B**). HCT-8 cells were assessed for Gö6976-induced cytotoxicity using two methods, propidium iodide (PI) staining and HCT-8 cell nuclei count relative to DMSO-treated controls (**Fig. 3.4**). Using the stoplight assay, we examined the effect of Gö6976 treatment of HCT-8 cells on *C. parvum* adherence and invasion. HCT-8 cells were treated with 2.5 nM Gö6976 for 1 h prior to infection with *C. parvum* sporozoites at an MOI of 4:1. At 2 h post-infection, we observed a significant reduction in adherent (FITC+/TRITC+) sporozoites for Gö6976-treated cells relative to DMSO-treated controls (**Fig. 3.5A**). Treatment with Gö6976 reduced total parasite number by 54.7% (26.5% to 12.0%,  $P < 0.0001$ ) relative to DMSO-treated controls showing that Gö6976 has anticryptosporidial activity early in infection (**Fig. 3.5C**). The decrease in total parasite number corresponded to a decrease in sporozoite adherence by 67.5% (11.5% to 4.40%,  $P = 0.0038$ ) and invasion by 45.1% (15.0% to 8.24%,  $P = 0.003$ ) (**Fig. 3.5C**). At higher concentrations of Gö6976, 7.5 nM and 12.5 nM, we observed a reduction in *C. parvum* total parasite number by 71.4% (19.7% to 5.65%,  $P = 0.001$ ) and 84.4% (19.7% to 3.08%,  $P = 0.0002$ ), respectively (**Fig. 3.5D**). This decrease in total parasite number corresponded to a decrease in sporozoite adherence by 71.5% (10.8% to 3.07%,  $P = 0.0038$ ) and 82.6%

(10.8% to 1.87%,  $P=0.0009$ ) and invasion by 71.3% (8.99% to 2.58%,  $P=0.0008$ ) and 86.5% (8.99% to 1.21%,  $P<0.0001$ ), respectively (**Fig. 3.5D**). We calculated the  $EC_{50}$  for Gö6976 inhibition of *C. parvum* invasion to be  $EC_{50}=1.99$  nM (**Fig. 3.5E**), within close range of the reported half-maximal inhibitory concentration ( $IC_{50}$ ) of Gö6976 for PKC $\alpha$  ( $IC_{50}=2.3$  nM) (Martiny-Baron et al., 1993). We also evaluated the impact of Gö6976 treatment of *C. parvum* sporozoites independently and found no significant difference in total parasite number, adherence, or invasion of HCT-8 cells relative to DMSO-treated sporozoites (**Fig. 3.6**). This suggests that Gö6976 acts primarily via host PKC $\alpha$  inhibition as opposed to other kinases (e.g., PKC $\beta$ 1 or TrkA) that are targeted by Gö6976 at higher concentrations or a parasite effector.

To further test the importance of PKC $\alpha$  we used an alternative inhibitor of PKC, calphostin C. Calphostin C induces inhibition of PKC $\alpha$  through an independent mechanism from Gö6976 and importantly this inhibition is irreversible, permitting removal of the compound prior to *C. parvum* exposure. Calphostin C (50 nM) treatment of HCT-8 cells resulted in a reduction in *C. parvum* total parasite number by 71.7% (22.9% to 6.47%,  $P=0.0015$ ) relative to DMSO-treated controls. This total parasite number decrease corresponded to a decrease in sporozoite adherence by 40.1% (5.48% to 3.28%,  $P=0.01$ ) and invasion by 81.7% (17.4% to 3.19%,  $P=0.0054$ ) (**Fig. 3.5F**). This data is summarized in **Table 3.1**. Altogether, these data support a primary role for host PKC $\alpha$  in mediating both sporozoite adherence and invasion.

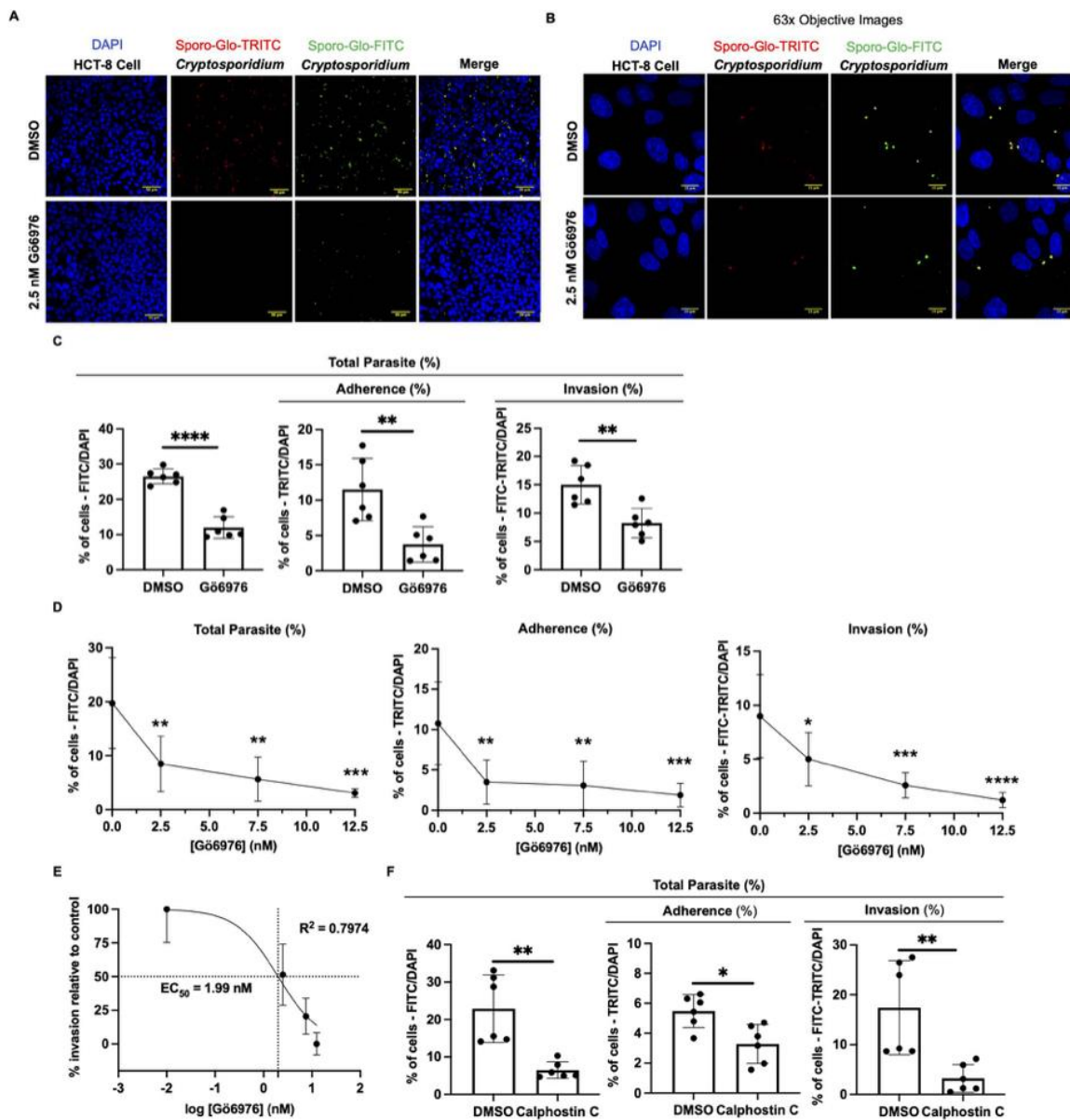
**Figure 3.4**



**Figure 3.4: Evaluating HCT-8 intestinal epithelial cells for pharmacologic**

**cytotoxicity.** (A) Intestinal epithelial cells were treated with DMSO, 2.5 nM Gö6976, 200 nM PMA, or *C. parvum* at an MOI of 4:1. To achieve maximum cytotoxicity, HCT-8 intestinal epithelial cells were fixed with 4% paraformaldehyde. Confocal fluorescence microscopy images of propidium iodide (PI) stained HCT-8 cells and differential interference contrast (DIC) are shown. (B) Bar graph quantification of HCT-8 cell cytotoxicity after exposure to DMSO, pharmacologic compounds, *C. parvum*, or 4% paraformaldehyde. (C) Confocal microscopy (20x objective) images of DAPI (HCT-8 cell nucleus) stained cells after treatment with DMSO, 2.5 nM Gö6976, or 200 nM PMA. (D) Bar graph quantification of HCT-8 cell cytotoxicity after exposure to DMSO or pharmacologic compounds. For PI experiments, asterisks denote results of one-way ANOVA and Tukey's posthoc test used to analyze percent (%) cytotoxicity (\* $P < 0.05$ ; \*\* $P < 0.01$ ; \*\*\* $P < 0.001$ ; \*\*\*\* $P < 0.00001$ ). When comparing HCT-8 cell nuclei counts to determine percent (%) cytotoxicity, asterisk denotes results of unpaired Student's t-test (\* $P < 0.05$ ; \*\* $P < 0.01$ ; \*\*\* $P < 0.001$ ; \*\*\*\* $P < 0.00001$ ).

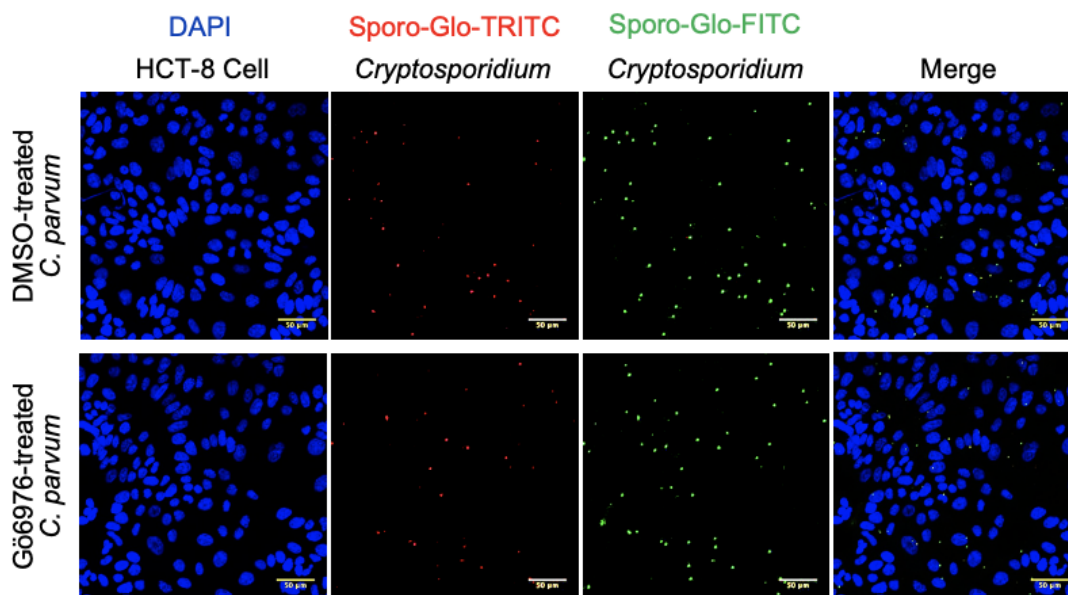
Figure 3.5



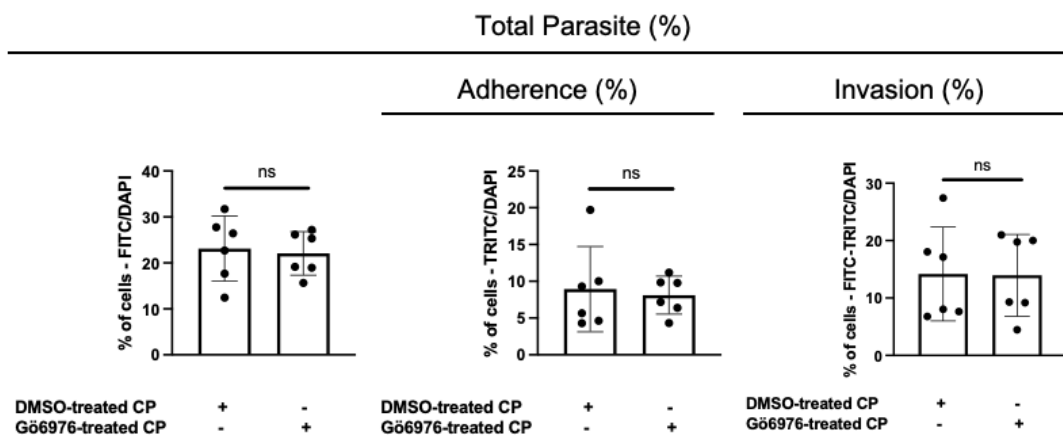
**Figure 3.5: Inhibition of PKC $\alpha$  decreases *Cryptosporidium parvum* adherence and invasion.** (A) Confocal microscopy (20x objective) images of DAPI (HCT-8 cell nucleus), TRITC-conjugated Sporo-Glo (adherent *C. parvum*), FITC-conjugated Sporo-Glo (total *C. parvum*), and merged channels. HCT-8 cells were either treated with DMSO (vehicle control) or 2.5 nM Gö6976 for 1 h. (B) High-magnification images (63x objective) denote differences in *C. parvum* total parasite number, adherence, and invasion. (C) From confocal microscopy images, bar graph quantification of *C. parvum* total parasite number, adherence, and invasion of HCT-8 cells after treatment with DMSO or 2.5 nM Gö6976. One of two independent experiments is shown. (D) Concentration curve of treatment with increasing doses of Gö6976 and effect on *C. parvum* total parasite number, adherence, and invasion relative to DMSO-treated control. One of two independent experiments is shown. (E) EC<sub>50</sub> calculation of Gö6976 treatment and *C. parvum* invasion. Gö6976 concentrations are log-transformed, and percent invasion is relative to DMSO-treated control. (F) Bar graph quantification of *C. parvum* total parasite number, adherence, and invasion of HCT-8 cells after treatment with DMSO or 50 nM calphostin C for 1 h. One of two independent experiments is shown. For figures C and F, asterisks denote results of one-tailed unpaired Student's t-test (\*P<0.05;\*\*P<0.01;\*\*\*P<0.001;\*\*\*\*P<0.00001). For figure D, asterisks denote results of a one-way ANOVA and Tukey's post hoc test (\*P<0.05;\*\*P<0.01;\*\*\*P<0.001;\*\*\*\*P<0.00001).

Figure 3.6

A



B



**Figure 3.6: Gö6976-treated *C. parvum* sporozoites exhibit no difference in infection of HCT-8 intestinal epithelial cells.** (A) Confocal microscopy (20x objective) images of DAPI (HCT-8 cell nucleus), TRITC-conjugated Sporo-Glo (adherent *C. parvum*), FITC-conjugated Sporo-Glo (total *C. parvum*), and merged channels. *C. parvum* sporozoites were either treated with DMSO (vehicle control) or 2.5 nM Gö6976 for 1 h. (B) From confocal microscopy images, bar graph quantification of *C. parvum* total parasite number, adherence, and invasion of HCT-8 cells after treatment with DMSO or 2.5 nM Gö6976. Asterisks denote results of one-tailed unpaired Student's t-test (\* $P < 0.05$ ; \*\* $P < 0.01$ ; \*\*\* $P < 0.001$ ; \*\*\*\* $P < 0.00001$ ).

**Table 3.1: Effect of PKC $\alpha$  pharmacologic compounds on *C. parvum* total parasite number, adherence, and invasion of HCT-8 cells.**

Compound	Effect on total parasite number	Effect on adherence	Effect on invasion
Gö6976	↓ <b>54.7%</b> (26.5 ± 2.13 to 12.0 ± 3.09, P<0.0001)	↓ <b>67.5%</b> (11.5 ± 4.40 to 3.74 ± 2.49, P=0.0038)	↓ <b>45.1%</b> (15.0 ± 3.38 to 8.24 ± 2.6, P=0.003)
Calphostin C	↓ <b>71.7%</b> (22.9 ± 9.00 to 6.47 ± 2.22, P=0.0015)	↓ <b>40.1%</b> (5.48 ± 1.10 to 3.28 ± 1.30, P=0.01)	↓ <b>81.7%</b> (17.4 ± 9.46 to 3.19 ± 2.76, P=0.0054)
PMA	↑ <b>149%</b> (26.5 ± 2.13 to 65.9 ± 5.14, P<0.0001)	↑ <b>142%</b> (11.5 ± 4.40 to 27.8 ± 5.46, P=0.0002)	↑ <b>154%</b> (15.0 ± 3.38 to 38.1 ± 8.52, P=0.0001)
Bryostatin 1	↑ <b>126%</b> (22.9 ± 9.00 to 51.8 ± 4.63, P<0.0001)	↑ <b>225%</b> (5.48 ± 1.10 to 17.8 ± 4.81, P=0.0001)	↑ <b>95.4%</b> (17.4 ± 9.46 to 34.0 ± 4.17, P=0.0029)

For all experiments performed in Table 1: Unpaired Student's t-test conducted to calculate statistical differences between means of groups of data.

### 3.3.4. Pharmacologic activation of PKC $\alpha$ increases *Cryptosporidium parvum* infection

We next investigated the impact of activation of PKC $\alpha$  on *C. parvum* adherence and invasion. Prior to infection, we activated PKC $\alpha$  by treating HCT-8 cells with PMA (200 nM) for 1 h. HCT-8 cells were assessed for PMA-induced cytotoxicity using PI staining and HCT-8 cell nuclei count relative to DMSO-treated controls as described previously (**Fig. 3.4**). Using the stoplight assay, at 2 hours post-infection we observed significant increases in both adherent and invaded (TRITC and FITC-labeled) *C. parvum*-infected HCT-8 cells (**Fig. 3.7A and 3.7B**). PMA-treated HCT-8 cells showed an increase in *C. parvum* total parasite number by 149% (26.5% to 65.9%,  $P < 0.0001$ ) (**Fig. 3.7C**). This increased total parasite number, corresponded with an increase in both sporozoite adherence by 142% (11.5% to 27.8%,  $P = 0.0002$ ) and invasion by 154% (15.0% to 38.1%,  $P = 0.0001$ ) relative to DMSO-treated controls (**Fig. 3.7C**). Duration of exposure to PMA has been correlated with the degree of PKC $\alpha$  activation, with extended incubation leading to a paradoxical inhibition caused by ubiquitination and degradation (Jalava et al., 1993; Lee et al., 1996). To determine the optimal time required to achieve maximum PKC $\alpha$  activation in HCT-8 cells, we varied the length of exposure to PMA. We observed a rapid translocation of PKC $\alpha$  to the plasma membrane as early as 15 min post-treatment with PMA (**Fig. 3.7D**). Since PMA-induced activation of PKC $\alpha$  occurred so rapidly, we next examined if priming of PKC $\alpha$  activation accelerates early *C. parvum* infection. To test this, we challenged HCT-8 cells with *C. parvum* and

quantified total parasite number at 15 min, 30 min, and 1 h with or without exposure to 200 nM PMA for 1 h. At the earliest recorded time point of 15 min, we observed an increase in *C. parvum* total parasite number by 160% (12.8% to 33.3%,  $P < 0.0001$ ) (**Fig. 3.7E**). This increase in *C. parvum* total parasite number was significant across all experimental timepoints relative to DMSO-treated controls resulting in an increase of 131% (21.2% to 49.0%,  $P < 0.0001$ ) and 115% (25.9% to 55.6%,  $P < 0.0001$ ) at 30 min and 1 h, respectively (**Fig. 3.7E**). To determine if this increased *C. parvum* total parasite number was specific to PMA, we introduced an alternative pharmacologic agonist of PKC $\alpha$ , bryostatin 1 (Szallasi et al., 1994). Bryostatin 1 activates PKC via binding to the C1 domain of PKC, which is distinct from PMA (Lorenzo et al., 1999). At 2 h post-infection, bryostatin 1 treatment of HCT-8 cells for 20 min resulted in an increase in *C. parvum* total parasite number from 126% (22.9% to 51.8%,  $P < 0.0001$ ) relative to DMSO-treated controls (**Fig. 3.7F**). This increase in total parasite number, corresponded with an increase in sporozoite adherence by 225% (5.48% to 17.8%,  $P = 0.0001$ ) and invasion by 95.4% (17.4% to 34.0%,  $P = 0.0029$ ). These findings indicate that PKC $\alpha$  activation enhances *C. parvum* adherence and invasion.

Figure 3.7

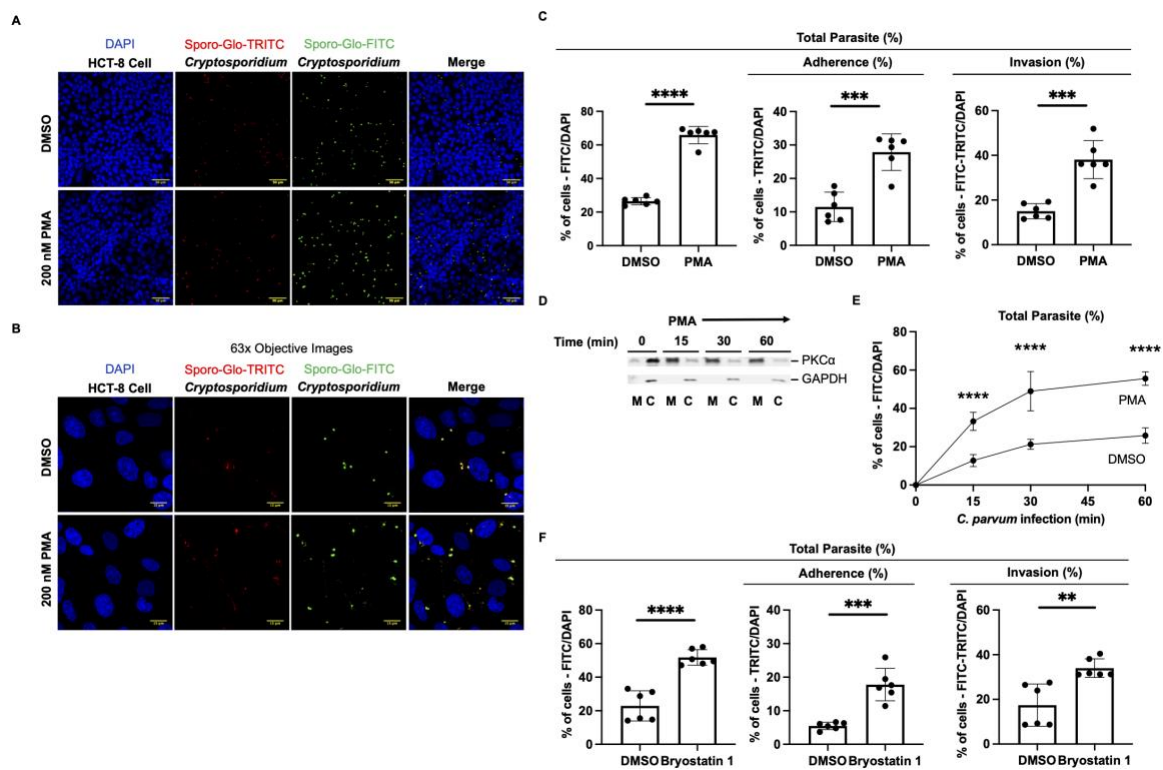


**Figure 3.7: Activation of PKC $\alpha$  increases *Cryptosporidium parvum***

**adherence and invasion.** (A) Confocal microscopy (20x objective) images of DAPI (HCT-8 cell nucleus), TRITC-conjugated Sporo-Glo (adherent *C. parvum*), FITC-conjugated Sporo-Glo (total *C. parvum*), and merged channels. HCT-8 cells were either treated with DMSO or 200 nM PMA for 1 h. (B) High-magnification images (63x objective) denote differences in *C. parvum* total parasite number, adherence, and invasion of HCT-8 cells. (C) From confocal microscopy images, bar graph quantification of *C. parvum* total parasite number, adherence, and invasion of HCT-8 cells after treatment with DMSO or 200 nM PMA. One of two independent experiments is shown. (D) Immunoblot of membrane and cytoplasmic HCT-8 cell fractions treated with 200 nM PMA over time (n=2). (E) Time-course of *C. parvum* infection  $\pm$  treatment with 200 nM PMA for 1 h relative to DMSO-treated control. One of two independent experiments is shown. (F) Bar graph quantification of *C. parvum* total parasite number, adherence, and invasion of HCT-8 cells after treatment with 100 nM bryostatin 1 or DMSO for 20 min. One of two independent experiments is shown. For figures C and F, asterisks denote results of one-tailed unpaired Student's t-test (\*P<0.05;\*\*P<0.01;\*\*\*P<0.001;\*\*\*\*P<0.00001). For figure E, asterisks denote results of a one-way ANOVA and Tukey's post hoc test (\*P<0.05;\*\*P<0.01;\*\*\*P<0.001;\*\*\*\*P<0.00001).

### 3.4 Discussion

Two major findings emerged from this study. First, *C. parvum* activated PKC $\alpha$  in human intestinal epithelial cells. Second, host PKC $\alpha$  mediated the initial adherence of parasites as well as internalization resulting in invasion which we discovered using our stoplight imaging assay. PKC $\alpha$  activity was directly related to parasite infection as pharmacologic antagonists blocked *C. parvum* adherence and invasion, while pharmacologic agonists promoted *C. parvum* adherence and invasion (**Table 3.1**). Our studies, therefore, provide insight into how polymorphisms in human *PRKCA* may increase susceptibility to cryptosporidiosis in children (Wojcik et al., 2020) suggesting that increased PKC $\alpha$  activity may increase permissibility to infection at the intestinal epithelium. We now have shown a novel role for host PKC $\alpha$  in *Cryptosporidium* adherence and invasion of human intestinal epithelial cells. The fact that *Cryptosporidium* targets intestinal epithelial cell PKC $\alpha$  during early infection and PKC $\alpha$  activity is critical to a pathogenic host-mediated cellular process makes it an attractive target for host-directed therapy.

Pharmacologic inhibition of intestinal epithelial cell PKC $\alpha$  reduced, while activation of PKC $\alpha$  enhanced *C. parvum* adherence and invasion. These findings implicate host PKC $\alpha$  activity in promoting both parasite adherence and invasion. Importantly, we observed treatment with the competitive inhibitor Gö6976 and the irreversible antagonist calphostin C resulted in comparable reductions in adherence and invasion. Mechanistically these compounds alter PKC $\alpha$  through dissimilar actions. Gö6976 inhibits PKC $\alpha$  through competition with ATP (Martiny-

Baron et al., 1993) while calphostin C inhibits PKC $\alpha$  through C1 domain binding (Bruns et al., 1991; Redman et al., 1995). The use of pharmacologic antagonists to target PKC $\alpha$  with differing mechanisms of action further supports a role for PKC $\alpha$ -mediated parasite entry. Moreover, *C. parvum* sporozoites showed no significant difference in infection of intestinal epithelial cells upon treatment with Gö6976. This finding was expected as no known homologs of PKC $\alpha$  have been reported in any *Cryptosporidium* spp. adding additional support for a host-inhibitory effect. We additionally found that treatment with a PKC $\alpha$  agonist alters the kinetics of infection *in vitro*. Altogether, these findings confirm a role for PKC $\alpha$  in parasite adherence and invasion and suggest activation of PKC $\alpha$  as a preliminary event to *C. parvum* infection.

PKC $\alpha$  alters the morphology of the host cell F-actin cytoskeleton thereby regulating processes that are affected by reorganization of these microfilaments (Hryciw et al., 2005; Peng et al., 2011). PKC $\alpha$  is active at the cell membrane, the same site as parasite adherence and invasion. Hence, it is biologically plausible for PKC $\alpha$  to have activity at the host-parasite interface. Two kinases important for regulating actin polymerization have been implicated in the required rearrangement of F-actin during *Cryptosporidium* infection: proto-oncogene tyrosine-protein kinase Src (c-Src) and phosphatidylinositol 3-kinase (PI3K) (Elliott et al., 2001; Chen et al., 2003; Chen et al., 2004a; Chen et al., 2004b). Inhibition of c-Src via a dominant-negative mutant blocked *C. parvum* mediated rearrangement of F-actin and subsequently *C. parvum* invasion of human biliary epithelial cells (Chen et al., 2003). Similarly, genetic and pharmacologic inhibition

of PI3K decreased *C. parvum*-induced actin rearrangements and blocked invasion of human biliary epithelial cells (Chen et al., 2004b). PKC $\alpha$  has been reported upstream to regulate c-Src (Brandt et al., 2002; Li et al., 2013) and PI3K (Ziemba et al., 2016; Hsu et al., 2018). Though these studies did not discern parasite adherence from invasion, we speculate sporozoite adherence results in activation and recruitment of host PKC $\alpha$  to the cell membrane. This results in a PKC $\alpha$  phosphorylation cascade leading to the F-actin remodeling required for invasion. This research furthers our current understanding of the anticryptosporidial activity of PKC $\alpha$  antagonists by pinpointing activity to specific life-cycle stages. Furthermore, we have established *C. parvum*-induced activation of PKC $\alpha$  as a critical event during invasion. Thus, PKC $\alpha$  is a key host protein target meriting further investigation as its activity will yield additional insight into the molecular mechanisms of parasite invasion.

Host-directed therapy is an emerging approach in the field of anti-infectives. Recent insights into pathogen-host interactions are leading to the identification of a wide array of host targets involved in pathogenesis. We show here that PKC $\alpha$  activity mediates *Cryptosporidium* adherence and invasion of intestinal epithelial cells *in vitro*. Evidence from our *in vitro* analyses suggests that PKC $\alpha$  is a potential host target for therapy in human infection with *Cryptosporidium* though further experimentation is necessary, in particular as our analysis only examined the addition of inhibitors prior to infection with sporozoites. Remarkably, there remains no PKC $\alpha$ -specific FDA-approved drug despite isozyme-specific contrasts in activity being linked to a number of human

disease states (Chen et al., 2001; Song et al., 2002; Braun et al., 2003; Liu et al., 2008). However, PKC agonist bryostatin 1 is currently in phase 2 of clinical trials for the treatment of moderately severe to severe Alzheimer's disease (Neurotrope Bioscience, Inc 2018). Consequently, the pharmacologic antagonists used in this study may serve as suitable options for future anticryptosporidial studies.

Using our fluorescence-based approach to examine PKC $\alpha$  activity, we observed activation of PKC $\alpha$  in not only *Cryptosporidium*-infected cells but also adjacent uninfected intestinal epithelial cells. Our pharmacologic data suggest the host cell baseline PKC $\alpha$  activation state may determine hospitality to *Cryptosporidium* infection. Therefore, the activation of PKC $\alpha$  in adjacent uninfected intestinal epithelial cells may have biological relevance. We speculate PKC $\alpha$  activation in adjacent uninfected cells to be the result of a cell contact signaling event. A host pathway for PKC activation has been found for other protozoan parasites during invasion (Rawal et al., 2005). *E. histolytica* and *Cryptosporidium* spp. recognize the same surface sugar for adherence to human cells. We hypothesize that *Cryptosporidium* sporozoite adherence to an intestinal epithelial cell induces a rapid influx of calcium ions (Ca<sup>2+</sup>) and subsequently in adjacent uninfected cells through cellular gap junctions. The intracellular Ca<sup>2+</sup> influx activates host PKC $\alpha$  in *Cryptosporidium*-infected cells and adjacent uninfected cells. Delineating intracellular Ca<sup>2+</sup> signaling and PKC $\alpha$  activation during epithelial cell *Cryptosporidium* infection is an important next step.

This study directly builds on the identification of *PRKCA* in a forward genetic screen by defining a role experimentally, at an enzymatic level, for susceptibility in human intestinal epithelial cells *in vitro*. Our pharmacologic analyses suggest the previously identified polymorphisms in *PRKCA* would increase PKC $\alpha$  activity, via increased mRNA expression or protein stability. Furthermore, these data suggest that the polymorphisms associated with increased susceptibility, act through exerting changes in the intestinal epithelium. Expression quantitative trait loci (eQTL) analyses have linked the associated SNP with decreased *PRKCA* mRNA expression in the esophagus and colon (GTEx Consortium 2015). However, the impact on small intestinal expression, which is the major site of *Cryptosporidium* infection, has not been determined. Our findings suggest that SNPs associated with increased susceptibility to *Cryptosporidium* might act via increased PKC $\alpha$  activity during *Cryptosporidium* infection, either by increasing *PRKCA* mRNA expression or via compensatory gene regulation of PKC $\alpha$  regulators. Alternatively, the activation of human intestinal cell PKC $\alpha$  may be *Cryptosporidium* specific resulting in altered expression only upon exposure to parasites.

A limitation of the *in vitro* system is that HCT-8 are cancer cells and may have abhorrent PKC $\alpha$  activity (Baltuch et al., 1995). This concern is somewhat mitigated by the observation that PKC $\alpha$  was activated and inhibited as expected in HCT-8 cells. An additional limitation of our system is the inability to investigate the immune response to infection. Th17 cells have been implicated in response to infection with increased levels of Th17-related cytokines reported in the gut

(Zhao et al., 2016) and PKC $\alpha$  is a positive regulator of Th17 cell function (Meisel et al., 2013). Moreover, gut infection has been linked to immune-mediated alterations leading to functional changes in the intestinal epithelium (Solaymani-Mohammadi and Singer 2013). Here, modifications of intestinal epithelial cell actin-binding proteins, ezrin and villin, played a role in *Giardia* pathophysiology and are CD4<sup>+</sup> and CD8<sup>+</sup> T cell-dependent (Solaymani-Mohammadi and Singer 2013). To address a secondary role for PKC $\alpha$  in the immune response to *Cryptosporidium* infection further examination *in vivo* is needed. A major strength of this study is the identification of intestinal epithelial cell PKC $\alpha$  activation by *C. parvum* which implicates yet another host kinase in infection. Second, we used a well-characterized intestinal cell model which allowed for examination of PKC $\alpha$  activity at precise stages of parasite infection. Using this intestinal cell system also allowed for investigation of PKC $\alpha$  devoid of the influence of immune cell regulation. Lastly, the introduction of the stoplight assay for differentiation of parasite adherence from invasion and downstream quantification is an asset for future studies in the field.

In conclusion, using an *in vitro* system of intestinal epithelial cell cryptosporidiosis, we expand on the role of PKC $\alpha$  and susceptibility to infection. We elucidated the parasite stages PKC $\alpha$  is involved by demonstrating changes in PKC $\alpha$  activity impact downstream *C. parvum* adherence and invasion. We have shown in this study, *C. parvum* sporozoites activate intestinal epithelial cell PKC $\alpha$  and prove PKC $\alpha$  activation as critical for *C. parvum* adherence and invasion (**Fig. 3.8**). These results lead us to conclude activation of PKC $\alpha$  by *C. parvum* is

deliberate and an important component of infection of intestinal epithelial cells.

Thus, the mechanisms by which PKC $\alpha$  promotes *C. parvum* invasion and its role *in vivo* warrant further exploration.

Figure 3.8

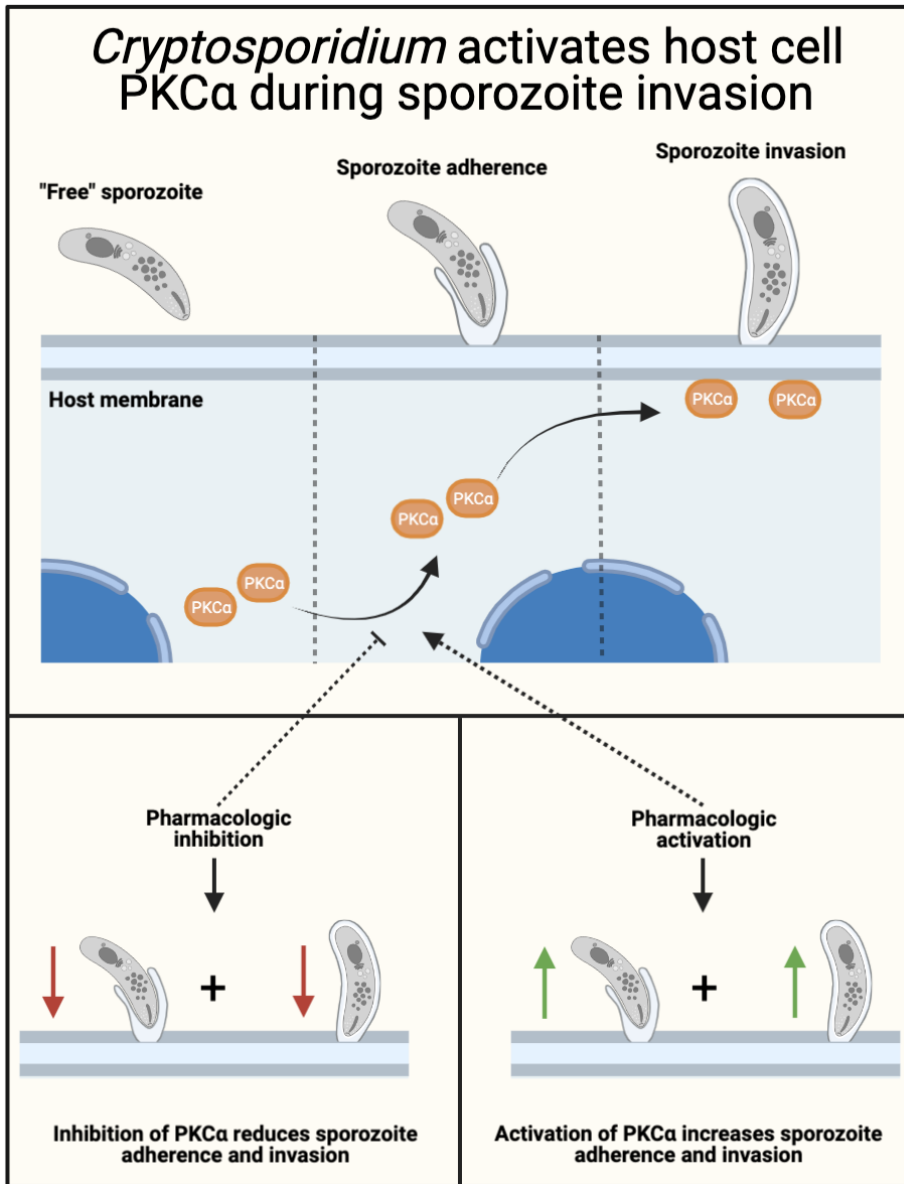


**Figure 3.8: PKC $\alpha$  is a gatekeeper of *Cryptosporidium* adherence and invasion.** Infection by *C. parvum* in intestinal epithelial cells results in activation and translocation of host PKC $\alpha$  to the host cell membrane. The addition of pharmacologic antagonists of PKC $\alpha$  reduces *C. parvum* sporozoite adherence and invasion. Contrarily, the addition of pharmacologic agonists of PKC $\alpha$  increases *C. parvum* sporozoite adherence and invasion.

## **Chapter 4: Conclusions and Future Directions**

The way the host immune system responds, for many pathogens, determines susceptibility and severity of disease. The host response to infection includes activation of the innate and adaptive immune system, the consequences of which consist of inflammatory signaling, pathogen clearance, and programmed cell death. Successful pathogens have learned to escape the immune system by avoiding or inactivating host defenses to promote their survival and replication within the host. Importantly, how the host responds to infection can be protective or deleterious depending on a combination of factors ranging from pathogen genetics or magnitude of the immune response to class of infectious agent or pre-existing medical conditions.

In this thesis, we examined the role of the host epithelium and host genetics in the defense against enteric infection. We investigated *Cryptosporidium* as our primary pathogen due to its known variability in the severity of symptoms ranging from asymptomatic to severe and life-threatening disease. Here we report *in vitro* findings that validate an observation initially made in a clinical cohort of infants using genome-wide scans. We found that targeting intestinal epithelial cell PKC $\alpha$  altered subsequent *Cryptosporidium* infection in an established *in vitro* model system of *Cryptosporidium* infection. This line of inquiry was inspired by previous work establishing a genetic link between *PRKCA* and susceptibility to pediatric cryptosporidiosis in Bangladeshi infants (Wojcik et al., 2020). To better understand genetic links to enteric infection we further probed the archetypal candidates of genetic susceptibility, HLA loci, in infants. When examining the contribution of HLA in infants with or

without *Cryptosporidium*-positive diarrhea we observed multiple HLA class I and II alleles associated with increased risk supporting a role for both CD4+ and CD8+ T cells in resistance to and clearance of infection (Ungar et al., 1991; McDonald et al., 2004; Korbel et al., 2011; McDonald et al., 1994; Pantenburg et al., 2009; Pantenburg et al., 2010). As HLA genes are the central drivers of recognition and presentation of antigens in humans, the significant alleles identified may encode HLA molecules that exhibit altered effectiveness in response to a specific pathogenic antigen. Independently, our *in vitro* PKC $\alpha$  findings suggest the previously reported genetic link between *PRKCA* and cryptosporidiosis in infants may have relevance in the intestinal epithelium. This is biologically plausible as it is also the role of the intestinal epithelium to facilitate environmental pathogen clearance autonomously as well as to initiate communication with immune cells. Furthermore, F-actin rearrangements have been implicated in several stages of the *Cryptosporidium* life cycle and host PKC $\alpha$  may function to regulate these filaments. While studies to determine whether changes in immune cell PKC $\alpha$  activity impacts *Cryptosporidium* infection remain to be performed (discussed below), our findings in the intestinal epithelium suggest invasion is likely a PKC $\alpha$ -mediated event. Altogether, this report explores two distinct host responses to *Cryptosporidium* and other common enteric infections.

#### **4.1 PKC $\alpha$ a mediator of *Cryptosporidium* infection**

*Cryptosporidium* infection requires the hijacking of a myriad of host cellular processes to establish a replicative infection. During invasion of intestinal

epithelial cells, activation of host actin polymerization creates a membrane protrusion that forms the intracellular yet extra-cytoplasmic parasitophorous vacuole (Forney et al., 1999; Besteiro et al., 2011). Actin is a globular protein that exists throughout the cell and polymerizes into a filamentous form with important cellular function (Cooper 2000). In most cell types, one or more PKC isoforms act to regulate this F-actin cytoskeletal morphology by interacting directly with F-actin-binding proteins such as ezrin (Bonnin et al., 1999; Ng et al., 2001; Solaymani-Mohammadi and Singer 2013; Singh et al., 2017). Based on this, we hypothesized that *Cryptosporidium*-induced host cell actin rearrangements rely on PKC $\alpha$  signaling. To investigate genetic links to *Cryptosporidium* infection, we examined genome differences in infants with or without *Cryptosporidium*-associated diarrhea (Wojcik et al., 2020). In this previous analysis, each copy of the SNP most highly associated (rs58296998) conferred a 2.4 times the odds of symptomatic *Cryptosporidium* infection during the first year of life (Wojcik et al., 2020). Notably, this SNP alters expression of *PRKCA* in humans (GTEx Consortium 2015; Stranger et al., 2017). Each copy harbored is associated with a tissue-specific decrease in *PRKCA* expression: esophageal muscularis ( $P = 3.12 \times 10^{-5}$ ), the sigmoid colon ( $P = 4.61 \times 10^{-4}$ ), and the esophageal mucosa ( $P = 7.50 \times 10^{-4}$ ) (GTEx Consortium 2015). However, the effect of this SNP on *PRKCA* expression in the small intestine, the primary site of *Cryptosporidium* infection, has not been characterized. Thus, our findings linking the most highly associated SNP with susceptibility to cryptosporidiosis paired with its variance in *PRKCA* expression suggests an indirect association between expression of

*PRKCA* and susceptibility to pediatric cryptosporidiosis. However, our pharmacologic *in vitro* findings contradict this association. One explanation for this contradiction is that the activity of PKC $\alpha$  in immune cells that respond to cryptosporidiosis have contrasting effects on infection to what we observed in intestinal epithelial cells. Alternatively, *PRKCA* expression may be dependent on exposure to *Cryptosporidium* as the host may downregulate *PRKCA* in response to infection, while the aforementioned *PRKCA* expression data was collected from explicitly healthy donor adults (GTEx Consortium 2015; Stranger et al., 2017). Overall, this work has demonstrated involvement of *PRKCA* expression and protein activity in *Cryptosporidium* infection of humans.

PKC $\alpha$  maintains a role in many human disease processes (Hempel et al., 1997; Koivunen et al., 2004; Palaniyandi et al., 2009; Bar-Am et al., 2004; Talman et al., 2016; Hahn et al., 1999; Skvara et al., 2008; Yang and Yan 2014). More applicable to this thesis, PKC $\alpha$  has repeatedly been implicated in regulation of host actin rearrangements during invasion of other intracellular enteric pathogens (Sukumaran et al., 2002; Mittal et al., 2016; Bhalla et al., 2017). Our observation that pharmacologic inhibition of PKC $\alpha$  activity blocks *Cryptosporidium* adherence and invasion suggests that PKC $\alpha$  is critical in early pathogenesis. Still, this work did not examine the activity of alternative PKC isoforms which may have opposing effects or exert redundancy in function thus compensating for absence of PKC $\alpha$  activity. Gastrointestinal cells express at least 12 known isoforms constituting all major subfamilies of PKC: conventional, novel, and atypical (Farhadi et al., 2006). Investigating *Cryptosporidium* infection

in a *PRKCA* absent setting will validate its role in the intestinal epithelium and shed light on the potential actions of alternate PKC isoforms.

The host epithelium remains the first defense against infection and is essential in the regulation of the innate and adaptive immune response. As such, we explored the role of PKC $\alpha$  activity in intestinal epithelial cells during *Cryptosporidium* infection. We show here that pharmacologic inhibition of intestinal epithelial cell PKC $\alpha$  with Gö6976 decreases *Cryptosporidium* adherence and invasion. While inhibition of PKC $\alpha$  with selective inhibitor Gö6976 at elevated concentrations led to a further decrease in *Cryptosporidium* adherence and invasion, the majority was inhibited at a PKC $\alpha$ -only relevant concentration. This finding suggested PKC $\alpha$  as the primary driver of *Cryptosporidium* adherence and invasion and thus the differences observed at higher concentrations were due to increased inhibition of PKC $\alpha$ . To further test PKC $\alpha$  we used an alternate pharmacologic inhibitor, calphostin C, which varies mechanistically and showed treatment replicated a decrease in adherence and invasion thus validating PKC $\alpha$  as a mediator of these events. We also identified the half-maximal effective concentration (EC<sub>50</sub>) in response to *Cryptosporidium* invasion and found the calculated EC<sub>50</sub> value fell below the reported IC<sub>50</sub> for Gö6976 inhibition of PKC $\alpha$  again signifying PKC $\alpha$  as the primary driver. Following these findings, we investigated whether activation of PKC $\alpha$  promoted *Cryptosporidium* infection. Pharmacologic activation of PKC $\alpha$  by PMA and bryostatin 1, separately, increased *Cryptosporidium* adherence and invasion of intestinal epithelial cells. Due to our finding of a causative role for PKC $\alpha$  activity

during *Cryptosporidium* infection, we further speculated that *Cryptosporidium* infection alters PKC $\alpha$  activity naturally as a step of pathogenesis. In chapter 3 of this thesis we address this, showing that *Cryptosporidium* does activate host PKC $\alpha$ . Notably, activation of PKC $\alpha$  occurred in neighboring uninfected intestinal epithelial cells as well. To explain this phenomenon, we hypothesize *Cryptosporidium* infection of intestinal epithelial cells results in a host Ca<sup>2+</sup> influx, to which the C2 domain of PKC $\alpha$  binds resulting in PKC $\alpha$  activation and translocation to the cell membrane (discussed below). In response to infection, the *Cryptosporidium*-infected cell communicates with adjacent host cells via Ca<sup>2+</sup> traveling through intercellular gap junctions resulting in PKC $\alpha$  activation in uninfected cells. Our findings suggest the increase in *Cryptosporidium* adherence and invasion via two distinct pharmacologic agonists is likely due to the increased availability of active PKC $\alpha$  at the start of adherence. However, due to the prevalence of PKC $\alpha$  in multiple tissues and its role as a regulator of cellular function and turnover, pharmacologic approaches targeting PKC $\alpha$  during infection will need to be developed further to establish a desirable method for therapy. Together, this data supports that PKC $\alpha$  is critical to the success of *Cryptosporidium* infection of intestinal epithelial cells and debuts this isoform as having potential efficacy against cryptosporidiosis.

#### **4.2 HLA, *Cryptosporidium*, and other common enteric infections**

Following laboratory closures at the University of Virginia caused by mandatory home confinements at the beginning of the COVID-19 pandemic coupled with my research interests in host-pathogen interactions, I pursued a

project designed to investigate how genetic variation in HLA genes expressed in infants impacts susceptibility to 12 common enteric pathogens during the first year of life. Genetic association studies are useful hypothesis-driven analyses that aim to identify gene variants linked to susceptibility and severity of disease. Previously, our lab performed an analysis similar to this; however, this previous analysis focused on HLA associations with *Cryptosporidium* infection in children 2-5 years of age (Kirkpatrick et al., 2008). Yet, enteric infections in particular disproportionately target pediatric populations during the first two years of life (George et al., 2018). Given the importance of HLA in human disease paired with the high burden of enteric infection we were particularly interested in understanding the contribution of HLA in infants living in an area endemic to enteric infection and diarrheal disease.

To investigate the role of HLA in the susceptibility to pediatric enteric infection, we analyzed data collected from Bangladeshi infants enrolled in the PROVIDE study, a prospective clinical trial of polio and rotavirus vaccine interventions. To determine which HLA alleles were advantageous or detrimental, we compared infants with pathogen-positive diarrhea to infants without. Seven novel HLA associations across five enteric pathogens were observed indicating that the influence of HLA on susceptibility to infection is immediate. HLA alleles are unique in that they are highly polymorphic in nature yet exhibit strong linkage disequilibrium with one another equipping the immune system with an advantage against a diversity of pathogens (Shiina et al., 2009). HLA molecules contain 6 individual binding pockets residing in the peptide-binding cleft designated A-F

(Nguyen et al., 2021). The B and F pockets are deemed the two primary anchor peptides thus determining the specificity of HLA molecules (Nguyen et al., 2021). The B pocket interacts with position 2 of the peptide antigen while the F pocket binds the C-terminal residue. HLA class I molecules can be clustered based on the overlap of their peptide binding specificity, designated “HLA supertypes” (Sidney et al., 2008). The five enteric pathogens we found to have HLA associations within the first year of life were EAEC, typical EPEC, astrovirus, adenovirus 40/41, and *Cryptosporidium*. Of the HLA alleles characterized by supertype to date, the sole pathogen associated with overlapping HLA alleles in our analysis is astrovirus infection (*A\*24:02*; *B\*15:01*; *B\*38:02*). For HLA *A\*24:02*, infants harboring this allele were protected against astrovirus infection while infants harboring *B\*15:01* or *B\*38:02* were at increased risk. Structurally, these encoded HLA molecules all share high peptide-binding similarity in the F pocket while their diversity in the B pocket is more diverse. Thus, according to B pocket supertype specificity, the astrovirus-derived peptide antigen that leads to a protective host immune response has residues which are aromatic and aliphatic in nature at position 2. Independently, this may also suggest the F pocket to not play as critical a role in peptide binding or stability of the peptide-HLA class I complex for this protective astrovirus-derived peptide antigen. HLA *B\*38:02* was also associated with increased risk of *Cryptosporidium* infection, suggesting poor presentation of the peptide antigen necessary to generate a protective CD8+ T cell response. Unfortunately, no protective HLA associations with *Cryptosporidium* infection were identified in this analysis for juxtaposition.

These novel HLA associations serve as an introduction to understanding the role of host genetics in enteric infection susceptibility and as such require additional validation in future studies. These findings have prospective clinical relevance in the screening of infants to determine those most at-risk of infection from a specified pathogen, inform severity of disease, and elucidate pathogen-derived peptide antigens that generate a protective immune response. Altogether, these findings depict the early importance of the HLA repertoire in the susceptibility and severity of pediatric diarrheal disease.

### **4.3 Future Directions**

The work presented here enhances our knowledge of *Cryptosporidium* pathogenesis. Furthermore, we add additional evidence for the role of HLA in pediatric enteric infection by reporting several novel HLA associations. In this section, we expand on this previous work and discuss future studies on how to address the questions left unanswered. Our unresolved questions and future directions to be discussed below: 1) Does *Cryptosporidium* infection cause an intracellular  $\text{Ca}^{2+}$  influx in intestinal epithelial cells? And is this  $\text{Ca}^{2+}$  required for PKC $\alpha$  activation? 2) What is the target(s) of PKC $\alpha$  activity during *Cryptosporidium* adherence and invasion, and does this involve regulation of the host actin cytoskeleton? 3) Is the activity of PKC $\alpha$  important in immune cell responses to *Cryptosporidium* infection? 4) Lastly, regarding our reported HLA allele-pathogen associations, do these encoded HLA molecules display altered presentation of pathogen-derived peptide antigens?

#### 4.3.1 Ca<sup>2+</sup> influx as an activator of PKC $\alpha$ during invasion

Calcium-mediated activation of PKC has been observed in the pathogenesis of at least one other protozoan parasite during invasion. Epithelial cells stimulated with an *E. histolytica*-derived lectin showed a rapid rise in intracellular Ca<sup>2+</sup> followed by a significant increase in expression of PKC, thereby correlating *E. histolytica* adherence with changes in host PKC (Rawal et al., 2005). Interestingly, *E. histolytica* and *Cryptosporidium* both express lectins that recognize host galactose and N-acetyl-D-galactosamine (GalNAc) cell surface sugars facilitating adherence to human epithelial cells (Bhat et al., 2007).

Parasite intracellular calcium signaling promotes *Cryptosporidium* infection, as chelation with highly specific Ca<sup>2+</sup>-chelator, BAPTA-AM, inhibited apical organelle discharge which mediates parasite entry into host cells (Chen et al., 2004c). This effect on infection was partially rescued by adding a Ca<sup>2+</sup> ionophore (A23187) in the presence of extracellular Ca<sup>2+</sup> (Chen et al., 2004c). Furthermore, *Cryptosporidium*-expressed CDPKs display distinct roles in infection supported by differences in gene expression and localization in the sporozoite (Zhang et al., 2020; Zhang et al., 2021). Selective inhibitors of CDPKs are an emerging therapeutic option displaying extensive anticryptosporidial activity *in vitro* and *in vivo* (Castellanos-Gonzalez et al., 2016; Voorhis et al., 2017; Hulverson et al., 2017; Lee et al., 2018). Calcium has also been implicated in parasite virulence via facilitating adhesion of *Cryptosporidium* oocysts to surfaces (Considine et al., 2002; Kuznar et al., 2004; Luo et al., 2016). Several studies have explored a calcium-mediated interaction between oocysts and

negatively charged groups present on surfaces, termed “calcium bridging” (Gao et al., 2009; Luo et al., 2016; Sarkhosh et al., 2019). *Cryptosporidium* oocysts were observed to bind to their external environment through a calcium-dependent mechanism mediated by the outer layer of the oocyst shell (Sarkhosh et al., 2019). Despite the many roles of calcium in parasite pathogenesis, little is reported as to what transpires within the host epithelial cell during infection.

To investigate if *Cryptosporidium* induces an epithelial cell  $\text{Ca}^{2+}$  influx that activates PKC $\alpha$  will require a multipronged approach. First, we must determine if *Cryptosporidium* infection causes a  $\text{Ca}^{2+}$  influx in the host cell. To accomplish this, we employed a fluorescent calcium indicator, fluo-4-AM, to label  $\text{Ca}^{2+}$  in HCT-8 intestinal epithelial cells (calcium indicators are commercially available molecules that fluoresce once bound to free  $\text{Ca}^{2+}$ ). Following challenge with *C. parvum* sporozoites, we performed live-cell imaging of HCT-8 cells during the course of infection and compared intracellular fluorescence (fluo-4-AM bound to  $\text{Ca}^{2+}$ ) intensity over time prior to and following addition of the parasite. Given previous work with other apicomplexan parasites, *Toxoplasma gondii* and *Plasmodium* spp., noting the importance of calcium entry and signaling (Wasserman et al., 1982; Ojo et al., 2010; Pace et al., 2014) we expected *Cryptosporidium* infection to result in a rapid  $\text{Ca}^{2+}$  influx. Shown in **Fig. 4.1**, we labeled HCT-8 intestinal epithelial cells with a fluo-4-AM dye. As assay controls, we treated HCT-8 cells with  $\text{Ca}^{2+}$ -ionophore ionomycin or a recipe of ionomycin followed by treatment with  $\text{Ca}^{2+}$ -chelator BAPTA-AM. Ionomycin stimulates a  $\text{Ca}^{2+}$  influx increasing accessibility to free intracellular  $\text{Ca}^{2+}$  (Liu et al., 1978; Bennett et al., 1979;

Lorenzo and Raisz 1981). BAPTA-AM is a cell-permeant chelator with high selectivity for  $\text{Ca}^{2+}$  used in the manipulation of intracellular free  $\text{Ca}^{2+}$  (Tsien 1980; Ochs et al., 1985; Barritt and Lee 1985). We observed no difference in fluo-4-AM intensity when HCT-8 cells were treated with BAPTA-AM alone relative to vehicle controls suggesting steady-state cytosolic free  $\text{Ca}^{2+}$  is low (data not shown). Ionomycin was used as a positive control and significantly increased intracellular  $\text{Ca}^{2+}$  as expected (**Fig. 4.1A**). Following treatment with BAPTA-AM this abundance of intracellular free  $\text{Ca}^{2+}$  was extinguished (**Fig. 4.1A**). When fluo-4-AM labeled HCT-8 cells were exposed to *Cryptosporidium* sporozoites we observed a rapid (<2 minutes)  $\text{Ca}^{2+}$  influx. Maximum fluo-4 AM fluorescence intensity is reached in HCT-8 cells approximately 10 minutes after challenge with sporozoites (**Fig. 4.1A**). Statistical analysis comparing fluo-4 AM fluorescence intensity of individual HCT-8 cells for each experimental condition found significant differences relative to control (**Fig. 4.1B**). This preliminary data suggests *Cryptosporidium* induces a host cell  $\text{Ca}^{2+}$  influx, however, this does not prove that the resultant  $\text{Ca}^{2+}$  influx is essential for infection. To ascertain if host free intracellular  $\text{Ca}^{2+}$  is required for *Cryptosporidium* infection we can utilize calcium modulators, ionomycin and BAPTA-AM, prior to challenge with *Cryptosporidium*. If intestinal epithelial cell free intracellular  $\text{Ca}^{2+}$  is required for *Cryptosporidium* infection, BAPTA-AM treatment of HCT-8 cells will decrease infection, an analogous phenotype to our observations using PKC $\alpha$  antagonists. Furthermore, we expect this phenotype to be partially rescuable by replenishing HCT-8 cell free intracellular  $\text{Ca}^{2+}$ . In contrast, HCT-8 cells treated with ionomycin

before challenge with *Cryptosporidium* will show increased infection mirroring treatment with PKC $\alpha$  agonists. Overall, the findings from these experiments have linked *Cryptosporidium* to host intracellular Ca<sup>2+</sup> and aim to further deduce if host Ca<sup>2+</sup> is essential for *Cryptosporidium* early infection.

In **Fig. 4.1**, we observed a multicellular influx of Ca<sup>2+</sup> in response to *Cryptosporidium* infection. A possible explanation for this observation is a high infection rate as we challenged HCT-8 cells with an elevated MOI (20:1) of *Cryptosporidium* sporozoites than used traditionally to increase our likelihood of finding a Ca<sup>2+</sup> influx event. For reference, in our previous *in vitro* findings, at an MOI of 4:1 we report 26.5%  $\pm$  2.13 of HCT-8 cells infected with *Cryptosporidium* sporozoites. Thereby increasing the MOI to 20:1, five times the standard infectious dose, we expect 100% of HCT-8 cells to be *Cryptosporidium* infected. However, the *Cryptosporidium* sporozoites were not labeled prior to live-cell imaging and therefore we are unable to quantify infection rate as it correlates with Ca<sup>2+</sup> influx. Future experiments will include labeling of *Cryptosporidium* sporozoites to allow for tractability as well as the distinction of *C. parvum*-infected cells to compare intracellular fluo-4 AM fluorescence intensity to uninfected cells from the same well. Alternatively, the multicellular influx of Ca<sup>2+</sup> in response to *Cryptosporidium* infection may be the result of a communication between HCT-8 intestinal epithelial cells. In Chapter 3, we report *in vitro* PKC $\alpha$  activation in *Cryptosporidium*-infected cells as well as neighboring uninfected cells. As we hypothesize activation of host PKC $\alpha$  occurs via binding to Ca<sup>2+</sup>, the observation of a multicellular increase in host intracellular Ca<sup>2+</sup> as a cell: cell communication

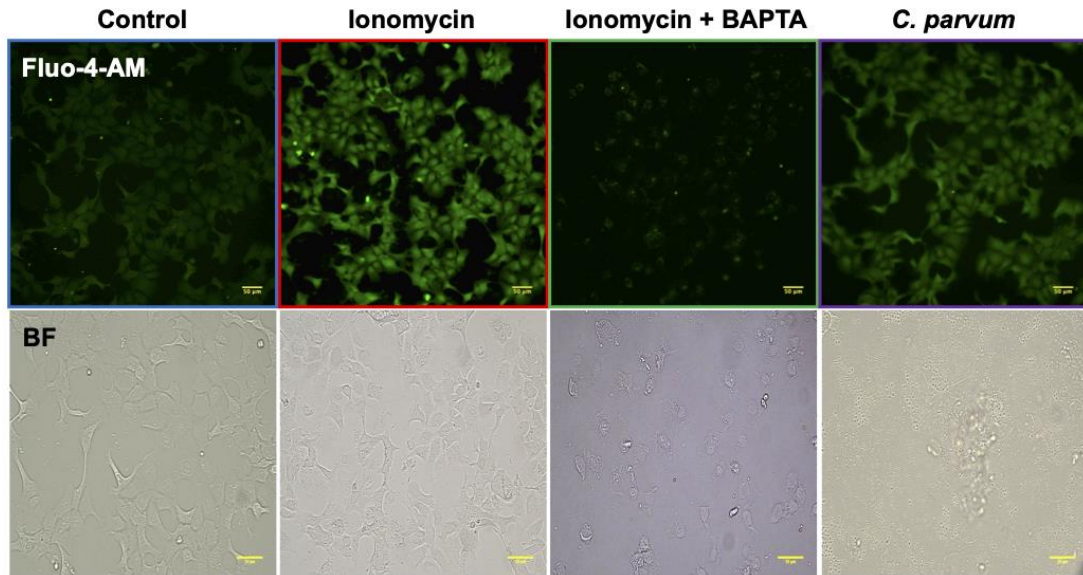
event has biological plausibility. Taken together, these findings suggest *Cryptosporidium* induces an influx of  $\text{Ca}^{2+}$  which inactive PKC $\alpha$  binds to causing activation and translocation to the host membrane in the *Cryptosporidium*-infected cell and uninfected neighboring cells.

When measuring intracellular  $\text{Ca}^{2+}$  in response to *Cryptosporidium* we fell short of differentiating sporozoite adherence from invasion and thus cannot determine the contribution of these life-cycle stages on  $\text{Ca}^{2+}$  influx. As we have now linked *Cryptosporidium* to an influx of  $\text{Ca}^{2+}$ , we can explicitly delineate the role of each life-cycle stage in this process. During *Cryptosporidium* sporozoite adherence to intestinal epithelial cells, parasite surface lectins interact with host cell surface sugars (Joe et al., 1994; Nesterenko et al., 1999; Bhat et al., 2007). Like *E. histolytica*, one hypothesis is that lectin-surface sugar interactions cause a host intracellular signaling cascade leading to a  $\text{Ca}^{2+}$  influx (Rawal et al., 2005). To test this interaction, we can expose HCT-8 intestinal epithelial cells to *Cryptosporidium*-derived lectins and then measure intracellular free  $\text{Ca}^{2+}$ . If treatment with *Cryptosporidium*-derived lectins replicates the influx of  $\text{Ca}^{2+}$  when challenged with *Cryptosporidium* sporozoites then this implicates *Cryptosporidium* adherence as responsible. If no  $\text{Ca}^{2+}$  influx is observed after treatment with *Cryptosporidium*-derived lectins, then the triggering event must occur after initial adherence and therefore during invasion. To explicitly test *Cryptosporidium* invasion as the culprit of host  $\text{Ca}^{2+}$  influx, we can first compare intracellular  $\text{Ca}^{2+}$  after challenge with heat-killed or live *Cryptosporidium* sporozoites. Exposure to high heat renders *Cryptosporidium* sporozoites inactive

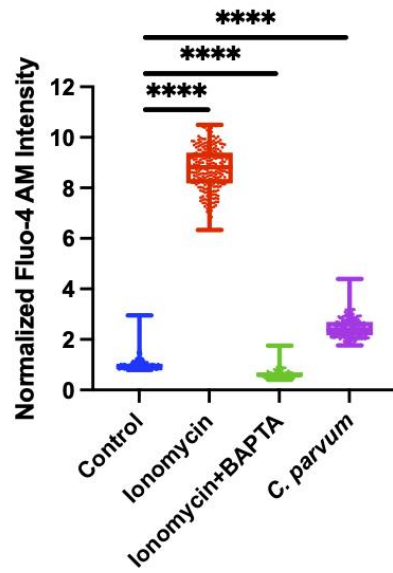
and thereby unable to seize host machinery necessary to facilitate invasion (Moriarty et al., 2005). If sporozoite invasion is responsible for the influx of  $\text{Ca}^{2+}$  we expect HCT-8 cells challenged with heat-killed sporozoites to be phenotypically similar to uninfected controls. Notably, in apicomplexan parasite invasion, the apically localized rhoptry bulb has been implicated (Dubremetz et al., 1998; Guérin et al., 2021). However, the complete catalog of rhoptry proteins expressed by *Cryptosporidium* spp. and the function of many identified rhoptry proteins remain uncharacterized. To explore sporozoite rhoptry protein secretion as the signal for host  $\text{Ca}^{2+}$  influx during invasion we can screen reported *Cryptosporidium*-expressed rhoptry genes as well as homologs from more documented apicomplexan parasites for binding to regulators of intracellular calcium. In this case, after binding to the host epithelial cell the sporozoite secretes a rhoptry protein across the host-parasite interface which instigates a host  $\text{Ca}^{2+}$  influx ultimately activating PKC $\alpha$ . Altogether, this work will uncover the stage for the *Cryptosporidium*-induced host  $\text{Ca}^{2+}$  influx and if host free intracellular  $\text{Ca}^{2+}$  is a requisite for infection.

Figure 4.1

A



B



**Figure 4.1: *C. parvum* infection signals a host intestinal epithelial cell  $\text{Ca}^{2+}$  influx.** Human ileocecal adenocarcinoma (HCT-8) cells were seeded on glass chamber microslides. After 24 h, cells were incubated with a fluo-4 AM, a cell-permeable fluorescent  $\text{Ca}^{2+}$  indicator for 30 min at 37°C. The fluo-4 AM indicator was removed and replaced with assay medium (Chapter 3.2 Materials and Methods). Maximum fluo-4 AM fluorescence intensity from live-cell images was measured for each experimental condition. A) 20x objective respective images from fluo-4 AM labeled HCT-8 intestinal epithelial cells treated with DMSO, ionomycin, ionomycin followed by BAPTA-AM, or *Cryptosporidium* at an MOI of 20:1 (sporozoite: cell). B) Quantification of maximum fluo-4 AM fluorescence intensity for each condition normalized to control. For figure B, asterisks denote results of a one-way ANOVA and Tukey's post hoc test (\* $P < 0.05$ ; \*\* $P < 0.01$ ; \*\*\* $P < 0.001$ ; \*\*\*\* $P < 0.00001$ ). N=92-314 cells/condition.

We hypothesize activation of host PKC $\alpha$  by *Cryptosporidium* is through a parasite induction of a host cell Ca $^{2+}$  influx, increasing the availability of free intracellular Ca $^{2+}$  for inactive PKC $\alpha$  to interact. This interaction can be studied further using two independent yet interactive analyses. To investigate a direct relationship between free intracellular Ca $^{2+}$  and activation of PKC $\alpha$ , we can generate a PKC $\alpha$  reporter intestinal epithelial cell line. By transiently transfecting HCT-8 cells with a plasmid expressing a wild-type construct of PKC $\alpha$  (PKC $\alpha$ -WT) tagged with hemagglutinin (HA) (Soh et al., 2003) we can track the localization of HA-tagged PKC $\alpha$ -WT (as a proxy for PKC $\alpha$ ) with fluorescent HA labeling antibodies (Zhao et al., 2019). Originally developed for imaging protein dynamics *in vivo*, these anti-HA probes have high affinity and specificity for HA epitopes (Zhao et al., 2019). To follow the influx of Ca $^{2+}$  over time, we can label transfected HA-tagged PKC $\alpha$ -WT plasmid HCT-8 cells with fluo-4 AM. Then, we can infect with *Cryptosporidium* sporozoites and live-cell image HA-tagged PKC $\alpha$  and intracellular Ca $^{2+}$ . If the influx of Ca $^{2+}$  caused by *Cryptosporidium* is the catalyst for PKC $\alpha$  activation, then after *Cryptosporidium* infection Ca $^{2+}$  will enter the host cell, colocalize with cytosolic HA-tagged PKC $\alpha$ , and this HA-PKC $\alpha$ -Ca $^{2+}$  complex will translocate to the plasma membrane. An alternative approach to further define the relationship between influx of Ca $^{2+}$  and PKC $\alpha$  is to perform western blotting of subcellular fractions of HCT-8 cells treated with ionomycin, BAPTA-AM, *Cryptosporidium*, or BAPTA-AM followed by *Cryptosporidium*. As Ca $^{2+}$  activates and translocates PKC $\alpha$  to the membrane, we expect ionomycin to increase membrane-associated PKC $\alpha$  relative to controls. Ionomycin has been

found to synergize with phorbol esters in promoting activity of the typical PKC isoforms (Altman et al., 1992; Genot et al., 1995; Salerno et al., 2017) however the contribution of ionomycin solely in the activation of PKC $\alpha$  has not been reported. For BAPTA-AM treated cells, we expect a decrease in membrane-associated PKC $\alpha$  relative to controls. This phenotype has been reported previously as treatment with BAPTA-AM blocks PKC $\alpha$  activation and translocation in a range of cell types (Li et al., 2002; Dieter et al., 1993; Zhou et al., 2006; Chow et al., 2008). In our previous analysis, we observed HCT-8 cells treated with *Cryptosporidium* exhibit increased PKC $\alpha$  in the membrane fraction when compared to uninfected controls. Hence, if a Ca<sup>2+</sup> influx is required for activation of PKC $\alpha$  during *Cryptosporidium* infection we expect a reduction in membrane-associated PKC $\alpha$  for cells treated with BAPTA-AM and then *Cryptosporidium* when compared to *Cryptosporidium*-only treated cells.

If the influx of Ca<sup>2+</sup> is demonstrated to not affect activation of PKC $\alpha$  by *Cryptosporidium*, there remain alternative mechanisms *Cryptosporidium* may impose to accomplish this. Activation of PKC $\alpha$  may occur through a direct interaction with a secreted parasite effector (i.e. rhoptry bulb protein). Notably, host protein LMO7 which also has links to host cell F-actin was found to interact with *Cryptosporidium* rhoptry protein 1 in the host cytoplasm and influence invasion (Du et al., 2019; Guérin et al., 2021). Furthermore, LIM domains are regulated via protein-protein interactions and was identified as a PKC-interacting protein by a yeast 2-hybrid screen *in vitro* (Kuroda et al., 1996). Thus, this suggests LIM domain-containing proteins such as LMO7 may serve as a target of

PKC activity during *Cryptosporidium* invasion and introduces an indirect interaction between parasite ROP1 and host PKC $\alpha$  through regulation of the intermediary host protein LMO7. Depending on our findings from Ca<sup>2+</sup> influx experiments, examining rhoGTPase protein binding interactions with PKC $\alpha$  will serve as an alternative approach. Altogether, the findings from the experiments laid out here will answer the role, if any, host influx of Ca<sup>2+</sup> exerts on PKC $\alpha$  activity and resultant *Cryptosporidium* infection.

#### **4.3.2 PKC $\alpha$ regulation of F-actin as a mechanism of action**

We show here that *Cryptosporidium* activates host PKC $\alpha$  and that host PKC $\alpha$  activity is directly related to susceptibility. While we have observed that host PKC $\alpha$  activity facilitates *Cryptosporidium* adherence and invasion, a few unanswered questions remain as to the mechanism of PKC $\alpha$  activity and prospective intermediate targets.

Remodeling of host F-actin is a requirement for progression of the *Cryptosporidium* life cycle and without it, entry of the parasite into the host cell is blocked (Elliot et al., 2000; Elliot et al., 2001). During invasion, F-actin traffics to the host-parasite interface colocalizing with the *Cryptosporidium* sporozoites (Chen et al., 2003). PKC $\alpha$  has been connected to regulation of cytoskeleton-driven processes in cells (Hryciw et al., 2005; Peng et al., 2011) and now, regulation of *Cryptosporidium* sporozoite adherence and invasion of intestinal epithelial cells. Therefore, we hypothesize host cell PKC $\alpha$  mediates adherence and invasion through the regulation of F-actin. To determine if PKC $\alpha$  in this manner, during infection, we can visualize F-actin colocalization with

*Cryptosporidium* post-treatment with pharmacologic PKC $\alpha$  agonists or antagonists by IF microscopy. Phalloidin, a toxin with high selectivity for F-actin, can be used to label F-actin in *Cryptosporidium*-infected cells (Huang et al., 1992). If PKC $\alpha$  is responsible for remodeling of host F-actin during *Cryptosporidium* infection, we expect to observe reduced and increased colocalization of F-actin with *Cryptosporidium* for PKC $\alpha$  antagonists and PKC $\alpha$  agonists, respectively. Additionally, we can directly probe this interaction by following F-actin accumulation using live-cell imaging. To do this we can generate a stable transgenic intestinal epithelial cell model expressing lifeact, a 17-amino-acid peptide that stains F-actin without disturbing actin dynamics, fused to a fluorescent protein (Riedel et al., 2008; Guérin et al., 2021). Using this approach, we can collect a time-lapse of infection following F-actin during *Cryptosporidium* adherence and invasion after treatment with PKC $\alpha$  agonists or antagonists.

If we observe differences in F-actin during *Cryptosporidium* infection post-treatment with PKC $\alpha$  modulators, we will explore known regulators of F-actin during *Cryptosporidium* invasion for potential interactions with PKC $\alpha$ . Several F-actin-associated proteins are involved during *Cryptosporidium* invasion and many of these proteins are regulated by PKC $\alpha$ . The actin-associated proteins observed at the parasite adherence site include neural Wiskott-Aldrich syndrome protein (N-WASP) and the Arp2/3 complex (Elliott et al., 2001). Notably, localization of Arp2/3 was reported at every site of invasion (Elliott et al., 2001). Additionally, activation of the tyrosine kinase c-Src and phosphatidylinositol 3-kinase (PI3K)

leading to subsequent recruitment of host Rho-GTPase Cdc42-substrate, frabin, has been observed during invasion (Chen et al., 2004b). Activation of Cdc42 is necessary for recruitment and activation of N-WASP and the Arp2/3 complex (Chen et al., 2004a; Chen et al., 2004b). Inhibition of host cell Arp2/3 (Elliott et al., 2001), PI3K (Forney et al., 1999; Chen et al., 2003), c-Src, and N-WASP (Chen et al., 2004a) independently resulted in reduced invasion, supporting a role for host actin polymerization (**Fig. 4.2**).

To investigate the activity of PKC $\alpha$  on F-actin-associated proteins previously implicated in *Cryptosporidium* invasion, we can inhibit PKC $\alpha$  activity and then probe for these messengers. Activation of each of these hypothesized targets regulated by PKC $\alpha$  can be measured: MARCKS, PI3K, and c-Src (Überall et al., 1997; Brandt et al., 2002; Li et al., 2013; Ziemba et al., 2016; Hsu et al., 2018). Since PI3K and c-Src are recruited to the host-parasite interface during invasion, we can compare the colocalization of each kinase with *Cryptosporidium* sporozoites in HCT-8 cells treated with PKC $\alpha$  antagonists relative to controls. However, there remains no reported role for activity of MARCKS during *Cryptosporidium* infection, rather independently PKC phosphorylation of MARCKS was found to increase PI3K activity (Ziemba et al., 2016). In this pathway, recruitment and activation of PI3K is accomplished by release of PIP<sub>2</sub> from MARCKS. Thus, free intracellular PIP<sub>2</sub> serves as a substrate for PI3K to control many processes at the membrane including cytoskeletal organization (Ziemba et al., 2016; Czech 2000). To determine if regulation of MARCKS by PKC $\alpha$  impacts actin rearrangements during invasion we can measure

intracellular PIP<sub>2</sub> in the presence or absence of *Cryptosporidium*. Using IF microscopy, we can label HCT-8 cells with antibodies specific to PIP<sub>2</sub> and MARCKS and then measure intracellular colocalization. We previously reported activation of PKC $\alpha$  during *Cryptosporidium* invasion and PKC $\alpha$  regulates MARCKS (Ziemba et al., 2016). If activation of PI3K occurs through MARCKS regulation by PKC $\alpha$  then we expect *Cryptosporidium* invasion to reduce colocalization of MARCKS with PIP<sub>2</sub>, an indicator of PIP<sub>2</sub> release from MARCKS. Furthermore, if PKC $\alpha$  induces the PIP<sub>2</sub> release from MARCKS, this event will be hindered in the presence of PKC $\alpha$  antagonists. Understanding the mechanism of PKC $\alpha$  activity during *Cryptosporidium* infection has the potential to uncover additional host factors participating in pathogenesis and relay how the parasite seizes host cell machinery.

Figure 4.2

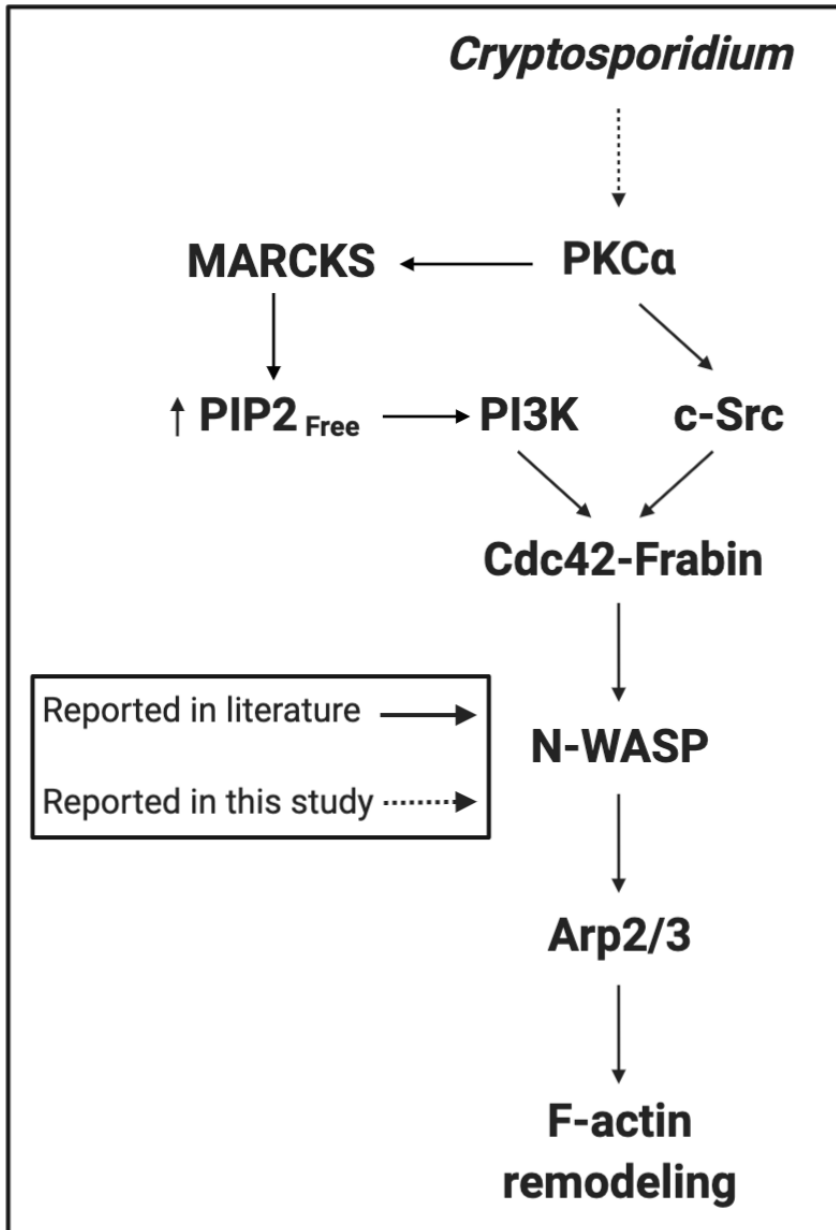


**Figure 4.2: Hypothetical pathway for *Cryptosporidium* activation of PKC $\alpha$  and F-actin remodeling.** *Cryptosporidium* infection results in activation and translocation of host intestinal epithelial cell PKC $\alpha$  to the plasma membrane, which leads to a PKC $\alpha$ -induced phosphorylation cascade and activation of kinases, c-Src and PI3K. This causes recruitment of Cdc42 and activation of N-WASP, leading to activation of the Arp2/3 complex and subsequent F-actin cytoskeletal remodeling required for complete parasite invasion.

### 4.3.3 A genetic role for PKC $\alpha$ in the host immune response

Here, we report that PKC $\alpha$  activity promotes *C. parvum* infection of intestinal epithelial cells however the role of PKC $\alpha$  in immune cells warrants further exploration. Our work thus far closely examined *Cryptosporidium* infection in an *in vitro* setting, an intrinsic limitation of which is the absence of input from immune cells which have an established role in protection. We, therefore, are unaware if PKC $\alpha$  plays a role in the immune cell response to *Cryptosporidium* infection and clearance of disease. PKC $\alpha$  was found to be physiologically important in signaling pathways necessary for T cell-dependent IFN $\gamma$  production (Pfeifhofer et al., 2006). CD4 $^+$  T cells are a primary source of IFN $\gamma$  secretion for the adaptive immune system and immunologically protect against *Cryptosporidium* infection in mice (Ungar et al., 1991). Furthermore, IFN $\gamma$  has repeatedly been identified as the most critical host cytokine secreted during infection due to its high activity against cryptosporidiosis (Griffiths et al., 1998; White et al., 2000). Hence, a secondary role for PKC $\alpha$  in the host response to infection may be as a gatekeeper of IFN $\gamma$  secretion from CD4 $^+$  T cells during cryptosporidiosis. PKC $\alpha$  is also involved in the proliferation and differentiation of immature thymocytes (Iwamoto et al., 1992; Michie et al., 2001). Notably, these thymocytes extensively produce interleukin-2 (IL-2) implicating PKC $\alpha$  as a second messenger of the T cell receptor (Iwamoto et al., 1992). High IL-2 levels have been reported in response to *Cryptosporidium* infection (Gomez Morales et al., 1999; Kaushik et al., 2009). Lastly, PKC $\alpha$  is a positive regulator of Th17 cell effector function with *PRKCA*-deficient cells lacking IL-17A production (Meisel et

al., 2013). In *C. parvum* infection *in vivo*, the Th17 response has been observed with increased levels of IL-17 mRNA and Th17-related cytokines reported in gut-associated lymphoid tissue of BALB/c mice (Zhao et al., 2015).

A commercially available *PRKCA* deletion mouse can be used to study *Cryptosporidium* infection in the complete absence of PKC. For these mice, the exon encoding the PKC $\alpha$  ATP-binding region was replaced with a neomycin resistance cassette (Braz et al., 2004). Notably, our *in vitro* analysis demonstrated pharmacologically the role of PKC $\alpha$  during infection, while use of a murine model will provide genetic input. We can use mouse-adapted *C. parvum* oocysts expressing nanoluciferase (Nluc) (provided by Dr. B. Striepen University of Pennsylvania, Philadelphia, PA) to compare infection between sex- and age-matched *PRKCA* deletion, *PRKCA* heterozygous, and *PRKCA* wild-type mice. The Nluc reporter system allows for quantification of parasite burden and shedding by measuring luminescence in gut and stool, respectively. (Vinayak et al., 2016). To delineate the role of PKC $\alpha$  activity in the immune cell response to *Cryptosporidium* infection we can examine immune cells from *PRKCA* deletion and *PRKCA* wild-type mice. To investigate the relationship between CD4<sup>+</sup> T cells and PKC $\alpha$ , we can challenge *PRKCA* deletion mice with *Cryptosporidium* and measure IFN $\gamma$  mRNA expression, IFN $\gamma$  cytokine production, and proportion of Th1 cells relative to *Cryptosporidium*-infected wild-type controls. To test the role of PKC $\alpha$  in thymocyte proliferation, we can measure IL-2 production and monitor the differentiation of immature thymocytes over the course of infection in *PRKCA* deletion and *PRKCA* wild-type mice. To examine the Th17 response, we can

challenge *PRKCA* deletion mice with *Cryptosporidium* and measure expression of IL-17 mRNA, Th17-related cytokines (e.g., IL-17A, IL-17F, IL-21, IL-22, and IL-26), and proportion of Th17 cells relative to *Cryptosporidium*-infected wild-type mice. Since PKC $\alpha$  positively regulates effector T cell function, we expect *PRKCA* deletion mice to show decreased levels of these protective T cell lineages (e.g., Th1 and Th17) and related cytokines, coinciding with increased parasite burden. Regardless, the putative contribution of host PKC $\alpha$  in the T cell response to cryptosporidiosis is an unexplored area of enteric infection research.

Investigating *Cryptosporidium* infection in the absence of *PRKCA*, we can validate our *in vitro* pharmacologic findings by measuring parasite burden in the mouse intestinal epithelium. As activity of PKC $\alpha$  exhibited a direct relationship with *Cryptosporidium*, we expect the *PRKCA* deletion to confer resistance to infection. Based on genetic associations in heterozygous children (Wojcik et al., 2020), we might also expect an allele-dosage effect in *PRKCA* heterozygous mice. We can further examine sections of small intestinal tissue by performing immunohistochemistry to compare histopathology between the distinct *PRKCA* genotyped mice. If PKC $\alpha$  plays a role in *Cryptosporidium* pathogenesis, in *PRKCA* deletion mice we expect a reduction in villus blunting (increased villus-crypt height ratio), lymphocyte infiltration, epithelial dysplasia, villus hyperplasia, and parasites in association with the intestinal epithelium.

In a previous study of expression profiles following infection, *PRKCA* was identified as the most significantly down-regulated gene in *C. parvum*-infected HCT-8 cells (Liu et al., 2018). To explore if *Cryptosporidium* infection alters

*PRKCA* expression *in vivo*, we can compare mRNA expression of *Cryptosporidium*-infected relative to uninfected wild-type mice. To accomplish this we can collect fecal stool samples from genotyped mice daily and extract total RNA, over a 20-day infection course. An advantage of examining fecal material is the analysis of *PRKCA* expression at the site of infection as opposed to quantification of *PRKCA* expression systemically. Moreover, we can compare PKC $\alpha$  activity in the intestinal epithelium of *Cryptosporidium*-infected mice relative to uninfected wild-type mice using IFA for PKC $\alpha$  membrane localization.

The intestinal epithelium exists at the interface of microbes and the immune system. The dialogue between intestinal epithelial and immune cells during various disease states is increasingly important (Soderholm et al., 2019). Intestinal epithelial cell secretion of immunomodulatory molecules retinoic acid, transforming growth factor (TGF)- $\beta$ , and IL-10 have been observed to affect a broad range of immune cells (Ihara et al., 2017; Oliveira et al., 2018; Andrews et al., 2018). The latter two represent immune-suppressive cytokines and exhibit importance in the regulation of immune homeostasis (Komai et al., 2018). In addition to these cytokines, intestinal epithelial cells secrete IL-15, a ligand that activates human natural killer cells, a significant contributor to innate immune system IFN $\gamma$  production (Zhu et al., 2020; Carson et al., 1994; Lodolce et al., 1998; Kennedy et al., 2000). Furthermore, in response to microbial attachment, intestinal epithelial cells have also been observed to secrete serum amyloid A1 promoting maturation of Th17 cells and IL-17 production which already have an established connection to PKC $\alpha$  (Meisel et al., 2013; Atarashi et al., 2016). To

investigate the role of PKC $\alpha$  activity in intestinal epithelial cell crosstalk with immune cells, we can conduct single-cell RNA-sequencing analysis of murine small intestines in homeostasis and during infection to detect differentially expressed genes. Concurrently, we can also measure levels of secreted cytokines TGF- $\beta$ , IL-10, retinoic acid, IL-15, and serum amyloid A1 in the gut of *PRKCA* deletion relative to wild-type mice.

Altogether, the analyses laid out in this section will provide a steppingstone to address the role of host PKC $\alpha$  in the immune response to cryptosporidiosis. Further characterization of PKC $\alpha$  in the intestinal epithelium and immune cells is instrumental as a tool in immunological diagnostics and understanding the contributions of the host responses to disease.

#### **4.3.4 Functional differences in HLA class I and II alleles**

HLA refers to a set of genes that encode the major histocompatibility complex (MHC) proteins in humans. In this thesis, we report novel associations between HLA alleles and susceptibility to enteric pathogens during the first year of life. HLA alleles encode cell surface molecules capable of presenting peptide antigens to the T cell receptor (TCR) on T cells. Following specialized binding of the TCR to pathogenic-derived peptides, the appropriate repertoire of T cells expands which in turn impacts effector properties (Rudolph et al., 2006; Springer et al., 2020). To recognize such a diverse breadth of peptide antigens and generate the appropriate response, the HLA locus is the most polymorphic cluster of genes in the human genome (Robinson et al., 2014). Therefore, an individual's ability to defend against a pathogen is dependent on their genotype.

An important next step to build on our findings is to confirm our HLA allele-pathogen associations at the molecular level. We can purify the HLA molecules encoded by the five HLA alleles identified in our study: *A\*24:02*, *A\*24:17*, *B\*15:01*, *B\*38:02*, and *DQA1\*01:01* from transgenic mice expressing human HLA molecules. Methods for purification of class I and II molecules from mice and humans have been described previously (Buus et al., 1986; Buus et al., 1987; Buus et al., 1988; O'Sullivan et al., 1990; Sette et al., 1994). Briefly, HLA molecules are purified from cell lines expressing the HLA allele of interest by affinity chromatography (Sidney et al., 2013). Pathogen-derived peptide antigens can be synthesized *in vitro* and radiolabeled (Greenwood et al., 1963). The purified HLA molecules and pathogen-derived peptide antigens can be introduced and the total labeled peptide antigen bound can be measured using gel filtration or captured with monoclonal antibodies (Sidney et al., 2013). We expect for an HLA allele found to have a deleterious association with an enteric pathogen, the encoded HLA molecule will display a lower binding affinity for the pathogen-derived peptide antigen. For example, in the case of *HLA B\*15:01* associated with increased risk of astrovirus infection in our analysis, the encoded *HLA B\*15:01* molecule may show a poor affinity for astrovirus-derived peptide antigens thus leading to poor TCR presentation. It is also possible for the *HLA B\*15:01* molecule to have a normal binding affinity for the astrovirus-derived peptide antigen however, presentation to the TCR induces an ineffective immune cell response. Conducting this analysis will allow us to validate the HLA allele-pathogen associations we previously reported.

Fundamentally, murine MHC class I and II are different from that of human MHC class I and II (i.e., HLA class I and II) leading to difficulty using mice to evaluate MHC. However, transgenic mouse strains have been developed to study cytotoxic T cell responses and used as a model to develop human vaccines (Epstein et al., 1989; Le et al., 1989). More recently, knock-in experiments to generate transgenic mice to evaluate the induction of the CD8+ T cell response to viral epitopes were accomplished (Harada et al., 2017). To study the presentation of pathogen-derived peptide antigens by the encoded HLA molecules we can generate a series of HLA class I and II knock-in mouse strains. Fortunately, Harada and colleagues have produced an HLA-A\*24:02 knock-in mouse which in our genetic study was highly associated with protection from EAEC infection. With permission, we can use this published transgenic mouse to evaluate the CD8+ T cell response to EAEC-derived peptide antigens. Based on our HLA findings, we expect EAEC infection of A\*24:02 knock-in mice to result in an expansion of CD8+ T cells expressing a TCR with a high affinity for a protective EAEC-derived peptide antigen and clearance of infection.

Our study of HLA associations with enteric infection found seven associations that maintained statistical significance after correction for multiple comparisons. However, there exist 23 other HLA allele-pathogen associations that were ultimately not investigated further (**Fig. 2.1**). Furthermore, the highly associated HLA alleles only corresponded with 5 of the 12 enteric pathogens analyzed. Though the remaining HLA associations did not pass the threshold for significance in our cohort, the associates may have relevance in future studies.

Due to the limited size of our cohort, these HLA associations warrant validation in additional genetic studies of separate ethnic groups to understand the relevance in the context of all children. Overall, the HLA allele-pathogen associations this study has reported may serve as a reference for future HLA-infection genetic association studies in an unrelated population.

Overall, our comprehension of how host cells recognize, present, and respond to pathogen-derived peptide antigens will provide insight into adaptive immunity and for the development of targeted therapeutics.

#### **4.4 Final Conclusions**

The nature of the host response to foreign pathogens is integral for protection against an array of diseases. However, the intensity of this response depends on pathogen virulence as well as an interplay between the host's innate and adaptive immune systems. Characterizing the role of distinct host cells during enteric pathogenesis can help to identify mechanisms facilitating protection through manipulation of these responses and concurrently inform us on the requisite pathways to promote disease.

*Cryptosporidium spp.* infection is a leading cause of diarrhea globally, with diarrhea responsible for over 1 million deaths annually (GBD Diarrheal Disease Collaborators 2017). *Cryptosporidium* was recognized as the second most common cause of diarrhea-associated mortality after rotavirus in children under 5 years of age (GBD Diarrheal Disease Collaborators 2017). Efforts to improve therapeutics for cryptosporidiosis are under development however no options have been approved by the FDA to date (Hayley et al., 2015). While the current

treatment, nitazoxanide, has proven beneficial in the management of cryptosporidiosis in healthy adults, its limited efficacy in immunocompromised patients paired with its unknown safety in infants warrants efforts toward a more effective drug. In the absence of a viable treatment option, policies have been implemented in areas most endemic to reduce cases of cryptosporidiosis, such as filtration and treatment of wastewater (Nasser et al., 2016). The causes for variability in severity of cryptosporidiosis are undetermined and therefore prove problematic in identifying those persons most at-risk for severe disease. Hence, the identification of host factors mediating infection and the development of host-targeted therapeutics against *Cryptosporidium* is critical in the management of this diarrheal disease. The data we report here shows host PKC $\alpha$  mediates *Cryptosporidium* infection and suggests localized targeted inhibition of PKC $\alpha$  may serve as a satisfactory option for pre-exposure prophylaxis.

Enteric infections have a particularly detrimental effect during early childhood leading to long-lasting health deficits through poor nutritional absorption, diarrheal illness, disturbance of natural intestinal flora, and long-term inflammation (George et al., 2018). Work to improve diagnosis, prevention, and treatment of enteric infections with a high burden in child populations is a highly important area of research. Links between HLA and SNPs with susceptibility to infectious diseases have been found across the human genome (Kirkpatrick et al., 2008; Lopalco et al., 2010; Sveinbjornsson et al., 2016; Wojcik et al., 2018; Wojcik et al., 2020). Efforts to target these identified gene products offer a novel strategy for disease resistance. Historically the most well-characterized of which

is the targeting of human CCR5 as a component of HIV-1 therapy, developed from the original discovery that individuals with particular CCR5 gene mutations are resistant to early stages of HIV infection (Choe et al., 1996, Liu et al., 1996, Simmons et al., 1996, Lopalco et al., 2010). Studying the structure and binding affinity of HLA molecules and the immune response to the pathogen-derived peptide antigens presented will offer an understanding of more effective vaccine development for early childhood disease.

Our analyses support HLA genetics as a mediator of enteric infection during the first year of life. Further exploration into these HLA allele-pathogen associations is warranted as allele frequencies are often population-based (Mack et al., 2009). HLA typing as a genetic test to collect information regarding a person's HLA variations in immunity is an established concept. HLA allele typing is routinely performed to identify matched donor bone marrow or cord blood for transplantation (Choo et al., 2007). Applying this concept to screening for at-risk HLA genes during infancy to determine susceptibility to infectious diseases is one approach. Additionally, the use of protective HLA molecules to develop a targeted therapeutic option for infection by modulating the host's immune response represents an alternative powerful tool.

In conclusion, the activity of proteins from host-expressed genes such as *PRKCA* and HLA loci are associated with susceptibility to enteric infections in infancy (**Fig. 4.3**). Here, we expand on a previous genetic analysis noting host PKC $\alpha$  activity as critical in adherence and invasion of intestinal epithelial cells by *Cryptosporidium in vitro*. Identification of conserved host cell components able to

interfere with pathogen susceptibility offers an advantage over current pathogen-directed agents due to the increased barrier of the pathogen to evolve and develop resistance. Therefore, we find it important to further study these interactions resulting in the protection of the host as this will at minimum increase our understanding of the host response. This work establishes yet another link between the host and infectious diseases and furthers our understanding of the mechanisms exercised by host cells in the generation of protection.

Figure 4.3

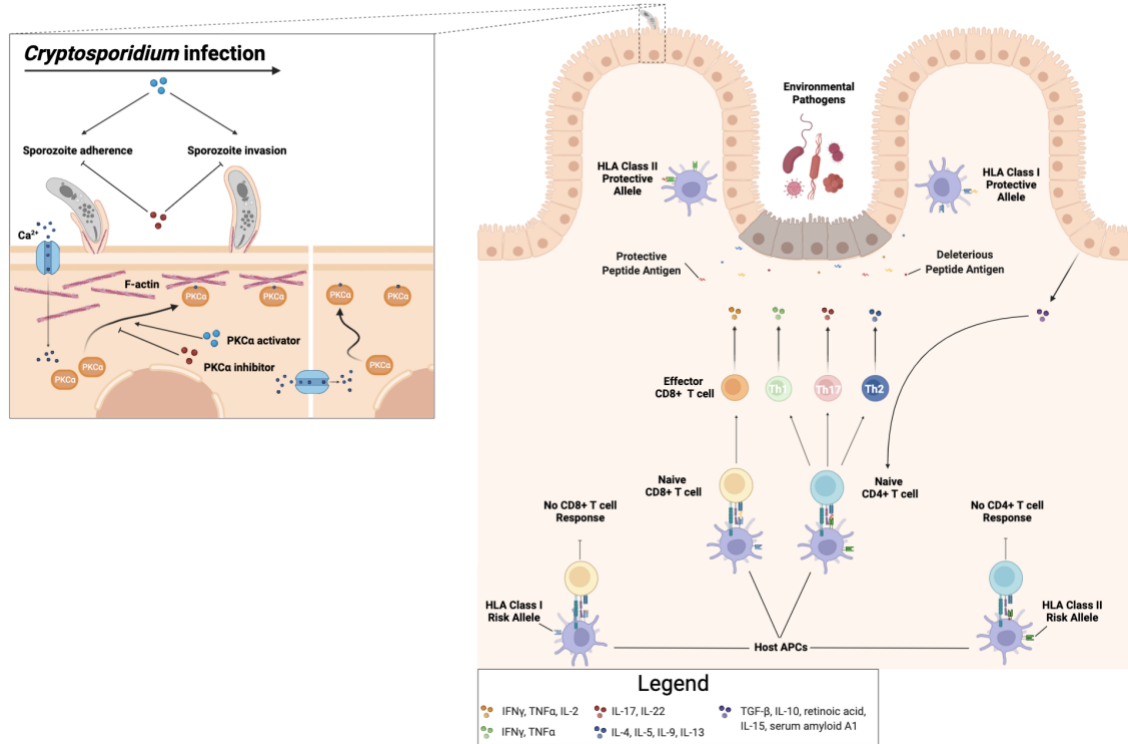


**Figure 4.3: Host factors underlying susceptibility to enteric infection. (A)**

*Cryptosporidium* adherence to the intestinal epithelium leads to rapid host intracellular free  $\text{Ca}^{2+}$  entry. This free intracellular  $\text{Ca}^{2+}$  activates and translocates PKC $\alpha$  from the cytoplasm to the plasma membrane. Here, PKC $\alpha$  can act to regulate F-actin at the site of parasite adherence resulting in rearrangement and invasion of the host intestinal epithelium. Residual free  $\text{Ca}^{2+}$  from the *Cryptosporidium*-infected cell traverses gap junctions to neighboring cells activating PKC $\alpha$  in these cells. Pharmacologic inhibitors and activators of PKC $\alpha$  decrease and increase *Cryptosporidium* adherence and invasion, respectively.

(B) The enteric infection leads to damage and apoptosis of the intestinal epithelium. Damage to the intestinal epithelium causes the secretion of signaling molecules that activate innate and adaptive immune responses to the infectious agent. Antigen-presenting cells (APCs) process and present pathogen-derived peptide antigens to naïve CD4 $^{+}$  and CD8 $^{+}$  T cells via cell surface HLA class I and II molecules. HLA class I and II alleles that encode protective molecules can recognize and present pathogen-derived peptide antigens resulting in activation and expansion of T cell subsets to combat the infectious agent. HLA class I and II alleles that encode molecules associated with increased risk of infection (1) cease to recognize a pathogen-derived peptide antigen and/or exhibit dysfunction in presentation or (2) recognize and present a pathogen-derived peptide antigen ineffective in producing a T cell response or that generate T cell subsets ineffective to clear the enteric infection.

## References

1. Abdullah, L.H., Conway, J.D., Cohn, J.A., Davis, C.W., 1997. Protein kinase C and Ca<sup>2+</sup> activation of mucin secretion in airway goblet cells. *Am J Physiol* 273, L201-210.
2. Ajene, A.N., Walker, C.L.F., Black, R.E., 2013. Enteric Pathogens and Reactive Arthritis: A Systematic Review of Campylobacter, Salmonella and Shigella-associated Reactive Arthritis. *J Health Popul Nutr* 31, 299–307.
3. Altman, A., Mally, M.I., Isakov, N., 1992. Phorbol ester synergizes with Ca<sup>2+</sup> ionophore in activation of protein kinase C (PKC)alpha and PKC beta isoenzymes in human T cells and in induction of related cellular functions. *Immunology* 76, 465–471.
4. Andrews, C., McLean, M.H., Durum, S.K., 2018. Cytokine Tuning of Intestinal Epithelial Function. *Front Immunol* 9, 1270.
5. Appanna, R., Ponnampalavanar, S., See, L.L.C., Sekaran, S.D., 2010. Susceptible and Protective HLA Class 1 Alleles against Dengue Fever and Dengue Hemorrhagic Fever Patients in a Malaysian Population. *PLOS ONE* 5, e13029.
6. Atarashi, K., Tanoue, T., Ando, M., Kamada, N., Nagano, Y., Narushima, S., Suda, W., Imaoka, A., Setoyama, H., Nagamori, T., Ishikawa, E., Shima, T., Hara, T., Kado, S., Jinnohara, T., Ohno, H., Kondo, T., Toyooka, K., Watanabe, E., Yokoyama, S., Tokoro, S., Mori, H., Noguchi, Y., Morita, H., Ivanov, I.I., Sugiyama, T., Nuñez, G., Camp, J.G., Hattori,

- M., Umesaki, Y., Honda, K., 2015. Th17 Cell Induction by Adhesion of Microbes to Intestinal Epithelial Cells. *Cell* 163, 367–380.
7. Baltuch, G.H., Dooley, N.P., Rostworowski, K.M., Villemure, J.G., Yong, V.W., 1995. Protein kinase C isoform alpha overexpression in C6 glioma cells and its role in cell proliferation. *J Neurooncol* 24, 241–250.
  8. Bar-Am, O., Yogev-Falach, M., Amit, T., Sagi, Y., Youdim, M.B.H., 2004. Regulation of protein kinase C by the anti-Parkinson drug, MAO-B inhibitor, rasagiline and its derivatives, in vivo. *J Neurochem* 89, 1119–1125.
  9. Bardou, P., Mariette, J., Escudié, F., Djemiel, C., Klopp, C., 2014. jvenn: an interactive Venn diagram viewer. *BMC Bioinformatics* 15, 293.
  10. Barnes, D.A., Bonnin, A., Huang, J.X., Gousset, L., Wu, J., Gut, J., Doyle, P., Dubremetz, J.F., Ward, H., Petersen, C., 1998. A novel multi-domain mucin-like glycoprotein of *Cryptosporidium parvum* mediates invasion. *Mol Biochem Parasitol* 96, 93–110.
  11. Barritt, G.J., Lee, A.M., 1985. Effects of electrical stimulation and an intracellular calcium chelator on calcium movement in suspensions of isolated myocardial muscle cells. *Cardiovasc Res* 19, 370–377.
  12. Benjamini, Y., Drai, D., Elmer, G., Kafkafi, N., Golani, I., 2001. Controlling the false discovery rate in behavior genetics research. *Behav Brain Res* 125, 279–284.

13. Bennett, J.P., Cockcroft, S., Gomperts, B.D., 1979. Ionomycin stimulates mast cell histamine secretion by forming a lipid-soluble calcium complex. *Nature* 282, 851–853.
14. Bentley, G., Higuchi, R., Hoglund, B., Goodridge, D., Sayer, D., Trachtenberg, E.A., Erlich, H.A., 2009. High-resolution, high-throughput HLA genotyping by next-generation sequencing. *Tissue Antigens* 74, 393–403.
15. Besteiro, S., Dubremetz, J.-F., Lebrun, M., 2011. The moving junction of apicomplexan parasites: a key structure for invasion. *Cellular Microbiology* 13, 797–805.
16. Bhalla, M., Law, D., Dowd, G.C., Ireton, K., 2017. Host Serine/Threonine Kinases mTOR and Protein Kinase C- $\alpha$  Promote InIB-Mediated Entry of *Listeria monocytogenes*. *Infection and Immunity*.
17. Bhat, N., Joe, A., PereiraPerrin, M., Ward, H.D., 2007. Cryptosporidium p30, a galactose/N-acetylgalactosamine-specific lectin, mediates infection in vitro. *J Biol Chem* 282, 34877–34887.
18. Billker, O., Lourido, S., Sibley, L.D., 2009. Calcium-dependent signaling and kinases in apicomplexan parasites. *Cell Host Microbe* 5, 612–622.
19. Black, A., Black, J., 2013. Protein kinase C signaling and cell cycle regulation. *Frontiers in Immunology* 3, 423.
20. Blackwell J.M., Jamieson S.E., Burgner D., 2009. HLA and infectious diseases. *Clin Microbiol Rev* 22(2):370–385. 112800048–08.

21. Bonnin, A., Lapillonne, A., Petrella, T., Lopez, J., Chaponnier, C., Gabbiani, G., Robine, S., Dubremetz, J.F., 1999. Immunodetection of the microvillous cytoskeleton molecules villin and ezrin in the parasitophorous vacuole wall of *Cryptosporidium parvum* (Protozoa: Apicomplexa). *European Journal of Cell Biology* 78, 794–801.
22. Borowski, H., Clode, P.L., Thompson, R.C.A., 2008. Active invasion and/or encapsulation? A reappraisal of host-cell parasitism by *Cryptosporidium*. *Trends in Parasitology* 24, 509–516.
23. Borowski, H., Thompson, R.C.A., Armstrong, T., Clode, P.L., 2010. Morphological characterization of *Cryptosporidium parvum* life-cycle stages in an in vitro model system. *Parasitology* 137, 13–26.
24. Boulter-Bitzer, J.I., Lee, H., Trevors, J.T., 2007. Molecular targets for detection and immunotherapy in *Cryptosporidium parvum*. *Biotechnol Adv* 25, 13–44.
25. Bouzid, M., Hunter, P.R., Chalmers, R.M., Tyler, K.M., 2013. *Cryptosporidium* Pathogenicity and Virulence. *Clin Microbiol Rev* 26, 115–134.
26. Bouzid, M., Kintz, E., Hunter, P.R., 2018. Risk factors for *Cryptosporidium* infection in low and middle income countries: A systematic review and meta-analysis. *PLoS Negl Trop Dis* 12, e0006553.
27. Brandt, D., Gimona, M., Hillmann, M., Haller, H., Mischak, H., 2002. Protein Kinase C Induces Actin Reorganization via a Src- and Rho-dependent Pathway. *J. Biol. Chem.* 277, 20903–20910.

28. Braun, M.U., Mochly-Rosen, D., 2003. Opposing effects of  $\delta$ - and  $\zeta$ -protein kinase C isozymes on cardiac fibroblast proliferation: use of isozyme-selective inhibitors. *Journal of Molecular and Cellular Cardiology* 35, 895–903.
29. Braz, J.C., Gregory, K., Pathak, A., Zhao, W., Sahin, B., Klevitsky, R., Kimball, T.F., Lorenz, J.N., Nairn, A.C., Liggett, S.B., Bodi, I., Wang, S., Schwartz, A., Lakatta, E.G., DePaoli-Roach, A.A., Robbins, J., Hewett, T.E., Bibb, J.A., Westfall, M.V., Kranias, E.G., Molkentin, J.D., 2004. PKC- $\alpha$  regulates cardiac contractility and propensity toward heart failure. *Nature Medicine* 10, 248–254.
30. Bruns, R.F., Miller, F.D., Merriman, R.L., Howbert, J.J., Heath, W.F., Kobayashi, E., Takahashi, I., Tamaoki, T., Nakano, H., 1991. Inhibition of protein kinase C by calphostin C is light-dependent. *Biochem Biophys Res Commun* 176, 288–293.
31. Bulgin R., Arbeloa A., Goulding D., Dougan G., Crepin V.F., Raymond B., 2009. The T3SS effector EspT defines a new category of invasive enteropathogenic *E. coli* (EPEC) which form intracellular actin pedestals. *PLoS Pathog* 5(12)
32. Buus, S., Sette, A., Colon, S.M., Grey, H.M., 1988. Autologous peptides constitutively occupy the antigen binding site on Ia. *Science* 242, 1045–1047.

33. Buus, S., Sette, A., Colon, S.M., Jenis, D.M., Grey, H.M., 1986. Isolation and characterization of antigen-Ia complexes involved in T cell recognition. *Cell* 47, 1071–1077.
34. Buus, S., Sette, A., Colon, S.M., Miles, C., Grey, H.M., 1987. The relation between major histocompatibility complex (MHC) restriction and the capacity of Ia to bind immunogenic peptides. *Science* 235, 1353–1358.
35. Carson, W.E., Giri, J.G., Lindemann, M.J., Linett, M.L., Ahdieh, M., Paxton, R., Anderson, D., Eisenmann, J., Grabstein, K., Caligiuri, M.A., 1994. Interleukin (IL) 15 is a novel cytokine that activates human natural killer cells via components of the IL-2 receptor. *J Exp Med* 180, 1395–1403.
36. Castellanos-Gonzalez, A., Sparks, H., Nava, S., Huang, W., Zhang, Z., Rivas, K., Hulverson, M.A., Barrett, L.K., Ojo, K.K., Fan, E., Van Voorhis, W.C., White, A.C., 2016. A Novel Calcium-Dependent Kinase Inhibitor, Bumped Kinase Inhibitor 1517, Cures Cryptosporidiosis in Immunosuppressed Mice. *J Infect Dis* 214, 1850–1855.
37. Chatila, T., Silverman, L., Miller, R., Geha, R., 1989. Mechanisms of T cell activation by the calcium ionophore ionomycin. *The Journal of Immunology* 143, 1283–1289.
38. Checkley, W., Buckley, G., Gilman, R.H., Assis, A.M., Guerrant, R.L., Morris, S.S., Mølbak, K., Valentiner-Branth, P., Lanata, C.F., Black, R.E., Childhood Malnutrition and Infection Network, 2008. Multi-country analysis

of the effects of diarrhoea on childhood stunting. *Int J Epidemiol* 37, 816–830.

39. Checkley, W., Epstein, L.D., Gilman, R.H., Black, R.E., Cabrera, L., Sterling, C.R., 1998. Effects of *Cryptosporidium parvum* Infection in Peruvian Children: Growth Faltering and Subsequent Catch-up Growth. *American Journal of Epidemiology* 148, 497–506.
40. Checkley, W., White, A.C., Jaganath, D., Arrowood, M.J., Chalmers, R.M., Chen, X.-M., Fayer, R., Griffiths, J.K., Guerrant, R.L., Hedstrom, L., Huston, C.D., Kotloff, K.L., Kang, G., Mead, J.R., Miller, M., Petri, W.A., Priest, J.W., Roos, D.S., Striepen, B., Thompson, R.C.A., Ward, H.D., Van Voorhis, W.A., Xiao, L., Zhu, G., Houpt, E.R., 2015. A review of the global burden, novel diagnostics, therapeutics, and vaccine targets for *cryptosporidium*. *Lancet Infect Dis* 15, 85–94.
41. Chen, L., Hahn, H., Wu, G., Chen, C.H., Liron, T., Schechtman, D., Cavallaro, G., Banci, L., Guo, Y., Bolli, R., Dorn, G.W., Mochly-Rosen, D., 2001. Opposing cardioprotective actions and parallel hypertrophic effects of delta PKC and epsilon PKC. *Proc Natl Acad Sci U S A* 98, 11114–11119.
42. Chen, X.-M., Huang, B.Q., Splinter, P.L., Cao, H., Zhu, G., Mcniven, M.A., Larusso, N.F., 2003. *Cryptosporidium parvum* invasion of biliary epithelia requires host cell tyrosine phosphorylation of cortactin via c-Src. *Gastroenterology* 125, 216–228.

43. Chen, X.-M., Huang, B.Q., Splinter, P.L., Orth, J.D., Billadeau, D.D., McNiven, M.A., LaRusso, N.F., 2004. Cdc42 and the Actin-Related Protein/Neural Wiskott-Aldrich Syndrome Protein Network Mediate Cellular Invasion by *Cryptosporidium parvum*. *Infection and Immunity* 72, 3011–3021.
44. Chen, X.-M., Splinter, P.L., Tietz, P.S., Huang, B.Q., Billadeau, D.D., LaRusso, N.F., 2004. Phosphatidylinositol 3-kinase and frabin mediate *Cryptosporidium parvum* cellular invasion via activation of Cdc42. *J Biol Chem* 279, 31671–31678.
45. Chen, X.-M., O'Hara, S.P., Huang, B.Q., Nelson, J.B., Lin, J.J.-C., Zhu, G., Ward, H.D., LaRusso, N.F., 2004. Apical Organelle Discharge by *Cryptosporidium parvum* Is Temperature, Cytoskeleton, and Intracellular Calcium Dependent and Required for Host Cell Invasion. *Infect Immun* 72, 6806–6816.
46. Chen, X.-M., O'Hara, S.P., Huang, B.Q., Splinter, P.L., Nelson, J.B., LaRusso, N.F., 2005. Localized glucose and water influx facilitates *Cryptosporidium parvum* cellular invasion by means of modulation of host-cell membrane protrusion. *Proc Natl Acad Sci U S A* 102, 6338–6343.
47. Chervin, A.S., Stone, J.D., Holler, P.D., Bai, A., Chen, J., Eisen, H.N., Kranz, D.M., 2009. The impact of TCR-binding properties and antigen presentation format on T cell responsiveness. *J Immunol* 183, 1166–1178.
48. Choe, H., Farzan, M., Sun, Y., Sullivan, N., Rollins, B., Ponath, P.D., Wu, L., Mackay, C.R., LaRosa, G., Newman, W., Gerard, N., Gerard, C.,

- Sodroski, J., 1996. The  $\beta$ -Chemokine Receptors CCR3 and CCR5 Facilitate Infection by Primary HIV-1 Isolates. *Cell* 85, 1135–1148.
49. Choo, S.Y., 2007. The HLA System: Genetics, Immunology, Clinical Testing, and Clinical Implications. *Yonsei Med J* 48, 11–23.
50. Chow, J.Y.C., Dong, H., Quach, K.T., Van Nguyen, P.N., Chen, K., Carethers, J.M., 2008. TGF-beta mediates PTEN suppression and cell motility through calcium-dependent PKC-alpha activation in pancreatic cancer cells. *Am J Physiol Gastrointest Liver Physiol* 294, G899-905.
51. Considine, R.F., Dixon, D.R., Drummond, C.J., 2002. Oocysts of *Cryptosporidium parvum* and model sand surfaces in aqueous solutions: an atomic force microscope (AFM) study. *Water Res* 36, 3421–3428.
52. Cooper, G.M., 2000. Structure and Organization of Actin Filaments. *The Cell: A Molecular Approach*. 2nd edition.
53. Costa, L.B., Noronha, F.J., Roche, J.K., Sevilleja, J.E., Warren, C.A., Oriá, R., Lima, A., Guerrant, R.L., 2012. Novel In Vitro and In Vivo Models and Potential New Therapeutics to Break the Vicious Cycle of *Cryptosporidium* Infection and Malnutrition. *The Journal of Infectious Diseases* 205, 1464–1471.
54. Czech, M.P., 2000. PIP2 and PIP3: Complex Roles at the Cell Surface. *Cell* 100, 603–606.
55. Delling, C., Dauschies, A., Bangoura, B., Dengler, F., 2019. *Cryptosporidium parvum* alters glucose transport mechanisms in infected enterocytes. *Parasitol Res* 118, 3429–3441.

56. Dieter, P., Fitzke, E., Duyster, J., 1993. BAPTA induces a decrease of intracellular free calcium and a translocation and inactivation of protein kinase C in macrophages. *Biol Chem Hoppe Seyler* 374, 171–174.
57. Doggett, J.S., Ojo, K.K., Fan, E., Maly, D.J., Van Voorhis, W.C., 2014. Bumped kinase inhibitor 1294 treats established *Toxoplasma gondii* infection. *Antimicrob Agents Chemother* 58, 3547–3549.
58. Du, T.-T., Dewey, J.B., Wagner, E.L., Cui, R., Heo, J., Park, J.-J., Francis, S.P., Perez-Reyes, E., Guillot, S.J., Sherman, N.E., Xu, W., Oghalai, J.S., Kachar, B., Shin, J.-B., 2019. LMO7 deficiency reveals the significance of the cuticular plate for hearing function. *Nat Commun* 10, 1117.
59. Dubremetz, J.F., Garcia-Réguet, N., Conseil, V., Fourmaux, M.N., 1998. Apical organelles and host-cell invasion by Apicomplexa. *Int J Parasitol* 28, 1007–1013.
60. Duggal, P., Guo, X., Haque, R., Peterson, K.M., Ricklefs, S., Mondal, D., Alam, F., Noor, Z., Verkerke, H.P., Marie, C., Leduc, C.A., Jr., S.C.C., Jr., M.G.M., Leibel, R.L., Houpt, E., Gilchrist, C.A., Sher, A., Porcella, S.F., Jr., W.A.P., 2011. A mutation in the leptin receptor is associated with *Entamoeba histolytica* infection in children. *J Clin Invest* 121, 1191–1198.
61. Elahi, S., Dinges, W.L., Lejarcegui, N., Laing, K.J., Collier, A.C., Koelle, D.M., McElrath, M.J., Horton, H., 2011. Protective HIV-specific CD8+ T cells evade Treg cell suppression. *Nat Med* 17, 989–995.

62. Elliott, D.A., Clark, D.P., 2000. *Cryptosporidium parvum* Induces Host Cell Actin Accumulation at the Host-Parasite Interface. *Infect Immun* 68, 2315–2322.
63. Elliott, D.A., Coleman, D.J., Lane, M.A., May, R.C., Machesky, L.M., Clark, D.P., 2001. *Cryptosporidium parvum* Infection Requires Host Cell Actin Polymerization. *Infect Immun* 69, 5940–5942.
64. Epstein, H., Hardy, R., May, J.S., Johnson, M.H., Holmes, N., 1989. Expression and function of HLA-A2.1 in transgenic mice. *Eur J Immunol* 19, 1575–1583.
65. Etzold, M., Lendner, M., Dauschies, A., Dyachenko, V., 2014. CDPKs of *Cryptosporidium parvum*--stage-specific expression in vitro. *Parasitol Res* 113, 2525–2533.
66. Farhadi, A., Keshavarzian, A., Ranjbaran, Z., Fields, J.Z., Banan, A., 2006. The Role of Protein Kinase C Isoforms in Modulating Injury and Repair of the Intestinal Barrier. *J Pharmacol Exp Ther* 316, 1–7.
67. Fischer, T., Stone, R.M., DeAngelo, D.J., Galinsky, I., Estey, E., Lanza, C., Fox, E., Ehninger, G., Feldman, E.J., Schiller, G.J., Klimek, V.M., Nimer, S.D., Gilliland, D.G., Dutreix, C., Huntsman-Labed, A., Virkus, J., Giles, F.J., 2010. Phase IIB Trial of Oral Midostaurin (PKC412), the FMS-Like Tyrosine Kinase 3 Receptor (FLT3) and Multi-Targeted Kinase Inhibitor, in Patients With Acute Myeloid Leukemia and High-Risk Myelodysplastic Syndrome With Either Wild-Type or Mutated FLT3. *J Clin Oncol* 28, 4339–4345.

68. Forney, J.R., DeWald, D.B., Yang, S., Speer, C.A., Healey, M.C., 1999. A Role for Host Phosphoinositide 3-Kinase and Cytoskeletal Remodeling during *Cryptosporidium parvum* Infection. *Infect Immun* 67, 844–852.
69. Forney, J.R., Vaughan, D.K., Yang, S., Healey, M.C., 1998. Actin-Dependent Motility in *Cryptosporidium parvum* Sporozoites. *The Journal of Parasitology* 84, 908–913.
70. Gao, X., Metge, D.W., Ray, C., Harvey, R.W., Chorover, J., 2009. Surface complexation of carboxylate adheres *Cryptosporidium parvum* oocysts to the hematite-water interface. *Environ Sci Technol* 43, 7423–7429.
71. GBD Diarrheal Diseases Collaborators, 2017. Estimates of global, regional, and national morbidity, mortality, and etiologies of diarrheal diseases: a systematic analysis for the Global Burden of Disease Study 2015. *Lancet Infect Dis* 17, 909–948.
72. Genot, E.M., Parker, P.J., Cantrell, D.A., 1995. Analysis of the Role of Protein Kinase C- $\alpha$ , - $\epsilon$ , and - $\zeta$  in T Cell Activation (\*). *Journal of Biological Chemistry* 270, 9833–9839.
73. George, C.M., Burrowes, V., Perin, J., Oldja, L., Biswas, S., Sack, D., Ahmed, S., Haque, R., Bhuiyan, N.A., Parvin, T., Bhuyian, S.I., Akter, M., Li, S., Natarajan, G., Shahnaij, M., Faruque, A.G., Stine, O.C., 2018. Enteric Infections in Young Children are Associated with Environmental Enteropathy and Impaired Growth. *Tropical Medicine & International Health* 23, 26–33.

74. Gomez Morales, M.A., La Rosa, G., Ludovisi, A., Onori, A.M., Pozio, E., 1999. Cytokine Profile Induced by Cryptosporidium Antigen in Peripheral Blood Mononuclear Cells from Immunocompetent and Immunosuppressed Persons with Cryptosporidiosis. *The Journal of Infectious Diseases* 179, 967–973.
75. Grandage, V.L., Everington, T., Linch, D.C., Khwaja, A., 2006. Gö6976 is a potent inhibitor of the JAK 2 and FLT3 tyrosine kinases with significant activity in primary acute myeloid leukemia cells. *British Journal of Hematology* 135, 303–316.
76. Greenwood F.C., Hunter W.M., Glover J.S., 1963. The preparation of I-labelled human growth hormone of high specific radioactivity. *Biochemical Journal* 89:114-23.
77. Griffiths, J.K., Theodos, C., Paris, M., Tzipori, S., 1998. The Gamma Interferon Gene Knockout Mouse: a Highly Sensitive Model for Evaluation of Therapeutic Agents against *Cryptosporidium parvum*. *Journal of Clinical Microbiology*.
78. GTEx Consortium., 2015. The Genotype-Tissue Expression (GTEx) pilot analysis: multitissue gene regulation in humans. *Science* 348(6235):648-60. doi: 10.1126/science.1262110. PMID: 25954001; PMCID: PMC4547484.
79. Guérin, A., Roy, N.H., Kugler, E.M., Berry, L., Burkhardt, J.K., Shin, J.-B., Striepen, B., 2021. *Cryptosporidium* rhoptry effector protein ROP1 injected

during invasion targets the host cytoskeletal modulator LMO7. *Cell Host & Microbe* 29, 1407-1420.e5.

80. Guerrant, D.I., Moore, S.R., Lima, A.A., Patrick, P.D., Schorling, J.B., Guerrant, R.L., 1999. Association of early childhood diarrhea and cryptosporidiosis with impaired physical fitness and cognitive function four-seven years later in a poor urban community in northeast Brazil. *Am J Trop Med Hyg* 61, 707–713.
81. Hahn, C.G., Friedman, E., 1999. Abnormalities in protein kinase C signaling and the pathophysiology of bipolar disorder. *Bipolar Disord* 1, 81–86.
82. Harada, N., Fukaya, S., Wada, H., Goto, R., Osada, T., Gomori, A., Ikizawa, K., Sakuragi, M., Oda, N., 2017. Generation of a Novel HLA Class I Transgenic Mouse Model Carrying a Knock-in Mutation at the  $\beta$ 2-Microglobulin Locus. *J Immunol* 198, 516–527.
83. Hashim, A., Clyne, M., Mulcahy, G., Akiyoshi, D., Chalmers, R., Bourke, B., 2004. Host Cell Tropism Underlies Species Restriction of Human and Bovine *Cryptosporidium parvum* Genotypes. *Infect Immun* 72, 6125–6131.
84. Hashim, A., Mulcahy, G., Bourke, B., Clyne, M., 2006. Interaction of *Cryptosporidium hominis* and *Cryptosporidium parvum* with Primary Human and Bovine Intestinal Cells. *Infect Immun* 74, 99–107.
85. Helmberg, W., Lanzer, G., Zahn, R., Weinmayr, B., Wagner, T., Albert, E., 1998. Virtual DNA analysis--a new tool for combination and standardized

evaluation of SSO, SSP and sequencing-based typing results. *Tissue Antigens* 51, 587–592.

86. Hempel, A., Maasch, C., Heintze, U., Lindschau, C., Dietz, R., Luft, F.C., Haller, H., 1997. High glucose concentrations increase endothelial cell permeability via activation of protein kinase C alpha. *Circ Res* 81, 363–371.
87. Heo, I., Dutta, D., Schaefer, D.A., Iakobachvili, N., Artegiani, B., Sachs, N., Boonekamp, K.E., Bowden, G., Hendrickx, A.P.A., Willems, R.J.R., Peters, P.J., Riggs, M.W., O'Connor, R., Clevers, H., 2018. Modeling *Cryptosporidium* infection in human small intestinal and lung organoids. *Nat Microbiol* 3, 814–823.
88. Holaska, J.M., Kowalski, A.K., Wilson, K.L., 2004. Emerin caps the pointed end of actin filaments: evidence for an actin cortical network at the nuclear inner membrane. *PLoS Biol* 2, E231.
89. Holaska, J.M., Rais-Bahrami, S., Wilson, K.L., 2006. Lmo7 is an emerin-binding protein that regulates the transcription of emerin and many other muscle-relevant genes. *Human Molecular Genetics* 15, 3459–3472.
90. Holcomb, C.L., Höglund, B., Anderson, M.W., Blake, L.A., Böhme, I., Egholm, M., Ferriola, D., Gabriel, C., Gelber, S.E., Goodridge, D., Hawbecker, S., Klein, R., Ladner, M., Lind, C., Monos, D., Pando, M.J., Pröll, J., Sayer, D.C., Schmitz-Agheguian, G., Simen, B.B., Thiele, B., Trachtenberg, E.A., Tyan, D.B., Wassmuth, R., White, S., Erlich, H.A.,

2011. A multi-site study using high-resolution HLA genotyping by next generation sequencing. *Tissue Antigens* 77, 206–217.
91. Hollenbach, J.A., Mack, S.J., Thomson, G., Gourraud, P.-A., 2012. Analytical methods for disease association studies with immunogenetic data. *Methods Mol Biol* 882, 245–266.
92. Hong, X., Yu, R.-B., Sun, N.-X., Wang, B., Xu, Y.-C., Wu, G.-L., 2005. Human leukocyte antigen class II DQB1\*0301, DRB1\*1101 alleles and spontaneous clearance of hepatitis C virus infection: A meta-analysis. *World J Gastroenterol* 11, 7302–7307.
93. Hryciw, D.H., Pollock, C.A., Poronnik, P., 2005. PKC-alpha-mediated remodeling of the actin cytoskeleton is involved in constitutive albumin uptake by proximal tubule cells. *Am J Physiol Renal Physiol* 288, F1227-1235.
94. Hsu, A.H., Lum, M.A., Shim, K.-S., Frederick, P.J., Morrison, C.D., Chen, B., Lele, S.M., Sheinin, Y.M., Daikoku, T., Dey, S.K., Leone, G., Black, A.R., Black, J.D., 2018. Crosstalk between PKC $\alpha$  and PI3K/AKT Signaling Is Tumor Suppressive in the Endometrium. *Cell Rep* 24, 655–669.
95. Huang, Z., Haugland, Rosaria P., You, W., Haugland, Richard P., 1992. Phallotoxin and actin binding assay by fluorescence enhancement. *Analytical Biochemistry* 200, 199–204.
96. Hulverson, M.A., Vinayak, S., Choi, R., Schaefer, D.A., Castellanos-Gonzalez, A., Vidadala, R.S.R., Brooks, C.F., Herbert, G.T., Betzer, D.P., Whitman, G.R., Sparks, H.N., Arnold, S.L.M., Rivas, K.L., Barrett, L.K.,

- White, A.C., Maly, D.J., Riggs, M.W., Striepen, B., Van Voorhis, W.C., Ojo, K.K., 2017. Bumped-Kinase Inhibitors for Cryptosporidiosis Therapy. *J Infect Dis* 215, 1275–1284.
97. Ihara, S., Hirata, Y., Koike, K., 2017. TGF- $\beta$  in inflammatory bowel disease: a key regulator of immune cells, epithelium, and the intestinal microbiota. *J Gastroenterol* 52, 777–787.
98. Ishii, H., Jirousek, M.R., Koya, D., Takagi, C., Xia, P., Clermont, A., Bursell, S.E., Kern, T.S., Ballas, L.M., Heath, W.F., Stramm, L.E., Feener, E.P., King, G.L., 1996. Amelioration of vascular dysfunctions in diabetic rats by an oral PKC beta inhibitor. *Science* 272, 728–731.
99. Iwamoto, T., Hagiwara, M., Hidaka, H., Isomura, T., Kioussis, D., Nakashima, I., 1992. Accelerated proliferation and interleukin-2 production of thymocytes by stimulation of soluble anti-CD3 monoclonal antibody in transgenic mice carrying a rabbit protein kinase C alpha. *J Biol Chem* 267, 18644–18648.
100. Jakobi, V., Petry, F., 2008. Humoral immune response in IL-12 and IFN- $\gamma$  deficient mice after infection with *Cryptosporidium parvum*. *Parasite Immunology* 30, 151–161.
101. Jalava, A., Lintunen, M., Heikkila, J., 1993. Protein Kinase C- $\alpha$  But Not Protein Kinase C- $\epsilon$  Is Differentially Down-Regulated by Bryostatin 1 and Tetradecanoyl Phorbol 13-Acetate in SH-SY5Y Human Neuroblastoma Cells. *Biochemical and Biophysical Research Communications* 191, 472–478.

102. Jex, A.R., Gasser, R.B., 2010. Genetic richness and diversity in *Cryptosporidium hominis* and *C. parvum* reveals major knowledge gaps and a need for the application of “next generation” technologies--research review. *Biotechnol Adv* 28, 17–26.
103. Joe, A., Hamer, D.H., Kelley, M.A., Pereira, M.E., Keusch, G.T., Tzipori, S., Ward, H.D., 1994. Role of a Gal/GalNAc-specific sporozoite surface lectin in *Cryptosporidium parvum*-host cell interaction. *J Eukaryot Microbiol* 41, 44S.
104. Jones, R., 2008. Searching for the greatest Bengali: The BBC and shifting identity categories in South Asia. *National Identities* 10, 149–165.
105. Karanis, P., Aldeyarbi, H.M., 2011. Evolution of *Cryptosporidium* in vitro culture. *Int J Parasitol* 41, 1231–1242.
106. Kaushik, K., Khurana, S., Wanchu, A., Malla, N., 2009. Lymphoproliferative and Cytokine Responses to *Cryptosporidium parvum* in Patients Coinfected with *C. parvum* and Human Immunodeficiency Virus. *Clin Vaccine Immunol* 16, 116–121.
107. Kennedy, M.K., Glaccum, M., Brown, S.N., Butz, E.A., Viney, J.L., Embers, M., Matsuki, N., Charrier, K., Sedger, L., Willis, C.R., Brasel, K., Morrissey, P.J., Stocking, K., Schuh, J.C.L., Joyce, S., Peschon, J.J., 2000. Reversible Defects in Natural Killer and Memory Cd8 T Cell Lineages in Interleukin 15–Deficient Mice. *Journal of Experimental Medicine* 191, 771–780.

108. Khalil, I.A., Troeger, C., Rao, P.C., Blacker, B.F., Brown, A., Brewer, T.G., Colombara, D.V., Hostos, E.L.D., Engmann, C., Guerrant, R.L., Haque, R., Houpt, E.R., Kang, G., Korpe, P.S., Kotloff, K.L., Lima, A.A.M., Petri, W.A., Platts-Mills, J.A., Shoultz, D.A., Forouzanfar, M.H., Hay, S.I., Reiner, R.C., Mokdad, A.H., 2018. Morbidity, mortality, and long-term consequences associated with diarrhoea from *Cryptosporidium* infection in children younger than 5 years: a meta-analyses study. *The Lancet Global Health* 6, e758–e768.
109. Khan, A., Shams, S., Khan, Saima, Khan, M.I., Khan, Sardar, Ali, A., 2019. Evaluation of prevalence and risk factors associated with *Cryptosporidium* infection in rural population of district Buner, Pakistan. *PLoS One* 14, e0209188.
110. Kirkpatrick, B.D., Colgate, E.R., Mychaleckyj, J.C., Haque, R., Dickson, D.M., Carmolli, M.P., Nayak, U., Taniuchi, M., Naylor, C., Qadri, F., Ma, J.Z., Alam, M., Walsh, M.C., Diehl, S.A., PROVIDE Study Teams, Petri, W.A., 2015. The “Performance of Rotavirus and Oral Polio Vaccines in Developing Countries” (PROVIDE) study: description of methods of an interventional study designed to explore complex biologic problems. *Am J Trop Med Hyg* 92, 744–751.
111. Kirkpatrick, B.D., Haque, R., Duggal, P., Mondal, D., Larsson, C., Peterson, K., Akter, J., Lockhart, L., Khan, S., Petri, W.A., 2008. Association between *Cryptosporidium* Infection and Human Leukocyte Antigen Class I and Class II Alleles. *J Infect Dis* 197, 474–478.

112. Koivunen, J., Aaltonen, V., Koskela, S., Lehenkari, P., Laato, M., Peltonen, J., 2004. Protein kinase C alpha/beta inhibitor Go6976 promotes formation of cell junctions and inhibits invasion of urinary bladder carcinoma cells. *Cancer Res* 64, 5693–5701.
113. Komai, T., Inoue, M., Okamura, T., Morita, K., Iwasaki, Y., Sumitomo, S., Shoda, H., Yamamoto, K., Fujio, K., 2018. Transforming Growth Factor- $\beta$  and Interleukin-10 Synergistically Regulate Humoral Immunity via Modulating Metabolic Signals. *Frontiers in Immunology* 9.
114. Korbil, D.S., Barakat, F.M., Santo, J.P.D., McDonald, V., 2011. CD4+ T Cells Are Not Essential for Control of Early Acute *Cryptosporidium parvum* Infection in Neonatal Mice. *Infection and Immunity* 79, 1647–1653.
115. Korpe, P.S., Valencia, C., Haque, R., Mahfuz, M., McGrath, M., Houpt, E., Kosek, M., McCormick, B.J.J., Penataro Yori, P., Babji, S., Kang, G., Lang, D., Gottlieb, M., Samie, A., Bessong, P., Faruque, A.S.G., Mduma, E., Nshama, R., Havt, A., Lima, I.F.N., Lima, A.A.M., Bodhidatta, L., Shreshtha, A., Petri, W.A., Ahmed, T., Duggal, P., 2018. Epidemiology and Risk Factors for Cryptosporidiosis in Children From 8 Low-income Sites: Results From the MAL-ED Study. *Clin Infect Dis* 67, 1660–1669.
116. Kotloff, K.L., Nataro, J.P., Blackwelder, W.C., Nasrin, D., Farag, T.H., Panchalingam, S., Wu, Y., Sow, S.O., Sur, D., Breiman, R.F., Faruque, A.S., Zaidi, A.K., Saha, D., Alonso, P.L., Tamboura, B., Sanogo, D., Onwuchekwa, U., Manna, B., Ramamurthy, T., Kanungo, S., Ochieng, J.B., Omore, R., Oundo, J.O., Hossain, A., Das, S.K., Ahmed, S., Qureshi,

- S., Quadri, F., Adegbola, R.A., Antonio, M., Hossain, M.J., Akinsola, A., Mandomando, I., Nhampossa, T., Acácio, S., Biswas, K., O'Reilly, C.E., Mintz, E.D., Berkeley, L.Y., Muhsen, K., Sommerfelt, H., Robins-Browne, R.M., Levine, M.M., 2013. Burden and etiology of diarrheal disease in infants and young children in developing countries (the Global Enteric Multicenter Study, GEMS): a prospective, case-control study. *The Lancet* 382, 209–222.
117. Kuhlenschmidt, T.B., Rutaganira, F.U., Long, S., Tang, K., Shokat, K.M., Kuhlenschmidt, M.S., Sibley, L.D., 2015. Inhibition of Calcium-Dependent Protein Kinase 1 (CDPK1) In Vitro by Pyrazolopyrimidine Derivatives Does Not Correlate with Sensitivity of *Cryptosporidium parvum* Growth in Cell Culture. *Antimicrob Agents Chemother* 60, 570–579.
118. Kuroda, S., Tokunaga, C., Kiyohara, Y., Higuchi, O., Konishi, H., Mizuno, K., Gill, G.N., Kikkawa, U., 1996. Protein-protein interaction of zinc finger LIM domains with protein kinase C. *J Biol Chem* 271, 31029–31032.
119. Kuznar, Z.A., Elimelech, M., 2004. Adhesion kinetics of viable *Cryptosporidium parvum* oocysts to quartz surfaces. *Environ Sci Technol* 38, 6839–6845.
120. Lamberti, L.M., Fischer Walker, C.L., Noiman, A., Victora, C., Black, R.E., 2011. Breastfeeding and the risk for diarrhea morbidity and mortality. *BMC Public Health* 11, S15.

121. Langer, R.C., Riggs, M.W., 1999. Cryptosporidium parvum apical complex glycoprotein CSL contains a sporozoite ligand for intestinal epithelial cells. *Infect Immun* 67, 5282–5291.
122. Lanteri, M.C., Kaidarova, Z., Peterson, T., Cate, S., Custer, B., Wu, S., Agapova, M., Law, J.P., Bielawny, T., Plummer, F., Tobler, L.H., Loeb, M., Busch, M.P., Bramson, J., Luo, M., Norris, P.J., 2011. Association between HLA class I and class II alleles and the outcome of West Nile virus infection: an exploratory study. *PLoS One* 6, e22948.
123. Le, A.X., Bernhard, E.J., Holterman, M.J., Strub, S., Parham, P., Lacy, E., Engelhard, V.H., 1989. Cytotoxic T cell responses in HLA-A2.1 transgenic mice. Recognition of HLA alloantigens and utilization of HLA-A2.1 as a restriction element. *The Journal of Immunology* 142, 1366–1371.
124. Lee, B., Damon, C.F., Platts-Mills, J.A., 2020. Pediatric acute gastroenteritis associated with adenovirus 40/41 in low-income and middle-income countries. *Curr Opin Infect Dis* 33, 398–403.
125. Lee, H.-W., Smith, L., Pettit, G.R., Vinitzky, A., Smith, J.B., 1996. Ubiquitination of Protein Kinase C- $\alpha$  and Degradation by the Proteasome\*. *Journal of Biological Chemistry* 271, 20973–20976.
126. Lee, S., Ginese, M., Beamer, G., Danz, H.R., Girouard, D.J., Chapman-Bonofiglio, S.P., Lee, M., Hulverson, M.A., Choi, R., Whitman, G.R., Ojo, K.K., Arnold, S.L.M., Van Voorhis, W.C., Tzipori, S., 2018. Therapeutic Efficacy of Bumped Kinase Inhibitor 1369 in a Pig Model of

- Acute Diarrhea Caused by *Cryptosporidium hominis*. *Antimicrob Agents Chemother* 62, e00147-18.
127. Leitch, G.J., He, Q., 2011. Cryptosporidiosis-an overview. *J Biomed Res* 25, 1–16.
128. Lekstrom-Himes, J.A., Hohman, P., Warren, T., Wald, A., Nam, J.M., Simonis, T., Corey, L., Straus, S.E., 1999. Association of major histocompatibility complex determinants with the development of symptomatic and asymptomatic genital herpes simplex virus type 2 infections. *J Infect Dis* 179, 1077–1085.
129. Li, C., Fultz, M.E., Wright, G.L., 2002. PKC- $\alpha$  shows variable patterns of translocation in response to different stimulatory agents. *Acta Physiologica Scandinavica* 174, 237–246.
130. Li, D., Shatos, M.A., Hodges, R.R., Dartt, D.A., 2013. Role of PKC $\alpha$  Activation of Src, PI-3K/AKT, and ERK in EGF-Stimulated Proliferation of Rat and Human Conjunctival Goblet Cells. *Invest. Ophthalmol. Vis. Sci.* 54, 5661–5674.
131. Lippuner, C., Ramakrishnan, C., Basso, W.U., Schmid, M.W., Okoniewski, M., Smith, N.C., Hässig, M., Deplazes, P., Hehl, A.B., 2018. RNA-Seq analysis during the life cycle of *Cryptosporidium parvum* reveals significant differential gene expression between proliferating stages in the intestine and infectious sporozoites. *International Journal for Parasitology* 48, 413–422.

132. Little, A.M., Parham, P., 1999. Polymorphism and evolution of HLA class I and II genes and molecules. *Rev Immunogenet* 1, 105–123.
133. Liu, C., Hermann, T.E., 1978. Characterization of ionomycin as a calcium ionophore. *Journal of Biological Chemistry* 253, 5892–5894.
134. Liu, J., Gratz, J., Amour, C., Kibiki, G., Becker, S., Janaki, L., Verweij, J.J., Taniuchi, M., Sobuz, S.U., Haque, R., Haverstick, D.M., Houpt, E.R., 2013. A laboratory-developed TaqMan Array Card for simultaneous detection of 19 enteropathogens. *J Clin Microbiol* 51, 472–480.
135. Liu, J., Platts-Mills, J.A., Juma, J., Kabir, F., Nkeze, J., Okoi, C., Operario, D.J., Uddin, J., Ahmed, S., Alonso, P.L., Antonio, M., Becker, S.M., Blackwelder, W.C., Breiman, R.F., Faruque, A.S.G., Fields, B., Gratz, J., Haque, R., Hossain, A., Hossain, M.J., Jarju, S., Qamar, F., Iqbal, N.T., Kwambana, B., Mandomando, I., McMurry, T.L., Ochieng, C., Ochieng, J.B., Ochieng, M., Onyango, C., Panchalingam, S., Kalam, A., Aziz, F., Qureshi, S., Ramamurthy, T., Roberts, J.H., Saha, D., Sow, S.O., Stroup, S.E., Sur, D., Tamboura, B., Taniuchi, M., Tennant, S.M., Toema, D., Wu, Y., Zaidi, A., Nataro, J.P., Kotloff, K.L., Levine, M.M., Houpt, E.R., 2016. Use of quantitative molecular diagnostic methods to identify causes of diarrhoea in children: a reanalysis of the GEMS case-control study. *Lancet* 388, 1291–1301.
136. Liu, J., Van Blitterswijk, C.A., De Boer, J., 2008. Different protein kinase C isozymes exert opposing effects on osteogenesis of human

mesenchymal stem cells: 8th World Biomaterials Congress 2008, WBC 2008. 8th World Biomaterials Congress 2008, 8th World Biomaterials Congress 2008.

137. Liu, R., Paxton, W.A., Choe, S., Ceradini, D., Martin, S.R., Horuk, R., MacDonald, M.E., Stuhlmann, H., Koup, R.A., Landau, N.R., 1996. Homozygous Defect in HIV-1 Coreceptor Accounts for Resistance of Some Multiply-Exposed Individuals to HIV-1 Infection. *Cell* 86, 367–377.
138. Liu, T.-L., Fan, X.-C., Li, Y.-H., Yuan, Y.-J., Yin, Y.-L., Wang, X.-T., Zhang, L.-X., Zhao, G.-H., 2018. Expression Profiles of mRNA and lncRNA in HCT-8 Cells Infected With *Cryptosporidium parvum* Ild Subtype. *Front Microbiol* 9.
139. Lodolce, J.P., Boone, D.L., Chai, S., Swain, R.E., Dassopoulos, T., Trettin, S., Ma, A., 1998. IL-15 Receptor Maintains Lymphoid Homeostasis by Supporting Lymphocyte Homing and Proliferation. *Immunity* 9, 669–676.
140. Lopalco, L., 2010. CCR5: From Natural Resistance to a New Anti-HIV Strategy. *Viruses* 2, 574–600.
141. Lorenzo, J.A., Raisz, L.G., 1981. Divalent Cation Ionophores Stimulate Resorption and Inhibit DNA Synthesis in Cultured Fetal Rat Bone. *Science*.
142. Lorenzo, P.S., Bögi, K., Hughes, K.M., Beheshti, M., Bhattacharyya, D., Garfield, S.H., Pettit, G.R., Blumberg, P.M., 1999. Differential Roles of the Tandem C1 Domains of Protein Kinase C  $\delta$  in the

- Biphasic Down-Regulation Induced by Bryostatin 1. *Cancer Res* 59, 6137–6144.
143. Love, M.S., Beasley, F.C., Jumani, R.S., Wright, T.M., Chatterjee, A.K., Huston, C.D., Schultz, P.G., McNamara, C.W., 2017. A high-throughput phenotypic screen identifies clofazimine as a potential treatment for cryptosporidiosis. *PLoS Negl Trop Dis* 11.
144. Lünemann, J.D., Münz, C., 2009. Autophagy in CD4+ T cell immunity and tolerance. *Cell Death Differ* 16, 79–86.
145. Luo, X., Jedlicka, S., Jellison, K., 2016. Pseudo-Second-Order Calcium-Mediated *Cryptosporidium parvum* Oocyst Attachment to Environmental Biofilms. *Applied and Environmental Microbiology*.
146. MacDonald, K.S., Fowke, K.R., Kimani, J., Dunand, V.A., Nagelkerke, N.J., Ball, T.B., Oyugi, J., Njagi, E., Gaur, L.K., Brunham, R.C., Wade, J., Luscher, M.A., Krausa, P., Rowland-Jones, S., Ngugi, E., Bwayo, J.J., Plummer, F.A., 2000. Influence of HLA supertypes on susceptibility and resistance to human immunodeficiency virus type 1 infection. *J Infect Dis* 181, 1581–1589.
147. Mack, S.J., Tu, B., Lazaro, A., Yang, R., Lancaster, A.K., Cao, K., Ng, J., Hurley, C.K., 2009. HLA-A, -B, -C, -DRB1 Allele and Haplotype Frequencies Distinguish Eastern European Americans from the General European American Population. *Tissue Antigens* 73, 17–32.
148. Martiny-Baron, G., Kazanietz, M.G., Mischak, H., Blumberg, P.M., Kochs, G., Hug, H., Marmé, D., Schächtele, C., 1993. Selective inhibition

- of protein kinase C isozymes by the indolocarbazole Gö 6976. *J. Biol. Chem.* 268, 9194–9197.
149. Matzaraki, V., Kumar, V., Wijmenga, C., Zhernakova, A., 2017. The MHC locus and genetic susceptibility to autoimmune and infectious diseases. *Genome Biology* 18, 76.
150. Mauzy, M.J., Enomoto, S., Lancto, C.A., Abrahamsen, M.S., Rutherford, M.S., 2012. The *Cryptosporidium Parvum* Transcriptome during In Vitro Development. *PLOS ONE* 7, e31715.
151. McDonald, S.A.C., O'Grady, J.E., Bajaj-Elliott, M., Notley, C.A., Alexander, J., Brombacher, F., McDonald, V., 2004. Protection against the Early Acute Phase of *Cryptosporidium parvum* Infection Conferred by Interleukin-4-Induced Expression of T Helper 1 Cytokines. *The Journal of Infectious Diseases* 190, 1019–1025.
152. McDonald, V., Deer, R., Uni, S., Iseki, M., Bancroft, G.J., 1992. Immune responses to *Cryptosporidium muris* and *Cryptosporidium parvum* in adult immunocompetent or immunocompromised (nude and SCID) mice. *Infection and Immunity*.
153. McDonald, V., Robinson, H.A., Kelly, J.P., Bancroft, G.J., 1994. *Cryptosporidium muris* in adult mice: adoptive transfer of immunity and protective roles of CD4 versus CD8 cells. *Infection and Immunity*.
154. Mead, J.R., Arrowood, M.J., Sidwell, R.W., Healey, M.C., 1991. Chronic *Cryptosporidium parvum* Infections in Congenitally

- Immunodeficient SCID and Nude Mice. *The Journal of Infectious Diseases* 163, 1297–1304.
155. Meisel, M., Hermann-Kleiter, N., Hinterleitner, R., Gruber, T., Wachowicz, K., Pfeifhofer-Obermair, C., Fresser, F., Leitges, M., Soldani, C., Viola, A., Kaminski, S., Baier, G., 2013. The Kinase PKC $\alpha$  Selectively Upregulates Interleukin-17A during Th17 Cell Immune Responses. *Immunity* 38, 41–52.
156. Mele, R., Gomez Morales, M.A., Tosini, F., Pozio, E., 2004. *Cryptosporidium parvum* at Different Developmental Stages Modulates Host Cell Apoptosis In Vitro. *Infect Immun* 72, 6061–6067.
157. Meloni B.P., Thompson R.C., 1996. Simplified methods for obtaining purified oocysts from mice and for growing *Cryptosporidium parvum* in vitro. *J Parasitol.* Oct;82(5):757-62. PMID: 8885885.
158. Mercado E.S., Espino F.E., Perez M.L., 2015. HLA-A\*33:01 as protective allele for severe dengue in a population of Filipino children. *PLOS One* 10(2) 13710115619.
159. Michie, A.M., Soh, J.W., Hawley, R.G., Weinstein, I.B., Zuniga-Pflucker, J.C., 2001. Allelic exclusion and differentiation by protein kinase C-mediated signals in immature thymocytes. *Proc Natl Acad Sci U S A* 98, 609–614.
160. Mittal, R., Grati, M., Yan, D., Liu, X.Z., 2016. *Pseudomonas aeruginosa* Activates PKC-Alpha to Invade Middle Ear Epithelial Cells. *Front. Microbiol.* 7.

161. Mondal, D., Haque, R., Sack, R.B., Kirkpatrick, B.D., Petri, W.A., 2009. Attribution of Malnutrition to Cause-Specific Diarrheal Illness: Evidence from a Prospective Study of Preschool Children in Mirpur, Dhaka, Bangladesh. *Am J Trop Med Hyg* 80, 824–826.
162. Monzani, E., Bazzotti, R., Perego, C., La Porta, C.A.M., 2009. AQP1 Is Not Only a Water Channel: It Contributes to Cell Migration through Lin7/Beta-Catenin. *PLoS One* 4.
163. Moore, S.R., Lima, N.L., Soares, A.M., Oriá, R.B., Pinkerton, R.C., Barrett, L.J., Guerrant, R.L., Lima, A.A.M., 2010. Prolonged episodes of acute diarrhea reduce growth and increase risk of persistent diarrhea in children. *Gastroenterology* 139, 1156–1164.
164. Moriarty, E. m., Duffy, G., McEvoy, J. m., Caccio, S., Sheridan, J. j., McDowell, D., Blair, I. s., 2005. The effect of thermal treatments on the viability and infectivity of *Cryptosporidium parvum* on beef surfaces. *Journal of Applied Microbiology* 98, 618–623.
165. Morrow, A.L., Rangel, J.M., 2004. Human milk protection against infectious diarrhea: implications for prevention and clinical care. *Semin Pediatr Infect Dis* 15, 221–228.
166. Müller, J., Hemphill, A., 2013. In vitro culture systems for the study of apicomplexan parasites in farm animals. *International Journal for Parasitology, International Meeting on Apicomplexan Parasites in Farm Animals (ApiCOWplexa)* 2012 43, 115–124.

167. Nakashima, S., 2002. Protein Kinase C $\alpha$  (PKC $\alpha$ ): Regulation and Biological Function. *The Journal of Biochemistry* 132, 669–675.
168. Nasser, A.M., 2015. Removal of *Cryptosporidium* by wastewater treatment processes: a review. *Journal of Water and Health* 14, 1–13.
169. Nataro, J.P., Guerrant, R.L., 2017. Chronic consequences on human health induced by microbial pathogens: Growth faltering among children in developing countries. *Vaccine* 35, 6807–6812.
170. Nesterenko, M.V., Woods, K., Upton, S.J., 1999. Receptor/ligand interactions between *Cryptosporidium parvum* and the surface of the host cell. *Biochimica et Biophysica Acta (BBA) - Molecular Basis of Disease* 1454, 165–173.
171. Neurotrope Bioscience, Inc., 2018. A Randomized, Double-Blind, Placebo-Controlled, Phase 2 Study Assessing the Safety, Tolerability and Efficacy of Bryostatin in the Treatment of Moderately Severe to Severe Alzheimer's Disease (Clinical trial registration No. NCT02431468). [clinicaltrials.gov](https://clinicaltrials.gov).
172. Newton, A.C., 1995. Protein kinase C: structure, function, and regulation. *J Biol Chem* 270, 28495–28498.
173. Ng, T., Parsons, M., Hughes, W.E., Monypenny, J., Zicha, D., Gautreau, A., Arpin, M., Gschmeissner, S., Verveer, P.J., Bastiaens, P.I.H., Parker, P.J., 2001. Ezrin is a downstream effector of trafficking PKC–integrin complexes involved in the control of cell motility. *EMBO J* 20, 2723–2741.

174. Nguyen, A.T., Szeto, C., Gras, S., 2021. The pockets guide to HLA class I molecules. *Biochemical Society Transactions* 49, 2319–2331.
175. O'Connor, R.M., Wanyiri, J.W., Wojczyk, B.S., Kim, K., Ward, H., 2007. Stable expression of *Cryptosporidium parvum* glycoprotein gp40/15 in *Toxoplasma gondii*. *Mol Biochem Parasitol* 152, 149–158.
176. O'Hara S.P., Chen X.M., 2011. The cell biology of *Cryptosporidium* infection. *Microbes Infect* 13:721–730.
177. O'Sullivan, D., Sidney, J., Appella, E., Walker, L., Phillips, L., Colón, S.M., Miles, C., Chesnut, R.W., Sette, A., 1990. Characterization of the specificity of peptide binding to four DR haplotypes. *J Immunol* 145, 1799–1808.
178. Ochs, D.L., Korenbrot, J.I., Williams, J.A., 1985. Relation between free cytosolic calcium and amylase release by pancreatic acini. *American Journal of Physiology-Gastrointestinal and Liver Physiology* 249, G389–G398.
179. Oettingen, J. von, Nath-Chowdhury, M., Ward, B.J., Rodloff, A.C., Arrowood, M.J., Ndao, M., 2008. High-yield amplification of *Cryptosporidium parvum* in interferon  $\gamma$  receptor knockout mice. *Parasitology* 135, 1151–1156.
180. Ojo, K.K., Larson, E.T., Keyloun, K.R., Castaneda, L.J., DeRocher, A.E., Inampudi, K.K., Kim, J.E., Arakaki, T.L., Murphy, R.C., Zhang, L., Napuli, A.J., Maly, D.J., Verlinde, C.L., Buckner, F.S., Parsons, M., Hol, W.G., Merritt, E.A., Van Voorhis, W.C., 2010. *Toxoplasma gondii* calcium-

- dependent protein kinase 1 is a target for selective kinase inhibitors. *Nat Struct Mol Biol* 17, 602–607.
181. Okhuysen, P.C., Chappell, C.L., Crabb, J.H., Sterling, C.R., DuPont, H.L., 1999. Virulence of Three Distinct *Cryptosporidium parvum* Isolates for Healthy Adults. *J Infect Dis* 180, 1275–1281.
182. Oliveira, L. de M., Teixeira, F.M.E., Sato, M.N., 2018. Impact of Retinoic Acid on Immune Cells and Inflammatory Diseases. *Mediators Inflamm* 2018, 3067126.
183. Pace, D.A., McKnight, C.A., Liu, J., Jimenez, V., Moreno, S.N.J., 2014. Calcium Entry in *Toxoplasma gondii* and Its Enhancing Effect of Invasion-linked Traits \*. *Journal of Biological Chemistry* 289, 19637–19647.
184. Packer, M., Narahara, K.A., Elkayam, U., Sullivan, J.M., Pearle, D.L., Massie, B.M., Creager, M.A., 1993. Double-blind, placebo-controlled study of the efficacy of flosequinan in patients with chronic heart failure. Principal Investigators of the REFLECT Study. *J Am Coll Cardiol* 22, 65–72.
185. Palaniyandi, S.S., Sun, L., Ferreira, J.C.B., Mochly-Rosen, D., 2009. Protein kinase C in heart failure: a therapeutic target? *Cardiovasc Res* 82, 229–239.
186. Pantenburg, B., Castellanos-Gonzalez, A., Dann, S.M., Connelly, R.L., Lewis, D.E., Ward, H.D., Arthur Clinton White, J., 2009. CD8+ T cells

- clear human intestinal *Cryptosporidium* infection through cytotoxic granule release (129.8). *The Journal of Immunology* 182, 129.8-129.8.
187. Pantenburg, B., Castellanos-Gonzalez, A., Dann, S.M., Connelly, R.L., Lewis, D.E., Ward, H.D., Clinton White, A., 2010. Human CD8+ T Cells Clear *Cryptosporidium parvum* from Infected Intestinal Epithelial Cells. *Am J Trop Med Hyg* 82, 600–607.
188. Pappas, D.J., Marin, W., Hollenbach, J.A., Mack, S.J., 2016. Bridging ImmunoGenomic Data Analysis Workflow Gaps (BIGDAWG): An integrated case-control analysis pipeline. *Hum Immunol* 77, 283–287.
189. Patil, C.L., Turab, A., Ambikapathi, R., Nesamvuni, C., Chandyo, R.K., Bose, A., Islam, M.M., Ahmed, A.M.S., Olortegui, M.P., de Moraes, M.L., Caulfield, L.E., MAL-ED network, 2015. Early interruption of exclusive breastfeeding: results from the eight-country MAL-ED study. *J Health Popul Nutr* 34, 10.
190. Pawlowic, M.C., Vinayak, S., Sateriale, A., Brooks, C., Striepen, B., 2017. Generating and maintaining transgenic *Cryptosporidium parvum* parasites. *Curr Protoc Microbiol* 46, 20B.2.1-20B.2.32.
191. Peng, J., He, F., Zhang, C., Deng, X., Yin, F., 2011. Protein kinase C- $\alpha$  signals P115RhoGEF phosphorylation and RhoA activation in TNF- $\alpha$ -induced mouse brain microvascular endothelial cell barrier dysfunction. *Journal of Neuroinflammation* 8, 28.

192. Petersen, C., Barnes, D.A., Gousset, L., 1997. Cryptosporidium parvum GP900, a unique invasion protein. *J Eukaryot Microbiol* 44, 89S-90S.
193. Petri, W.A., Haque, R., Mann, B.J., 2002. The bittersweet interface of parasite and host: lectin-carbohydrate interactions during human invasion by the parasite *Entamoeba histolytica*. *Annu Rev Microbiol* 56, 39–64.
194. Petri, W.A., Miller, M., Binder, H.J., Levine, M.M., Dillingham, R., Guerrant, R.L., 2008. Enteric infections, diarrhea, and their impact on function and development. *J Clin Invest* 118, 1277–1290.
195. Pfeifhofer, C., Gruber, T., Letschka, T., Thuille, N., Lutz-Nicoladoni, C., Hermann-Kleiter, N., Braun, U., Leitges, M., Baier, G., 2006. Defective IgG2a/2b Class Switching in PKC $\alpha$ -/- Mice. *The Journal of Immunology* 176, 6004–6011.
196. Platts-Mills, J.A., Babji, S., Bodhidatta, L., Gratz, J., Haque, R., Havt, A., McCormick, B.J., McGrath, M., Olortegui, M.P., Samie, A., Shakoor, S., Mondal, D., Lima, I.F., Hariraju, D., Rayamajhi, B.B., Qureshi, S., Kabir, F., Yori, P.P., Mufamadi, B., Amour, C., Carreon, J.D., Richard, S., Lang, D., Bessong, P., Mduma, E., Ahmed, T., Lima, A.A., Mason, C.J., Zaidi, A.K., Bhutta, Z., Kosek, M., Guerrant, R.L., Gottlieb, M., Miller, M., Kang, G., Houpt, E.R., 2015. Pathogen-specific burdens of community diarrhoea in developing countries (MAL-ED): a multisite birth cohort study. *Lancet Glob Health* 3, e564–e575.

197. Pontremoli, S., Melloni, E., Michetti, M., Salamino, F., Sparatore, B., Sacco, O., Horecker, B.L., 1986. Differential mechanisms of translocation of protein kinase C to plasma membranes in activated human neutrophils. *Biochem Biophys Res Commun* 136, 228–234.
198. Putignani, L., Possenti, A., Cherchi, S., Pozio, E., Crisanti, A., Spano, F., 2008. The thrombospondin-related protein CpMIC1 (CpTSP8) belongs to the repertoire of micronemal proteins of *Cryptosporidium parvum*. *Mol Biochem Parasitol* 157, 98–101.
199. R Core Team., 2020. R: A language and environment for statistical computing. R Foundation for Statistical Computing Vienna, Austria.
200. Ranade, D., Pradhan, R., Jayakrishnan, M., Hegde, S., Sengupta, K., 2019. Lamin A/C and Emerin depletion impacts chromatin organization and dynamics in the interphase nucleus. *BMC Molecular and Cell Biology* 20, 11.
201. Rawal, S., Majumdar, S., Vohra, H., 2005. Activation of MAPK kinase pathway by Gal/GalNAc adherence lectin of *E. histolytica*: gateway to host response. *Mol Cell Biochem* 268, 93–101.
202. Redman, C., Lefevre, J., MacDonald, M.L., 1995. Inhibition of diacylglycerol kinase by the antitumor agent calphostin C. Evidence for similarity between the active site of diacylglycerol kinase and the regulatory site of protein kinase C. *Biochem Pharmacol* 50, 235–241.

203. Reduker, D.W., Speer, C.A., 1985. Factors Influencing Excystation in *Cryptosporidium* Oocysts from Cattle. *The Journal of Parasitology* 71, 112–115.
204. Ribas-Silva, R.C., Ribas, A.D., dos Santos, M.C., da Silva, W.V., Lonardoní, M.V., Borelli, S.D., Silveira, T.G., 2013. Association between HLA genes and American cutaneous leishmaniasis in endemic regions of Southern Brazil. *BMC Infectious Diseases* 13, 198.
205. Riedl, J., Crevenna, A.H., Kessenbrock, K., Yu, J.H., Neukirchen, D., Bista, M., Bradke, F., Jenne, D., Holak, T.A., Werb, Z., Sixt, M., Wedlich-Soldner, R., 2008. Lifeact: a versatile marker to visualize F-actin. *Nat Methods* 5, 605–607.
206. Riggs, M.W., Stone, A.L., Yount, P.A., Langer, R.C., Arrowood, M.J., Bentley, D.L., 1997. Protective monoclonal antibody defines a circumsporozoite-like glycoprotein exoantigen of *Cryptosporidium parvum* sporozoites and merozoites. *J Immunol* 158, 1787–1795.
207. Robinson, J., Halliwell, J.A., Marsh, S.G.E., 2014. IMGT/HLA and the Immuno Polymorphism Database. *Methods Mol Biol* 1184, 109–121.
208. Rudolph, M.G., Stanfield, R.L., Wilson, I.A., 2006. How TCRs bind MHCs, peptides, and coreceptors. *Annu Rev Immunol* 24, 419–466.
209. Ryan, U., Fayer, R., Xiao, L., 2014. *Cryptosporidium* species in humans and animals: current understanding and research needs. *Parasitology* 141, 1667–1685.

210. Salerno, F., Paolini, N.A., Stark, R., von Lindern, M., Wolkers, M.C., 2017. Distinct PKC-mediated posttranscriptional events set cytokine production kinetics in CD8+ T cells. *Proc Natl Acad Sci U S A* 114, 9677–9682.
211. Sarkhosh, T., Zhang, X.F., Jellison, K.L., Jedlicka, S.S., 2019. Calcium-Mediated Biophysical Binding of *Cryptosporidium parvum* Oocysts to Surfaces Is Sensitive to Oocyst Age. *Applied and Environmental Microbiology*.
212. Schmid, D., Pypaert, M., Münz, C., 2007. Antigen-loading compartments for major histocompatibility complex class II molecules continuously receive input from autophagosomes. *Immunity* 26, 79–92.
213. Schnee, A.E., Haque, R., Taniuchi, M., Uddin, M.J., Alam, M.M., Liu, J., Rogawski, E.T., Kirkpatrick, B., Houpt, E.R., Petri, W.A., Jr., Platts-Mills, J.A., 2018. Identification of Etiology-Specific Diarrhea Associated With Linear Growth Faltering in Bangladeshi Infants. *American Journal of Epidemiology* 187, 2210–2218.
214. Sears, C.L., Kirkpatrick, B.D., 2007. Is nitazoxanide an effective treatment for patients with acquired immune deficiency syndrome-related cryptosporidiosis? *Nat Rev Gastroenterol Hepatol* 4, 136–137.
215. Sette, A., Sidney, J., del Guercio, M.F., Southwood, S., Ruppert, J., Dahlberg, C., Grey, H.M., Kubo, R.T., 1994. Peptide binding to the most frequent HLA-A class I alleles measured by quantitative molecular binding assays. *Mol Immunol* 31, 813–822.

216. Sheehan, N.J., 2004. The ramifications of HLA-B27. *J R Soc Med* 97, 10–14.
217. Shiina, T., Hosomichi, K., Inoko, H., Kulski, J.K., 2009. The HLA genomic loci map: expression, interaction, diversity and disease. *J Hum Genet* 54, 15–39.
218. Shimokawa, P.T., Targa, L.S., Yamamoto, L., Rodrigues, J.C., Kanunfre, K.A., Okay, T.S., 2016. HLA-DQA1/B1 alleles as putative susceptibility markers in congenital toxoplasmosis. *Virulence* 7, 456–464.
219. Sidney J., Southwood S., Moore C., Oseroff C., Pinilla C., Grey H.M., Sette A., 2013. Measurement of MHC/peptide interactions by gel filtration or monoclonal antibody capture. *Curr. Protoc. Immunol.*, Chapter 18 p. Unit 18.3.
220. Sidney, J., Peters, B., Frahm, N., Brander, C., Sette, A., 2008. HLA class I supertypes: a revised and updated classification. *BMC Immunology* 9, 1.
221. Simmons, G., Wilkinson, D., Reeves, J.D., Dittmar, M.T., Beddows, S., Weber, J., Carnegie, G., Desselberger, U., Gray, P.W., Weiss, R.A., Clapham, P.R., 1996. Primary, syncytium-inducing human immunodeficiency virus type 1 isolates are dual-tropic and most can use either Lestr or CCR5 as coreceptors for virus entry. *J Virol* 70, 8355–8360.
222. Singh, R.K., Kumar, S., Gautam, P.K., Tomar, M.S., Verma, P.K., Singh, S.P., Kumar, S., Acharya, A., 2017. Protein kinase C- $\alpha$  and the regulation of diverse cell responses. *Biomolecular Concepts* 8, 143–153.

223. Skvara, H., Dawid, M., Kleyn, E., Wolff, B., Meingassner, J.G., Knight, H., Dumortier, T., Kopp, T., Fallahi, N., Stary, G., Burkhart, C., Grenet, O., Wagner, J., Hijazi, Y., Morris, R.E., McGeown, C., Rordorf, C., Griffiths, C.E.M., Stingl, G., Jung, T., 2008. The PKC inhibitor AEB071 may be a therapeutic option for psoriasis. *J Clin Invest* 118, 3151–3159.
224. Soderholm, A.T., Pedicord, V.A., 2019. Intestinal epithelial cells: at the interface of the microbiota and mucosal immunity. *Immunology* 158, 267–280.
225. Soh, J.-W., Weinstein, I.B., 2003. Roles of specific isoforms of protein kinase C in the transcriptional control of cyclin D1 and related genes. *J Biol Chem* 278, 34709–34716.
226. Solaymani-Mohammadi, S., Singer, S.M., 2013. Regulation of Intestinal Epithelial Cell Cytoskeletal Remodeling by Cellular Immunity Following Gut Infection. *Mucosal Immunol* 6, 369–378.
227. Soldati, D., Dubremetz, J.F., Lebrun, M., 2001. Microneme proteins: structural and functional requirements to promote adhesion and invasion by the apicomplexan parasite *Toxoplasma gondii*. *Int J Parasitol* 31, 1293–1302.
228. Song, J.C., Rangachari, P.K., Matthews, J.B., 2002. Opposing effects of PKC $\alpha$  and PKC $\epsilon$  on basolateral membrane dynamics in intestinal epithelia. *American Journal of Physiology-Cell Physiology* 283, C1548–C1556.

229. Sow, S.O., Muhsen, K., Nasrin, D., Blackwelder, W.C., Wu, Y., Farag, T.H., Panchalingam, S., Sur, D., Zaidi, A.K.M., Faruque, A.S.G., Saha, D., Adegbola, R., Alonso, P.L., Breiman, R.F., Bassat, Q., Tamboura, B., Sanogo, D., Onwuchekwa, U., Manna, B., Ramamurthy, T., Kanungo, S., Ahmed, S., Qureshi, S., Quadri, F., Hossain, A., Das, S.K., Antonio, M., Hossain, M.J., Mandomando, I., Nhampossa, T., Acácio, S., Omere, R., Oundo, J.O., Ochieng, J.B., Mintz, E.D., O'Reilly, C.E., Berkeley, L.Y., Livio, S., Tennant, S.M., Sommerfelt, H., Nataro, J.P., Ziv-Baran, T., Robins-Browne, R.M., Mishcherkin, V., Zhang, J., Liu, J., Houpt, E.R., Kotloff, K.L., Levine, M.M., 2016. The Burden of *Cryptosporidium* Diarrheal Disease among Children < 24 Months of Age in Moderate/High Mortality Regions of Sub-Saharan Africa and South Asia, Utilizing Data from the Global Enteric Multicenter Study (GEMS). *PLoS Negl Trop Dis* 10, e0004729.
230. Spano, F., Putignani, L., Naitza, S., Puri, C., Wright, S., Crisanti, A., 1998. Molecular cloning and expression analysis of a *Cryptosporidium parvum* gene encoding a new member of the thrombospondin family. *Mol Biochem Parasitol* 92, 147–162.
231. Sparks, H., Nair, G., Castellanos-Gonzalez, A., White, A.C., 2015. Treatment of *Cryptosporidium*: What We Know, Gaps, and the Way Forward. *Curr Trop Med Rep* 2, 181–187.

232. Springer, I., Besser, H., Tickotsky-Moskovitz, N., Dvorkin, S., Louzoun, Y., 2020. Prediction of Specific TCR-Peptide Binding From Large Dictionaries of TCR-Peptide Pairs. *Frontiers in Immunology* 11.
233. Steiner, K.L., Ahmed, S., Gilchrist, C.A., Burkey, C., Cook, H., Ma, J.Z., Korpe, P.S., Ahmed, E., Alam, M., Kabir, M., Tofail, F., Ahmed, T., Haque, R., Petri, W.A., Faruque, A.S.G., 2018. Species of Cryptosporidia Causing Subclinical Infection Associated With Growth Faltering in Rural and Urban Bangladesh: A Birth Cohort Study. *Clin Infect Dis* 67, 1347–1355.
234. Stranger, B.E., Brigham, L.E., Hasz, R., Hunter, M., Johns, C., Johnson, M., Kopen, G., Leinweber, W.F., Lonsdale, J.T., McDonald, A., Mestichelli, B., Myer, K., Roe, B., Salvatore, M., Shad, S., Thomas, J.A., Walters, G., Washington, M., Wheeler, J., Bridge, J., Foster, B.A., Gillard, B.M., Karasik, E., Kumar, R., Miklos, M., Moser, M.T., Jewell, S.D., Montroy, R.G., Rohrer, D.C., Valley, D.R., Davis, D.A., Mash, D.C., Gould, S.E., Guan, P., Koester, S., Little, A.R., Martin, C., Moore, H.M., Rao, A., Struewing, J.P., Volpi, S., Hansen, K.D., Hickey, P.F., Rizzardi, L.F., Hou, L., Liu, Y., Molinie, B., Park, Y., Rinaldi, N., Wang, L., Van Wittenberghe, N., Claussnitzer, M., Gelfand, E.T., Li, Q., Linder, S., Zhang, R., Smith, K.S., Tsang, E.K., Chen, L.S., Demanelis, K., Doherty, J.A., Jasmine, F., Kibriya, M.G., Jiang, L., Lin, S., Wang, M., Jian, R., Li, X., Chan, J., Bates, D., Diegel, M., Halow, J., Haugen, E., Johnson, A., Kaul, R., Lee, K., Maurano, M.T., Nelson, J., Neri, F.J., Sandstrom, R., Fernando, M.S.,

- Linke, C., Oliva, M., Skol, A., Wu, F., Akey, J.M., Feinberg, A.P., Li, J.B., Pierce, B.L., Stamatoyannopoulos, J.A., Tang, H., Ardlie, K.G., Kellis, M., Snyder, M.P., Montgomery, S.B., eGTEx Project, 2017. Enhancing GTEx by bridging the gaps between genotype, gene expression, and disease. *Nat Genet* 49, 1664–1670.
235. Strong, W.B., Gut, J., Nelson, R.G., 2000. Cloning and sequence analysis of a highly polymorphic *Cryptosporidium parvum* gene encoding a 60-kilodalton glycoprotein and characterization of its 15- and 45-kilodalton zoite surface antigen products. *Infect Immun* 68, 4117–4134.
236. Strulovici, B., Daniel-Issakani, S., Oto, E., Nestor, J., Chan, H., Tsou, A.P., 1989. Activation of distinct protein kinase C isozymes by phorbol esters: correlation with induction of interleukin 1 beta gene expression. *Biochemistry* 28, 3569–3576.
237. Sukumaran, S.K., Quon, M.J., Prasadarao, N.V., 2002. *Escherichia coli* K1 internalization via caveolae requires caveolin-1 and protein kinase C- $\alpha$  interaction in human brain microvascular endothelial cells. *J. Biol. Chem.* 277, 50716–50724.
238. Sveinbjornsson, G., Gudbjartsson, D.F., Halldorsson, B.V., Kristinsson, K.G., Gottfredsson, M., Barrett, J.C., Gudmundsson, L.J., Blondal, K., Gylfason, A., Gudjonsson, S.A., Helgadottir, H.T., Jonasdottir, Adalbjorg, Jonasdottir, Aslaug, Karason, A., Kardum, L.B., Knežević, J., Kristjansson, H., Kristjansson, M., Love, A., Luo, Y., Magnusson, O.T., Sulem, P., Kong, A., Masson, G., Thorsteinsdottir, U., Dembic, Z.,

- Nejentsev, S., Blondal, T., Jonsdottir, I., Stefansson, K., 2016. HLA class II sequence variants influence tuberculosis risk in populations of European ancestry. *Nat Genet* 48, 318–322.
239. Szallasi, Z., Denning, M.F., Smith, C.B., Dlugosz, A.A., Yuspa, S.H., Pettit, G.R., Blumberg, P.M., 1994. Bryostatins protect protein kinase C- $\delta$  from down-regulation in mouse keratinocytes in parallel with its inhibition of phorbol ester-induced differentiation. *Mol Pharmacol* 46, 840–850.
240. Talman, V., Pascale, A., Jääntti, M., Amadio, M., Tuominen, R.K., 2016. Protein Kinase C Activation as a Potential Therapeutic Strategy in Alzheimer's Disease: Is there a Role for Embryonic Lethal Abnormal Vision-like Proteins? *Basic Clin Pharmacol Toxicol* 119, 149–160.
241. Tandel, J., English, E.D., Sateriale, A., Gullicksrud, J.A., Beiting, D.P., Sullivan, M.C., Pinkston, B., Striepen, B., 2019. Life cycle progression and sexual development of the apicomplexan parasite *Cryptosporidium parvum*. *Nat Microbiol* 4, 2226–2236.
242. Taniuchi M., Sobuz S.U., Begum S., Platts-Mills J.A., Liu J., Yang Z., 2013. Etiology of diarrhea in Bangladeshi infants in the first year of life analyzed using molecular methods. *J Infect Dis* 208(11):1794–1802.
243. Teixeira N.B., Rojas T.C., Silveira W.D., Matheus-Guimarães C., Silva N.P., Scaletsky I.C., 2015. Genetic analysis of enteropathogenic *Escherichia coli* (EPEC) adherence factor (EAF) plasmid reveals a new

deletion within the EAF probe sequence among O119 typical EPEC strains. *BMC Microbiol* 15(200):1186. 12866–015–0539–9.

244. Tessema, T.S., Schwamb, B., Lochner, M., Förster, I., Jakobi, V., Petry, F., 2009. Dynamics of gut mucosal and systemic Th1/Th2 cytokine responses in interferon-gamma and interleukin-12p40 knock out mice during primary and challenge *Cryptosporidium parvum* infection. *Immunobiology* 214, 454–466.
245. Tetley, L., Brown, S.M.A., McDonald, V., Coombs, G.H., 1998. Ultrastructural analysis of the sporozoite of *Cryptosporidium parvum*. *Microbiology (Reading)* 144 ( Pt 12), 3249–3255.
246. Tian S., Maile R., Collins E.J., Frelinger J.A., 2007. CD8+ T cell activation is governed by TCR-peptide/MHC affinity, not dissociation rate. *J Immunol* 179(5):2952–2960.
247. Troeger, C., Forouzanfar, M., Rao, P.C., Khalil, I., Brown, A., Reiner, R.C., Fullman, N., Thompson, R.L., Abajobir, A., Ahmed, M., Alemayohu, M.A., Alvis-Guzman, N., Amare, A.T., Antonio, C.A., Asayesh, H., Avokpaho, E., Awasthi, A., Bacha, U., Barac, A., Betsue, B.D., Beyene, A.S., Boneya, D.J., Malta, D.C., Dandona, L., Dandona, R., Dubey, M., Eshrati, B., Fitchett, J.R.A., Gebrehiwot, T.T., Hailu, G.B., Horino, M., Hotez, P.J., Jibat, T., Jonas, J.B., Kasaeian, A., Kissepp, N., Kotloff, K., Koyanagi, A., Kumar, G.A., Rai, R.K., Lal, A., Razek, H.M.A.E., Mengistie, M.A., Moe, C., Patton, G., Platts-Mills, J.A., Qorbani, M., Ram, U., Roba, H.S., Sanabria, J., Sartorius, B., Sawhney, M., Shigematsu, M.,

- Sreeramareddy, C., Swaminathan, S., Tedla, B.A., Jagiellonian, R.T.-M., Ukwaja, K., Werdecker, A., Widdowson, M.-A., Yonemoto, N., Zaki, M.E.S., Lim, S.S., Naghavi, M., Vos, T., Hay, S.I., Murray, C.J.L., Mokdad, A.H., 2017. Estimates of global, regional, and national morbidity, mortality, and etiologies of diarrheal diseases: a systematic analysis for the Global Burden of Disease Study 2015. *The Lancet Infectious Diseases* 17, 909–948.
248. Trowsdale, J., Knight, J.C., 2013. Major histocompatibility complex genomics and human disease. *Annu Rev Genomics Hum Genet* 14, 301–323.
249. Tsien, R.Y., 1980. New calcium indicators and buffers with high selectivity against magnesium and protons: design, synthesis, and properties of prototype structures. *Biochemistry* 19, 2396–2404.
250. Tzipori, S., Griffiths, J.K., 1998. Natural history and biology of *Cryptosporidium parvum*. *Adv Parasitol* 40, 5–36.
251. Überall, F., Giselbrecht, S., Hellbert, K., Fresser, F., Bauer, B., Gschwendt, M., Grunicke, H.H., Baier, G., 1997. Conventional PKC- $\alpha$ , Novel PKC- $\epsilon$  and PKC- $\theta$ , but Not Atypical PKC- $\lambda$  Are MARCKS Kinases in Intact NIH 3T3 Fibroblasts. *J. Biol. Chem.* 272, 4072–4078.
252. Ungar, B.L., Kao, T.C., Burris, J.A., Finkelman, F.D., 1991. *Cryptosporidium* infection in an adult mouse model. Independent roles for IFN-gamma and CD4<sup>+</sup> T lymphocytes in protective immunity. *The Journal of Immunology* 147, 1014–1022.

253. Unicomb, L.E., Banu, N.N., Azim, T., Islam, A., Bardhan, P.K., Faruque, A.S., Hall, A., Moe, C.L., Noel, J.S., Monroe, S.S., Albert, M.J., Glass, R.I., 1998. Astrovirus infection in association with acute, persistent and nosocomial diarrhea in Bangladesh. *Pediatr Infect Dis J* 17, 611–614.
254. Upton, S.J., Tilley, M., Brillhart, D.B., 1994. Comparative development of *Cryptosporidium parvum* (Apicomplexa) in 11 continuous host cell lines. *FEMS Microbiol Lett* 118, 233–236.
255. Van Voorhis, W.C., Doggett, J.S., Parsons, M., Hulverson, M.A., Choi, R., Arnold, S.L.M., Riggs, M.W., Hemphill, A., Howe, D.K., Mealey, R.H., Lau, A.O.T., Merritt, E.A., Maly, D.J., Fan, E., Ojo, K.K., 2017. Extended-spectrum antiprotozoal bumped kinase inhibitors: A review. *Exp Parasitol* 180, 71–83.
256. Vinayak, S., Pawlowic, M.C., Sateriale, A., Brooks, C.F., Studstill, C.J., Bar-Peled, Y., Cipriano, M.J., Striepen, B., 2015. Genetic modification of the diarrheal pathogen *Cryptosporidium parvum*. *Nature* 523, 477–480.
257. Wang, W., Zhang, W., Zhang, J., He, J., Zhu, F., 2020. Distribution of HLA allele frequencies in 82 Chinese individuals with coronavirus disease-2019 (COVID-19). *HLA* 96, 194–196.
258. Wasserman, M., Alarcón, C., Mendoza, P.M., 1982. Effects of Ca<sup>++</sup> depletion on the asexual cell cycle of *Plasmodium falciparum*. *Am J Trop Med Hyg* 31, 711–717.

259. Wetzel, D.M., Schmidt, J., Kuhlenschmidt, M.S., Dubey, J.P., Sibley, L.D., 2005. Gliding motility leads to active cellular invasion by *Cryptosporidium parvum* sporozoites. *Infect Immun* 73, 5379–5387.
260. White, A.C., Jr, Robinson, P., Okhuysen, P.C., Lewis, D.E., Shahab, I., Lahoti, S., DuPont, H.L., Chappell, C.L., 2000. Interferon- $\gamma$  Expression in Jejunal Biopsies in Experimental Human Cryptosporidiosis Correlates with Prior Sensitization and Control of Oocyst Excretion. *The Journal of Infectious Diseases* 181, 701–709.
261. Wickham, H., Averick, M., Bryan, J., Chang, W., McGowan, L.D., François, R., Golemund, G., Hayes, A., Henry, L., Hester, J., Kuhn, M., Pedersen, T.L., Miller, E., Bache, S.M., Müller, K., Ooms, J., Robinson, D., Seidel, D.P., Spinu, V., Takahashi, K., Vaughan, D., Wilke, C., Woo, K., Yutani, H., 2019. Welcome to the Tidyverse. *Journal of Open Source Software* 4, 1686.
262. Wilke, G., Funkhouser-Jones, L.J., Wang, Y., Ravindran, S., Wang, Q., Beatty, W.L., Baldridge, M.T., VanDussen, K.L., Shen, B., Kuhlenschmidt, M.S., Kuhlenschmidt, T.B., Witola, W.H., Stappenbeck, T.S., Sibley, L.D., 2019. A Stem-Cell-Derived Platform Enables Complete *Cryptosporidium* Development In Vitro and Genetic Tractability. *Cell Host Microbe* 26, 123-134.e8.
263. Wojcik, G.L., Korpe, P., Marie, C., Mentzer, A.J., Carstensen, T., Mychaleckyj, J., Kirkpatrick, B.D., Rich, S.S., Concannon, P., Faruque, A.S.G., Haque, R., Petri, W.A., Duggal, P., 2020. Genome-Wide

Association Study of Cryptosporidiosis in Infants Implicates PRKCA. *mBio* 11, e03343-19.

264. Wojcik, G.L., Marie, C., Abhyankar, M.M., Yoshida, N., Watanabe, K., Mentzer, A.J., Carstensen, T., Mychaleckyj, J., Kirkpatrick, B.D., Rich, S.S., Concannon, P., Haque, R., Tsokos, G.C., Petri Jr, W.A., Duggal, P., 2018. Genome-Wide Association Study Reveals Genetic Link between Diarrhea-Associated *Entamoeba histolytica* Infection and Inflammatory Bowel Disease. *mBio*.
265. Xiong, H., Huang, J., Rong, X., Zhang, M., Huang, K., Xu, R., Wang, M., Li, C., Liao, Q., Xia, W., Luo, G., Ye, X., Lu, L., Fu, Y., Guo, T., Nelson, K., 2015. HLA-B alleles B\*15:01 and B\*15:02: opposite association with hepatitis C virus infection in Chinese voluntary blood donors. *Intervirology* 58, 80–87.
266. Yang, L., Yan, Y., 2014. Protein kinases are potential targets to treat inflammatory bowel disease. *World J Gastrointest Pharmacol Ther* 5, 209–217.
267. Yang, Y.-L., Buck, G.A., Widmer, G., 2010. Cell Sorting-Assisted Microarray Profiling of Host Cell Response to *Cryptosporidium parvum* Infection. *Infection and Immunity* 78, 1040–1048.
268. You, X., Mead, J.R., 1998. Characterization of experimental *Cryptosporidium parvum* infection in IFN- $\gamma$  knockout mice. *Parasitology* 117, 525–531.

269. Zhang, Q., Guo, Y., Li, N., Li, Y., Su, J., Xu, R., Zhang, Z., Feng, Y., Xiao, L., 2020. Characterization of Calcium-Dependent Protein Kinases 3, a Protein Involved in Growth of *Cryptosporidium parvum*. *Frontiers in Microbiology* 11.
270. Zhang, Q., Shao, Q., Guo, Y., Li, N., Li, Y., Su, J., Xu, R., Zhang, Z., Xiao, L., Feng, Y., 2021. Characterization of Three Calcium-Dependent Protein Kinases of *Cryptosporidium parvum*. *Frontiers in Microbiology* 11.
271. Zhao, G.H., Fang, Y.Q., Ryan, U., Guo, Y.X., Wu, F., Du, S.Z., Chen, D.K., Lin, Q., 2016. Dynamics of Th17 associating cytokines in *Cryptosporidium parvum*-infected mice. *Parasitol Res* 115, 879–887.
272. Zhao, N., Kamijo, K., Fox, P.D., Oda, H., Morisaki, T., Sato, Y., Kimura, H., Stasevich, T.J., 2019. A genetically encoded probe for imaging nascent and mature HA-tagged proteins in vivo. *Nat Commun* 10, 2947.
273. Zhou, X., Yang, W., Li, J., 2006. Ca<sup>2+</sup>- and protein kinase C-dependent signaling pathway for nuclear factor-kappaB activation, inducible nitric-oxide synthase expression, and tumor necrosis factor-alpha production in lipopolysaccharide-stimulated rat peritoneal macrophages. *J Biol Chem* 281, 31337–31347.
274. Zhu, Y., Cui, G., Miyauchi, E., Nakanishi, Y., Mukohira, H., Shimba, A., Abe, S., Tani-ichi, S., Hara, T., Nakase, H., Chiba, T., Sehara-Fujisawa, A., Seno, H., Ohno, H., Ikuta, K., 2020. Intestinal epithelial cell-derived IL-15 determines local maintenance and maturation of intra-

epithelial lymphocytes in the intestine. *International Immunology* 32, 307–319.

275. Ziemba, B.P., Burke, J.E., Masson, G., Williams, R.L., Falke, J.J., 2016. Regulation of PI3K by PKC and MARCKS: Single-Molecule Analysis of a Reconstituted Signaling Pathway. *Biophys J* 110, 1811–1825.